
Wayne State University Dissertations

January 2021

Cardio-Renal Mechanisms Of Fructose-Induced Salt-Sensitive Hypertension

Peter Eric Levanovich
Wayne State University

Follow this and additional works at: https://digitalcommons.wayne.edu/oa_dissertations

 Part of the [Physiology Commons](#)

Recommended Citation

Levanovich, Peter Eric, "Cardio-Renal Mechanisms Of Fructose-Induced Salt-Sensitive Hypertension" (2021). *Wayne State University Dissertations*. 3446.
https://digitalcommons.wayne.edu/oa_dissertations/3446

This Open Access Dissertation is brought to you for free and open access by DigitalCommons@WayneState. It has been accepted for inclusion in Wayne State University Dissertations by an authorized administrator of DigitalCommons@WayneState.

**CARDIO-RENAL MECHANISMS OF FRUCTOSE-INDUCED SALT-SENSITIVE
HYPERTENSION**

by

PETER E. LEVANOVICH

DISSERTATION

Submitted to the Graduate School

of Wayne State University,

Detroit, Michigan

in partial fulfillment of the requirements

for the degree of

DOCTOR OF PHILOSOPHY

2021

MAJOR: PHYSIOLOGY

Approved By:

Advisor

Date

© COPYRIGHT BY
PETER E. LEVANOVICH
2021
All Rights Reserved

DEDICATION

This work is dedicated to those of us who continue to strive toward a better tomorrow. To dwell on the bleakness of the past is nothing short of futility. To hope for a brighter future is the seed from which progress grows. For those of us who continue to dream... follow your folly.

ACKNOWLEDGEMENTS

First and foremost, I would like to acknowledge my dear friend and mentor, Dr. Noreen F. Rossi. Her never ending support, encouragement, and enthusiasm in even the most challenging of studies and worst of circumstances were the fuel for my personal and professional growth. Completion of this work would not have been possible without the entirety of both - neither of which could have been brought forward to such extents by anyone else.

I would like to acknowledge my current and former lab mates who aided with so many aspects of this research - the diversity of skill sets, expertise, and guidance in techniques in which I was so very lacking is what enabled the depth this work required to produce the insights it did. I would particularly like to thank Min Wu. - A.K.A. *Mama Min* - who I could not have performed these studies without. Not only was I always kept well fed with her outstanding dumpling recipes, but for every failure was the continuous encouragement that enabled me to move forward to find success.

I would like to thank Dr. Charles Chung for his ongoing support and mentorship in ultrasonography, physiologic concepts, and overall approach to research.

I believe it goes without saying, my friends and most importantly my family were invaluable to helping me to maintain focus. They've always supported me in every endeavor, but it became clear these past several years just how devoted they were to helping me achieve my goals, despite how much complained.

Lastly, I would like to thank Department of Physiology, the sources of funding I've received (both the Detroit Cardiovascular T32 Training Grant and the Interdisciplinary Biomedical Sciences Fellowship). I extend this gratitude to the people that not only awarded

them but also stood behind me that were always eager to lend advice, assistance whenever needed, or simply held me together whenever things were looking so very bleak. I would like to thank Christine Cupps for all of this.

TABLE OF CONTENTS

Dedication.....	ii
Acknowledgements.....	iii
List of Tables.....	vii
List of Figures.....	viii
List of Abbreviations.....	ix
Chapter 1: Hypertension Associated with Fructose and High Salt: Renal and Sympathetic Mechanisms.....	1
Introduction.....	1
Fructose Consumption, Hypertension and Mortality.....	2
Fructose Influences Sodium Handling and Blood Pressure.....	5
Experimental Purpose and Design.....	12
Chapter 2: Aortic Stiffness and Diastolic Dysfunction in Sprague- Dawley Rats Consuming Short-term Fructose Plus High Salt Diet.....	14
Introduction.....	14
Materials and Methods.....	17
Results.....	22
Discussion.....	29
Chapter 3: Adolescent Fructose Consumption Induces Chronic Salt- Sensitivity and Renal Dysfunction.....	36
Introduction.....	36
Materials and Methods.....	38
Results.....	43
Discussion.....	53
Chapter 4: Acute and Chronic Cardiovascular Dysfunction in Response to Fructose-Induced Ontogenetic Programming of Salt-Sensitivity.....	59
Introduction.....	59

Materials and Methods.....	61
Results.....	67
Discussion.....	75
Chapter 5: Conclusions and Future Directions.....	82
Appendix A: IACUC Protocol Approval Letters.....	84
Appendix B: Copyright License Agreement for Chapter 1.....	86
Appendix C: Copyright License Agreement for Chapter 2.....	87
References.....	88
Abstract.....	112
Autobiographical Statement.....	114

LIST OF TABLES

Table 2.1: Rat, Kidney and Heart Weights for All Rat Groups.....	23
Table 2.2: Baseline Hemodynamics and Changes after 3-Week Diet Regimen.....	23
Table 2.3: Echocardiographic Parameters in Control Groups.....	26
Table 2.4: Values for Plasma Glucose, PRA and Ang II and Renal Cortical Tissue Ang II after 3-Week Diet Regimen.....	29
Table 3.1: Study-wide Changes in Hemodynamics.....	45
Table 3.2: Daily Metabolic Measurements.....	47
Table 3.3: Ion Consumption and Excretion.....	48
Table 3.4: Metabolic, Renal, and Endocrine Measurements.....	51
Table 4.1: Daily Consumption Measurements.....	68
Table 4.2: Hemodynamic Measurements.....	69
Table 4.3: Echocardiographic Parameters Assessed at the End of Phase 3.....	71
Table 4.4: Parameters Associated with Diastolic Function Assessed at the End of Phase III.....	73
Table 4.5: Metabolic and Endocrine Assessment.....	75

LIST OF FIGURES

Figure 2.1: Change in Mean Arterial Pressure Timeline.....	24
Figure 2.2: Aortic Pulse Wave Velocity.....	25
Figure 2.3: Ratio of Early to Late Transmitral Filling Velocities.....	26
Figure 2.4: Elastic Properties of the Ascending Aorta.....	27
Figure 2.5: Renal Resistive Index (RRI).....	28
Figure 2.6: Glucose:Insulin Ratio.....	29
Figure 3.1: Timeline of Experimental Protocols, Division of Phases, and Allotment of Dietary Regimens and Groups.....	39
Figure 3.2: Timeline of Daily Mean Arterial Pressure.....	44
Figure 3.3: Bodily Sodium Balance.....	50
Figure 3.4: Assessment of glomerular filtration rate.....	53
Figure 4.1: Timeline of Experimental Protocols, Division of Phases, and Allotment of Dietary Regimens and Groups.....	63
Figure 4.2: Assessment of Aortic Compliance.....	70
Figure 4.3: Assessment of Renal Resistive Index.....	71
Figure 4.4: Assessment of Left Ventricular Morphology in Phase III.....	72
Figure 4.5: Assessment of Diastolic Function.....	74

LIST OF ABBREVIATIONS

Ang II - angiotensin II

ANOVA – Analysis of Variance

AT1 - angiotensin receptor type 1

BW – Body Weight

CARDIA - Coronary Artery Risk Development in Young Adults

DBP – Diastolic Blood Pressure

DOCA – deoxycorticosterone-acetate

E/A – Ratio of early to late phase left ventricular filling

ECG – Echocardiogram

ET-1 – Endothelin 1

EDTA - Ethylenediaminetetraacetic Acid

FLS – Fructose Low (0.4%) Sodium

FHS – Fructose High (4.0%) Sodium

GFR – Glomerular Filtration Rate

G:I Ratio – Glucose to Insulin Ratio

GLUT - glucose transporter

GLUT5 - Glucose Transporter Isoform 5

HFCS - high fructose corn syrup

HR – Heart Rate

K⁺ - Potassium

LV – Left Ventricle

LVAW – Left Ventricular Anterior Wall Width

LVEF – Left Ventricular Ejection Fraction

LVDID – Left Ventricular Diastolic Internal Diameter

LVFS – Left Ventricular Fractional Shortening

LVPW – Left Ventricular Posterior Wall Width

LVSID – Left Ventricular Systolic Internal Diameter

LVAW – Left Ventricular Anterior Wall Width

LVTW – Left Ventricular Total Wall Width

MAP – Mean Arterial Pressure

Na⁺ - Sodium

NHANES - National Health and Nutrition Examination Survey

NHE - Sodium hydrogen exchanger

NKCC2 - Sodium potassium chloride transporter

PAT1 - Putative anion transporter 1

PKA - Protein kinase A

PKC - Protein kinase C

PRA - Plasma renin activity

PP – Pulse Pressure

PWV – Pulse Wave Velocity

RRI – Renal Resistive Index

RAS renin angiotensin system

RAS - Renin-Angiotensin System

ROS – Reactive Oxygen Species

SE – Standard Error of the Mean

SBP – Systolic Blood Pressure

TDI – Tissue Doppler Imaging

$U_x \times V$ – Urinary concentration of a defined ion X Volume

CHAPTER 1: HYPERTENSION ASSOCIATED WITH FRUCTOSE AND HIGH SALT: RENAL AND SYMPATHETIC MECHANISMS

(This Chapter contains previously published material. See Appendix B.)

INTRODUCTION

Hypertension is a multifactorial condition rather than a single disease entity whose onset can be brought about through a variety of factors originating from environmental, dietary, or hereditary factors. The complex interplay of these components has frustrated our understanding of hypertension, despite decades of research spent attempting to identify its causes and develop viable treatments. Even today, less than 20% of all hypertensive cases have a known etiology (referred to as secondary hypertension) with the basis for the remaining majority of cases being unknown (referred to as primary or essential hypertension) [1, 2]. Studies of the U.S. population have found that 29% of adults are hypertensive, and this number is only expected to increase dramatically in the near future [3]. Unfortunately, elevated blood pressure is becoming increasingly prevalent in people under the age of 40 years [4]. Despite the fact the proportion of individuals with controlled blood pressure (systolic < 140 mmHg; diastolic < 90 mmHg) in the U.S. has increased from 28.4% to 43.5%, in low and middle-income countries control of blood pressure has actually decreased to 7.7% [5, 6]. Indeed, even mild increases in either systolic or diastolic pressure (< 10 mmHg) are accompanied by increases in mortality rates [7]. The increased prevalence of hypertension has coincided with an equally sharp increase in the incidence of chronic kidney disease that has been attributed, at least in part, to substantial changes in dietary intake and sedentary lifestyle [4, 8]. Hence, there has been an increased effort to develop new models of hypertension that better reflect the environmental and dietary behaviors of modern society. Several models of diet-induced hypertension exist that are well established,

namely those high in fat or sodium [9, 10]. Models of metabolic syndrome induce a constellation of medical conditions accompanying insulin resistance such as obesity, hyperglycemia, hypertension, and dyslipidemia [11]. Given the widespread use of fructose as a sweetener in food products, several recent reviews have discussed the impact of fructose ingestion on obesity and hypertension within the metabolic syndrome [12, 13] and the hormones involved [14]. The present review focuses on recent interest on the consequences of even mild fructose consumption *independent* of full-blown metabolic syndrome with particular attention to the role of the kidney and the sympathetic nervous system on blood pressure.

FRUCTOSE CONSUMPTION, HYPERTENSION, AND MORTALITY

Total fructose consumption includes that which is found in high fructose corn syrup (HFCS) and sucrose. Generation of HFCS began in the late 1950s when it was discovered that glucose, hydrolyzed from corn starch extracts, could be partially converted to fructose through enzymatic isomerization [15]. Over time, this process was industrialized and led to the development of the corn-derived sweetener, HFCS, which can be synthesized with varying ratios of fructose to glucose content. Ease of synthesis, comparable flavor, and low cost of this ingredient have contributed to its widespread use as a sweetener [16]. Between 1970 and 2006, fructose consumption drastically increased, amounting to approximately 50% of all per capita added sugar consumption. This increase is accounted for solely by an exponential increase in free fructose consumption in the form of HFCS. During this time, caloric intake from total sugar (HFCS, sucrose, and other natural sugars) and fats increased significantly contributing to a 41% increase in total carbohydrate intake, of which fructose consumption provided a primary source [17].

HFCS appeals to nearly every demographic leading to its widespread use in food products. Statistical analysis of data collected in the National Health and Nutrition Examination Survey (NHANES I-III) determined that HFCS is most heavily consumed in the form sugar-sweetened beverages, and this trend is consistent throughout all age groups and sexes. Although a recent meta-analysis of three prospective studies fails to show incident hypertension associated with fructose, these studies relied on self-reports of dietary intake and physician-diagnosed hypertension and did not include concurrent sodium intake [18]. In contrast, another meta-analysis (n = 240,508) that includes data from the Coronary Artery Risk Development in Young Adults (CARDIA) cohort (n = 240,508) [19] and quoted by the recent American Heart Association update on stroke reports a 12% greater risk of hypertension with consumption of sugar sweetened beverages when controlled for sex, age, race, BMI and smoking behaviors [20]. Compared with the increased risk associated with more traditional factors such as alcohol consumption (61%), smoking (21%), and red meat intake (35%) and sedentary life style (48%) [21-24] or the non-traditional risk of stress (5-12%) [25], the risk associated with fructose intake may appear small but is nonetheless real. Whether the risk of hypertension associated with fructose is modified by combination with higher sodium intake has not yet been rigorously evaluated in humans, but the role of combined intake in preclinical studies is discussed below.

Adolescents and young adults are the highest consumers overall, and people in lower income population sectors are more likely to consume HFCS than those in more affluent demographic groups [13]. The rise in fructose consumption over the past several decades has been accompanied by an increase in obesity in the United States, and these rates parallel those of hypertension in a nearly linear relationship between body mass index and blood

pressure [26, 27]. Although several human studies have shown that high fructose consumption contributes to weight gain and blood pressure elevation, there is still controversy over the extent to which HFCS consumption is correlated with the historical obesity and hypertension trends [28]. Factors such as overall increase in national carbohydrate consumption make it challenging to discern increased fructose intake as a primary etiologic source for these disease states [17]. Nevertheless, the ingestion of fructose induces several physiologic responses that favor weight gain and increased blood pressure.

The most recent NHANES III survey found that as of 2004, the average daily intake of fructose (49 grams) in the U.S. equated to 9.1% of total energy intake [17]. Interestingly, commercially available drinks using HFCS have up to 140 calories from added sugars per 12 fluid ounce container. Given the most commonly used HFCS composition of 55% fructose and 45% glucose, this amounts to approximately 25 grams or 100 calories from fructose alone. This quantity from one drink alone nearly surpasses the American Heart Association recommendation of only 150 and 100 calories from added sugars per day for men and women, respectively [29]. Animal studies designed to model this trend in human dietary intake have used various dietary fructose compositions - many of which exceed 60% of total daily caloric intake [30-32]. Increased fructose ingestion in either humans or animal studies have demonstrated significant hemodynamic changes even after limited periods of time [28, 33, 34]. Interestingly, most animal studies were not accompanied by significant increases in body weight, suggesting that factors apart from obesity may contribute to the hypertensive phenotype [30, 31]. Chronic animal models using more moderate fructose intake that is consistent with heavy human consumption (15-20% of daily caloric intake) demonstrate cardiovascular and metabolic changes similar to human subjects, although the timeline by

which these occur may be skewed [35, 36]. The role of endothelial dysfunction has been reviewed in detail [37, 38]. Mechanisms involved in the early phases of sodium absorption by the intestine have been studied to a greater extent [39]; however, renal sodium reabsorption [40], the renal renin-angiotensin-aldosterone (RAS) system [41], and sympathetic nervous system [32, 42] have received more limited attention.

FRUCTOSE INFLUENCE ON SODIUM HANDLING AND BLOOD PRESSURE

Fructose influences on gastrointestinal sodium absorption

Sodium homeostasis is a critical component of blood pressure regulation and has been linked to various cardiovascular and renal complications, including hypertension [43-46]. Glucose intake is coupled to Na⁺ transport via the luminal sodium-glucose-linked transporters 1 and 2 (SGLT1 and SGLT2). Intracellular glucose concentration is largely maintained through the glucose transporter 2 (GLUT2) isoform along the basolateral membrane. Chronically, fructose and glucose (but not other sugars) lead to an increase in GLUT2 protein expression along the basolateral membrane [47]. Similar to GLUT5, GLUT2 has a much lower affinity for glucose than other isoforms and therefore functions primarily as a fructose transporter [48]. Fructose transport is facilitated by a downhill concentration gradient between the intestinal lumen and intracellular space [39, 49, 50].

On the other hand, sodium absorption occurs throughout the small intestine via a variety of transport systems. SLC26A6 (human), also known as the putative ion transporter 1 (PAT1), is a multifunctional apical chloride/base exchanger that increases with fructose feeding in both the jejunum [39, 51] and kidney [52]. The function of PAT1 is coupled with that of the intestinal Na/H exchanger 3 (NHE3) so that Na⁺ is reabsorbed with Cl⁻ in an electroneutral manner [53, 54]. The presence of fructose amplifies NHE3 function, thereby

enhancing absorption of Na⁺ and secretion of H⁺ [39, 40, 42]. PAT1 also co-localizes with GLUT5 (Slca5), a member of the glucose transporter family, with low affinity for glucose and high affinity for fructose. GLUT5 is the dominant fructose transporter in the jejunum.

Despite the changes in both sodium and sugar transporters, the impact of fructose on overall gastrointestinal absorption and ultimate fecal excretion of sodium has been given scant investigative attention. An increase in dietary sodium does not increase absolute fecal sodium excretion in Sprague Dawley rats independent of whether the high sodium chow is delivered with glucose or fructose in the drinking water or with water alone. Gastrointestinal sodium absorption increases as dietary intake of sodium increases regardless of the presence or type of sugars in the diet. Thus, the task for excretion of the greater total body sodium content relies on the kidney. Notably, urinary sodium excretion is significantly diminished in fructose-fed rats resulting in a positive sodium balance [41]. The renal mechanisms that are understood to date are detailed below.

Fructose influences renal sodium reabsorption and RAS

The bulk of Na⁺ reabsorption in the mammalian kidney occurs in the proximal tubule, which is responsible for reabsorption of 60-70% of all Na⁺ and fluid filtered by the glomerulus [55]. Similar to the intestine, GLUT2, GLUT5, NHE3, and several isoforms from the SGLT family facilitate the reabsorption of Na⁺. Proximal tubule Na⁺ reabsorption is reliant on secondary active transport by co-transporters such as NHE3 and SGLT isoforms, particularly SGLT2 [56]. Fine tuning of ionic concentrations and gradients is critical to blood pressure homeostasis. Perturbation such as augmented proximal tubule Na⁺ reabsorption results in increased fluid reabsorption, leading to a net positive sodium balance predisposing to hypertension. This mechanism has been linked to hypertension in spontaneously

hypertensive rats [57] and Dahl salt-sensitive rats [58]. In carefully executed balance studies, Gordish et al. [41] showed that rats given 20% fructose in their drinking water and placed on high salt diet displayed significantly greater cumulative Na^+ balance compared with rats given only water or 20% glucose in their drinking water. These findings strongly supported a role for fructose-feeding on renal Na^+ balance. Notably, except for elevated triglyceride levels in the fructose-fed high salt group, there were no differences in fasting plasma glucose and body weights between fructose-high salt-fed rats and glucose or water controls either with standard or high salt intake [41].

In the proximal tubule, the large proportion of filtered Na^+ and bicarbonate (HCO_3^-) reabsorption is linked to Na^+/H^+ exchange, via NHE3 [59]. Acute *in vivo* microperfusion studies of proximal tubules from Wistar rats exposed to fructose revealed enhanced NHE3 activity. The increase in NHE3 activity was corroborated by *in vitro* studies showing greater Na^+ dependent H^+ flux in the presence of fructose associated with diminished PKA activity in cultured LLC-PK1 cells, a porcine cell line [60]. Fructose, but not glucose, increased NHE3 activity by isolated rat proximal tubules via a PKC-dependent pathway and further potentiated the effects of picomolar concentrations of angiotensin II (Ang II) to increase Na^+/H^+ exchange. Na/K-ATPase activity did not change [40]. Moderate amounts of fructose consumption (approximately 40% of daily caloric intake provided as a 20% fructose solution in drinking water) increased tail cuff blood pressure in rats. Proximal tubule expression levels of NHE3 increased significantly in the fructose-fed compared to that of control rats, whereas $\alpha 1$ subunit of the basolateral Na/K-ATPase did not. Moreover, proximal tubules isolated from these rats also showed enhanced Na^+ reabsorption that was potentiated by Ang II [61, 62].

The proximal tubule thus appears to become sensitized to Ang II via a PKC mechanism, to which the addition of high Na⁺ intake leads to substantial reabsorption rates. Further, this sensitization extends beyond the proximal tubule into the thick ascending limb and other Na⁺ transport mechanisms in the distal nephron, although studies have reported some conflicting results. An early study with 65% dietary fructose failed to observe a change in overall NKCC2 abundance in the kidney [63]. *In vitro* and *in vivo* studies have shown similar effects on Na⁺/K⁺/2Cl⁻ co-transporter 2 (NKCC2) expression and activity. Acute *in vitro* administration of fructose to the thick ascending limb increases NKCC2 activity by increasing protein expression and not phosphorylation along the apical membrane [64]. Chronic *in vivo* studies using furosemide, an NKCC2 antagonist, to measure acute diuretic and natriuretic responses following NKCC2 blockade found that high fructose-induced hypertension led to significant increases in urine output as well as in urinary potassium, chloride, and sodium concentration. This was reflected by significant increases in NKCC2 mRNA and protein expression [65]. Together, these alterations in transporter expression and activity throughout the nephron facilitate plasma volume expansion which is responsible, at least in part, for the observed hypertension.

The importance of sensitization to Ang II also cannot be understated. Several preclinical studies have shown that even moderate consumption of fructose and Na⁺ can have considerable adverse effects on blood pressure [41, 42, 61, 66]. With the profound increases in Na⁺ retention observed in the various models of fructose-induced hypertension with expected extracellular volume expansion, it would be anticipated that plasma renin activity (PRA) would be suppressed. Further investigation by others reported blunted suppression of PRA in Sprague Dawley rats given 20% fructose for one week, followed by

one week of fructose plus 4% NaCl diet [41, 66]. In contrast, extending the high salt intake period to 3 weeks, Soncrant et al. confirmed the elevation in blood pressure using telemetric monitoring and were able to demonstrate inhibition of PRA and plasma Ang II in fructose-fed rats [42]. Thus, it appears that PRA which is typically inhibited by either high blood pressure or expanded extracellular volume requires a longer period of exposure to either of these inhibitory influences in the context of high fructose intake. In other words, a much greater expansion of extracellular volume and, therefore a longer period of positive cumulative Na⁺ balance, may be required to inhibit renin secretion with concomitant fructose-feeding.

It is also possible that intrarenal RAS contributes to hypertension and increased Na⁺ reabsorption with fructose feeding. Early studies indicated that renal tissue renin expression was suppressed in fructose-fed mice [39] yet increased in rats fed 20% fructose for 12 weeks [65]. Renal tissue Ang II levels were not statistically different from control glucose-fed rats on high salt diet for 3 weeks despite higher blood pressure [42]. Notably, renal angiotensin AT1 receptor mRNA was increased in adipose tissue but not kidney after three weeks of high fructose ingestion [67]. When fructose was given in greater amounts (60 to 66% in the drinking water) and for longer periods of time (8 to 16 weeks), both Ang I and Ang II as well as AT1 receptor protein expression was increased in kidney tissue [68, 69]. Alternatively, the third influence on renin secretion involves sympathetic inputs to the macula densa. Indeed, switching from standard diet (0.4% NaCl) to high salt (4% NaCl) diet in fructose-fed rats increases renal sympathetic nerve activity by ~ 50% [42]. Denervation of the kidneys bilaterally using cryo-techniques further decreased the already suppressed PRA suggesting sympathetic inputs to the kidney were responsible for the enhanced renin secretion.

Notably, neither the diets nor denervation altered tissue Ang II content compared with controls [42].

In addition to the experimental dietary manipulations, some of the variability in these studies likely stems from methodology used such as the technique for blood pressure assessment (tail cuff vs telemetry), the time when fructose is initiated relative to the high salt diet, the length of exposure to each component of the diet, and the methodology for collection of blood or tissue for measurements of renin, plasma Ang II or their tissue levels. Regardless of the impact of these factors, the findings that a diet enriched for fructose sensitizes the nephron to Ang II such that even minimal activation of the RAS can have profound sodium reabsorption effects.

Fructose influences on the renal sympathetic nervous system

The scientific interest in sympathetic innervation of the kidney has increased recently after the demonstration of marked reductions in blood pressure in individuals with resistant hypertension after denervation using the catheter-based approach [70, 71]. Renal sympathetic nerve activity (RSNA) is significantly increased in many forms of experimental hypertension (reviewed by Osborn and Foss [72]), reinforcing the vital role of RSNA in blood pressure regulation. The mechanisms of increased RSNA in the pathogenesis of hypertension include increased tubular sodium reabsorption and water retention, decreased renal blood flow and glomerular filtration rate, and increased renin secretion from the juxtaglomerular cells which activates the renin-angiotensin system [73]. Since moderately high dietary fructose and salt cause hypertension via similar mechanisms, it has been hypothesized that sympathetic activity increases in this dietary milieu. In fact, ingestion of fructose has been shown to result in changes in secretion of hormones that regulate energy balance [74], a shift

associated with increased sympathetic nervous system activity [75]. The hormone leptin which promotes satiety is released from adipose tissue cells to maintain energy balance by promoting satiety. In contrast, ghrelin opposes this action and promotes hunger. Ingestion of fructose leads to simultaneously increased secretion of ghrelin and decreased secretion of leptin. After chronic ingestion of excess dietary fructose (over 1 to 4 weeks), fasting plasma concentrations of leptin are significantly higher [76]. The mechanistic basis for elevated leptin levels likely stems from fructose-induced fatty acid re-esterification and synthesis of VLDL-triglycerides. This pathway causes a shift towards the fat-storing mode, prompting the adipose cells to respond by elevating leptin production. Simultaneously, augmentation of RSNA occurs initiating the onslaught of hypertension-promoting effects.

Fuctose-induced endothelial dysfunction

The general mechanisms by which the fructose induces increased sodium absorption and retention and how this ultimately leads to increased extracellular volume and hypertension are well defined. The hypertensive states are maintained by two additional overarching pathologies: increased sympathetic activity (regional and systemic) and endothelial dysfunction [77]. As noted, increased sympathetic activity to the kidney causes increased sodium reabsorption as well as blunts inhibition of renin secretion, despite increased plasma sodium levels. Sympathetic activity to the vasculature produces vasoconstriction which, in turn, increases arterial pressure. Chronic fructose feeding has been shown to induce over-activation of the sympathetic nervous system that leads to increased systemic resistance, accompanied by an increase in plasma norepinephrine. Increases in arterial pressure in this study were ameliorated by alpha1-adrenoreceptor blockade [78]. Much of this sympathetic drive is postulated to originate from increased

plasma insulin levels, which in turn exacerbate insulin resistance and a positive feed-back loop that promotes further sympathetic drive [32].

While increases in arterial pressure are occurring via sympathetic, humoral, and volume-dependent mechanisms, additional factors are simultaneously inducing further endothelial dysfunction that may lead to permanent vascular remodeling. Fructose-induced hyperinsulinemia leads to disruptions of endothelial systems such as lowered activity and expression of endothelial nitric oxide synthase (eNOS) and endothelin-1 (ET-1); both of which alter vascular tone and increase vasoconstriction [36, 79, 80]. Thromboxane A2 and angiotensin II (Ang. II) are also potent vasoconstrictors whose upregulation have been observed in fructose studies and have been linked, at least in part, to increased ET-1 expression [81-83]. Each of these vasoactive proteins - ET-1, Ang. II, and thromboxane A2 - can act independently or in concert to degrade endothelial membrane proteins by way of matrix metalloproteinase up-regulation. It has been proposed that this pathway of endothelial dysfunction ultimately leads to further degradation of eNOS and therefore increased arterial pressure. This situation is true in the context of hyperinsulinemia and has also been shown in instances of high dietary fructose consumption, where matrix metalloproteinases isoform 2 upregulation reduces nitric oxide (NO) levels. [84].

EXPERIMENTAL PURPOSE AND DESIGN

In vitro and *in vivo* research has provided us with extensive knowledge regarding the pathologies of fructose-induced hypertension. However, much of this research has been conducted using irrelevantly high quantities of fructose that without question implicate influential pathologic mechanisms such as hyperinsulinemia and hyperglycemia. The benefits of using a model with lower levels of fructose to induce states of salt-sensitivity are

not only particularly relevant to modern consumption trends, but also promote an avenue of study in which the multifactorial nature of hypertension can be further elucidated without confounding factors such as insulin resistance. The purpose of this research was to utilize a model of hypertension such as this to elucidate not only the mechanisms by which it occurs, but also to determine the extent by which such mechanisms induce end-organ damage. The studies detailed in the following chapters were designed to investigate the end-organ consequences of fructose-induced salt-sensitive hypertension in both acute and chronic settings.

CHAPTER 2: AORTIC STIFFNESS AND DIASTOLIC DYSFUNCTION IN SPRAGUE DAWLEY RATS CONSUMING SHORT-TERM FRUCTOSE PLUS HIGH SALT DIET

(This Chapter contains previously published material. See Appendix C.)

INTRODUCTION

Hypertension prevalence is currently estimated at 46% among adults in the United States and remains one of the top healthcare and societal burdens [85]. Chronic increases in arterial pressure contribute to the development of comorbidities and major adverse cardiac events (MACE) such as stroke, myocardial infarction, heart failure, and renal disease [86]. Despite the urgent need to implement strategies for incidence reduction, the etiologies underlying the majority of hypertensive states still remain unknown. In addition to genomic factors, environmental factors including suboptimal dietary habits also contribute to the development of hypertension. Consumption of fructose has been on the rise due to increasing use of high fructose corn syrup since the 1970's for sweetening beverages and pre-packaged foods [13]. A recent meta-analysis found that individuals consuming sugar-sweetened beverages in the highest versus lowest quantile displayed a greater risk for hypertension [19]. The association between fructose ingestion and hypertension is potentiated by increased salt intake [87]. Indeed, a typical Western diet is enriched in both fructose and salt.

Previous work in the fructose-induced salt sensitive hypertension rat model showed increased reactive oxygen species (ROS) production, diminished nitric oxide bioavailability and cumulative positive sodium balance [41, 88]. Activation of the renin-angiotensin-aldosterone system (RAS) and increased renal sympathetic nerve activity, both of which promote increased renal tubular sodium reabsorption, have also been implicated as mechanisms resulting in elevated arterial pressure [41, 42, 62, 66, 89]. Notably, bilateral

renal cryo-denervation [42] or daily treatment with the superoxide dismutase mimetic, 4-hydroxy-2,2,6,6-tetramethylpiperidine-1-oxyl (+T; Tempol), reduces 8-isoprostane excretion and ameliorates the hypertension.[66] In light of these findings, it is possible that combined fructose and high salt diet may exert a deleterious impact cardiac and vascular function either directly or indirectly via the elevated arterial pressure. If so, then it would be important to evaluate whether 4-hydroxy-2,2,6,6-tetramethylpiperidine-1-oxyl also ameliorates cardiovascular function in this model.

Data from the Framingham population highlight that aortic stiffening precedes hypertension.[90, 91] The force of ejected blood during cardiac systole exerts pressure on the aortic wall that makes the normal aorta expand and then recoil back during cardiac diastole. This property of healthy aorta is known as the Windkessel function, or capacitance, and functionally is responsible for reduction of systolic blood pressure and maintenance of peripheral perfusion during diastole. As the aorta stiffens such as occurs physiologically in aging and pathophysiologically in diabetes, obesity and hypertension, it loses the Windkessel function which is reflected in increases in pulse wave velocity (PWV) [92, 93]. Accordingly, aortic PWV is one of the most reliable predictors of cardiovascular mortality as demonstrated by two major meta-analyses [94, 95]. Elastic properties of major vessels can also be assessed with strain imaging as demonstrated by a recent study describing reductions in common carotid artery strain as a valuable tool for detection of atherosclerotic disease.[96] Likewise, a decrease in ascending aortic strain is an independent predictor of significant coronary artery disease in patients with coronary artery stenosis $\geq 70\%$ [97].

Given the interdependence of systemic and renal hemodynamics, it is tempting to speculate that aortic stiffening is expected to have deleterious consequences on the renal

vasculature. Renal resistive index (RRI) measured with intrarenal Doppler ultrasound is influenced by complex interactions between vascular wall properties and systemic factors and can be used to identify vascular dysfunction [98]. Higher RRI is associated with increased PWV [99] and leads to microvascular damage over time [100]. The effects of fructose-induced salt-sensitive hypertension on the elastic properties of conduit and resistance vessels are presently undefined. Even in the absence of hypertension, salt-sensitivity in humans constitutes a cardiovascular risk factor [101, 102]. It is unknown whether fructose predisposes to salt-sensitive hypertension by reduced aortic compliance, increased PWV and consequential perturbations in renal hemodynamics via the ROS system. However, such a process could link fructose and high salt ingestion with hypertension and may explain how fructose induced salt sensitive hypertension leads to systemic and renal hemodynamic derangements.

In the present investigation, we employed the fructose-induced salt sensitive hypertension rat model by feeding rats 20% (w/v) fructose for one week, followed by the addition of 4% NaCl for three more weeks, which results in increases in mean arterial pressure[42]. We hypothesized that dietary fructose, rather than glucose, in combination with high salt will lead to aortic stiffening, evidenced by increased aortic PWV, decreased strain, and decreased distensibility coefficient. This will, in turn, result in an increase in RRI. We hypothesize that daily supplementation with the antioxidant, 4-hydroxy-2,2,6,6-tetramethylpiperidine-1-oxyl, will ameliorate the increase in mean arterial pressure, and thereby mitigate vascular stiffening. These studies are aimed at identifying the diverse mechanisms that diminish aortic compliance, impair renal vascular function, and contribute to hypertension.

MATERIALS AND METHODS

Animals

Male Sprague-Dawley rats (Harlan Sprague Dawley, Indianapolis, IN) were housed under controlled conditions (21–23°C; 12 hr light and 12 hr dark cycles, light on at 7 am) and were permitted ad libitum access to water and standard rat chow containing 0.4% NaCl until they were enrolled into experimental protocols described below. Complete care provided to rats was in accordance with the principles of the National Institutes of Health Guide for the Care and Use of Laboratory Animals. All procedures and protocols were approved by the Wayne State University Institutional Animal Care and Use Committee (Protocol #19-01-1001).

Dietary regimen

Upon arrival of animals to the DLAR facilities, all rats were provided ad libitum access to 0.4% NaCl standard chow (Envigo Teklad, Madison, WI) and normal water. Three to five days later, hemodynamic telemetry devices were implanted, and rats allowed to recover for three-four days in single housing. Following previously established protocols, 6,9,10 the rats were randomized to either 20% (w/v) glucose (Sigma-Aldrich, St. Louis, MO) or 20% (w/v) fructose (Sigma-Aldrich, St. Louis, MO) and maintained 0.4% NaCl chow. The age of rats at enrollment was 10-12 weeks and the average weight was 228.6 ± 5.9 g in the control group and 225 ± 2.5 g in the Tempol group. Glucose was provided in the control groups to match both caloric and fluid intake. The consumption of glucose and fructose was similar throughout the protocol (~65 kcal per day as carbohydrate). After one week, the rats were randomly assigned to one of eight groups: 1) glucose and normal (0.4%) salt (Glu+NS), 2), glucose and high (4.0%) salt (Glu+HS), 3) fructose and normal salt (Fru+NS), 4) fructose and

high salt (Fru+HS), 5) Glu+NS with the addition of 4-hydroxy-2,2,6,6-tetramethyl-piperidine-1-oxyl (+T) (Glu+NS+T), 6) Glu+HS+T, 7) Fru-NS+T or 8) Fru+HS+T).

To assure that each rat in the groups receiving +T (Santa Cruz, Santa Cruz, CA) received the full dose, 35 ml of the respective drinking mixture was supplemented with +T, 15 mg/400 g body weight. After the rat completed drinking the allotted antioxidant solution, a fresh water bottle with the respective glucose or fructose supplement alone was provided. This approach allowed verification that each rat received its full dose of anti-oxidant and that fructose or glucose ingestion across all groups was similar. The respective dietary regimens were continued for three weeks with monitoring of hemodynamic parameters via telemetry.

Surgical procedures

Hemodynamic telemetry transmitter placement. All rats were instrumented with hemodynamic telemeters at ten weeks of age (~225 g body weight) under ketamine (80 mg/kg) and xylazine (10 mg/ml) anesthesia. An incision was made in the groin and a hemodynamic telemetry transmitter (TA11PA-C40, Data Sciences International) implanted by exposing the right femoral artery, temporarily occluding the proximal end, and inserting the gel-filled catheter attached to the transmitter device into the artery with a 21-gauge needle. The catheter was advanced into the abdominal aorta and the transmitter tunneled subcutaneously. The incision was closed using surgical staples. Post-operative analgesia was provided with buprenorphine SR (0.3 mg/kg subcutaneously).

Vascular catheter placement. At the end of the fourth week (1 week glucose/fructose + 3 weeks \pm Tempol®), the rats were instrumented with carotid arterial catheters for hemodynamic monitoring during ultrasonography and for collection of aortic blood at the conclusion of experiments.

Telemetry, echocardiography and renal Doppler studies

Data acquisition of hemodynamic parameters was performed using Dataquest ART software (Data Sciences International, Saint Paul, MN). Measurements of heart rate, systolic (SBP), diastolic (DBP), and mean arterial pressures (MAP) as well as the derived pulse pressure (PP) were sampled for 10 sec at a sampling rate of 500 samples/sec every 1 hr for the remainder of the 3-week protocol. The average of hemodynamic recordings initiated during the last three days of the week during which the rats were on glucose or fructose and 0.4% NaCl were taken as baseline. Once assigned to one of the eight groups (see above), hemodynamic measurements over the next three weeks were taken for 24 hr beginning at 7 am (lights on) during Mondays and Thursdays in order to avoid cage cleaning days and disruptions (e.g., weekend changes in veterinary staff) that could impact the parameters as well as conserve transmitter battery time. Values are the 24-hr average for a given day.

Two days after placement of vascular catheters, echocardiography and renal Doppler scans were completed by an investigator blinded to the group assignments. Blood pressure and heart rate were monitored continuously with PowerLab (ADInstruments, Colorado Springs, CO) connected to the LabChart 8.0 software.

Rats were anesthetized with 3% isoflurane in an induction chamber, and maintenance of anesthesia was achieved with 1.5% isoflurane delivered via a nose cone. Scans were performed on the heated platform (Fujifilm Visualsonics, Inc., Toronto, Canada) in a supine position with all four limbs secured to ECG electrodes with tape. Fur was removed from the chest and abdominal areas first by shaving the area followed by a cream depilatory (Pharmaceutical Innovations, Newark, NJ), before applying contact gel preheated to 37°C. Body temperature was monitored using a rectal probe. Echocardiographic recordings were

made according to standard methods[103, 104] at the conclusion of the three-week dietary intervention. Images were acquired using a Vevo3100 with an MX-250S transducer (Fujifilm Visualsonics Inc.). A parasternal short axis view was used to obtain images in M-mode at the level of papillary muscles to assess systolic function and left ventricular dimensions. Left ventricular diastolic function was ascertained using pulse wave Doppler recordings of transmitral flow velocities aligned in the apical four chamber view. Aortic PWV was determined using B-mode and pulse wave Doppler of aortic flow velocities at two positions along the aortic arch [105]. Briefly, the time to initiation of flow was determined relative to the ECG and the difference calculated. The distance between the two flow positions, determined along the B-mode image, was then divided by the time to calculate the PWV.

The renal resistive index (RRI) was ascertained using pulse wave Doppler imaging of flow through the left main renal artery. The RRI was calculated as the difference between the peak systolic and minimum diastolic velocity, divided by the peak systolic velocity [98]. Aortic distensibility and strain were derived from the B-mode images. Some measurements were not able to be technically ascertained in each animal due to anatomical constraints. Data analysis was completed offline in blinded fashion using VevoLab and VevoVasc software (Fujifilm Visualsonics, Inc.).

After all scans were completed, the rats were permitted to recover from isoflurane anesthesia and allowed to regain normal activities for ~4-6 hr. Arterial blood was then collected in the conscious animals using the carotid catheter for hormone analyses. Blood (1 ml) was taken over 90-sec period into pre-chilled tubes containing 50 μ l sodium ethylenediaminetetraacetic acid (EDTA) for PRA. Another 1.5 ml of blood was taken into a separate pre-chilled tube with 120 μ l of 500 mM sodium EDTA, 125 mM phenanthroline, 1

mM phenylmethanesulfonyl fluoride, 20 mM pepstatin, 1 mM enalapril and 10X phosphatase inhibitor cocktail for Ang II. The blood was immediately centrifuged at 3000 rpm at 4°C, and the plasma stored at -70°C until assay.

The rats were then euthanized with pentobarbital (100mg/kg) and hearts and kidneys harvested and weighed while keeping them cold in saline. The renal cortex was then rapidly and sharply dissected, and the tissue frozen at -70°C until analyzed for tissue Ang II.

Hormone assays

All tests were performed on blood samples obtained simultaneously between 1 pm and 4 pm. Non-fasting blood glucose concentrations were measured with One Touch Ultra 2 (Lifescan, Switzerland). Plasma renin activity (PRA) (IBL International, Hamburg, Germany) and insulin (Cayman, Ann Arbor, MI) were measured by enzyme-linked immunosorbant assays according to the product directions. Plasma and tissue angiotensin II (Ang II) concentrations were assessed by radioimmunoassay as previously described by our laboratory [106].

Analyses and statistics

Heart rate and arterial pressures were collected using Dataquest ART software (Data Sciences Intl, St. Paul, MN) and averaged over a 24 hr period. All analyses were performed by a researcher blinded to the group assignments. Results are presented as mean \pm SE. Comparisons among groups were completed with one-way ANOVA; comparisons among groups over time were accomplished using two- factor ANOVA. A repeated measures design requires that every participant participates in every condition of the experiment, historically called a within-subjects design. Our data was unbalanced, that is, there were slightly different but unequal sample sizes across each group since some procedures were not able

to be performed in each animal due to technical reasons (e.g., catheter malfunction). The repeated measures design drops sample sizes in the analysis until the same, or equal, numbers are in each group across all time points. Ideally the repeated measures design (with time point) would be preferred. However, this selection of analysis would drop the already small sample size until the numbers were equal across all time points and in each group observed – until they all have the same sample size. The two-factor approach (group and time point) allows us to keep all the data available and conduct mean comparisons, using a Sidak *post hoc* test for multiple pair-wise comparisons. Homogeneity of variance was checked and verified using Leven's test. Comparisons of ultrasound parameters between Fru+HS and Fru+HS+T groups were done using Student's unpaired t-test. Differences were deemed statistically significant when the P-value was less than 0.05.

RESULTS

Baseline body weight and heart weight of fructose-fed and glucose-fed rats with and without antioxidant supplementation were similar. Kidney weights were significantly greater in control fructose-fed rats on either normal or high salt diets. In +T-treated rats, mean kidney weights were also higher but the differences were only significant for the left kidneys since right kidney weights displayed greater variability (Table 1).

Baseline SBP, DBP, MAP and heart rate were similar across all groups (Table 2.2). Baseline PP appeared to be greater in the Fru+HS group but this did not achieve significance ($P = 0.16$). SBP and MAP increased significantly after three weeks of high salt diet in fructose-fed but not glucose-fed animals; supplementation with antioxidant prevented this increase (Figure 2.1). After three weeks, the change in DBP, PP and heart rate did not differ among

Table 2.1: Rat, Kidney and Heart Weights for All Rat Groups.

	N	Initial Rat Body Weight (g)	Final Rat Body Weight (g)	Kidney Weight (g/kg BW)		Heart Weight (g/kg BW)
Control						
Glu+NS	8	230 ± 8	327 ± 7	2.9 ± 0.1	2.9 ± 0.2	3.8 ± 0.8
Glu+HS	12	224 ± 5	329 ± 8	2.9 ± 0.1	2.9 ± 0.3	3.9 ± 0.5
Fru+NS	8	227 ± 7	330 ± 13	3.1 ± 0.1*	3.2 ± 0.3*	4.1 ± 0.7
Fru+HS	10	226 ± 5	313 ± 5	3.2 ± 0.1*	3.1 ± 0.3*	3.9 ± 0.4
Tempol						
Glu+NS+T	10	222 ± 5	332 ± 10	2.9 ± 0.1	2.9 ± 0.2	3.7 ± 0.4
Glu+HS+T	12	228 ± 8	329 ± 5	2.8 ± 0.1	2.9 ± 0.3	3.9 ± 0.4
Fru+NS+T	9	224 ± 6	329 ± 9	3.2 ± 0.1†	3.2 ± 0.2	3.7 ± 0.4
Fru+HS+T	9	222 ± 5	337 ± 14	3.1 ± 0.1†	3.1 ± 0.4	3.7 ± 0.4

Glu+NS, 20% glucose+0.4% NaCl; Glu+HS, 20% glucose+4% NaCl; Fru+NS, 20% fructose+0.4% NaCl; Fru+HS, 20% fructose+4% NaCl; +T, indicates addition of 15 mg/400g BW Tempol®; BW, body weight. Values are mean ± SE. * $P < 0.05$ vs corresponding glucose-fed group. † $P < 0.05$ vs corresponding glucose-fed plus Tempol® group.

Table 2.2: Baseline Hemodynamics and Changes after 3-Week Diet Regimen

Diet	N	Baseline MAP (mmHg)	ΔMAP (mmHg)	Baseline SBP (mmHg)	ΔSBP (mmHg)	Baseline DBP (mmHg)	ΔDBP (mmHg)	Baseline PP (mmHg)	ΔPP (mmHg)	Baseline Heart Rate (bpm)	ΔHR (bpm)
Control											
Glu+NS	8	107 ± 3	0.2 ± 1.5	123 ± 4	0.3 ± 1.7	93 ± 5	4.7 ± 1.5	29 ± 3	1.6 ± 2.2	411 ± 20	-28 ± 20
Glu+HS	12	106 ± 2	1.5 ± 1.0	122 ± 2	1.9 ± 1.2	93 ± 3	5.6 ± 2.8	30 ± 2	-1.6 ± 1.6	437 ± 27	-30 ± 20
Fru+NS	8	107 ± 3	-0.9 ± 1.8	124 ± 4	-1.3 ± 2.5	93 ± 4	5.6 ± 2.1	31 ± 3	1.2 ± 2.6	408 ± 21	-26 ± 26
Fru+HS	10	107 ± 2	5.5 ± 0.8‡	126 ± 4	5.6 ± 1.5**	91 ± 2	6.7 ± 2.8	37 ± 3	0.9 ± 1.7	409 ± 19	-16 ± 20
Tempol											
Glu+NS+T	10	104 ± 2	1.2 ± 1.1	121 ± 4	-0.4 ± 2.0	93 ± 3	4.9 ± 1.8	28 ± 3	-0.3 ± 2.0	431 ± 24	-25 ± 11
Glu+HS+T	12	107 ± 2	1.1 ± 1.1	121 ± 4	2.7 ± 1.2	87 ± 3	5.1 ± 3.5	34 ± 3	-0.8 ± 1.2	421 ± 22	-26 ± 20
Fru+NS+T	9	108 ± 3	1.2 ± 0.8	128 ± 4	0.3 ± 1.1	98 ± 6	6.1 ± 3.0	29 ± 4	-0.6 ± 0.7	422 ± 15	-31 ± 13
Fru+HS+T	9	110 ± 2	0.8 ± 0.8†	129 ± 3	1.9 ± 0.7†	91 ± 1	5.3 ± 3.3	39 ± 3	0.9 ± 1.5	422 ± 13	-23 ± 16

Group definitions as in Table 1. Values are mean ± SE. * $P < 0.05$ vs Glu-NS; ‡ $P < 0.05$ vs Fru-NS; † $P < 0.05$ vs Fru-HS.

the groups. For clarity, Figure 2.2 depicts the progression of MAP over time only for fructose-fed rats. By day 10, MAP rose significantly compared with baseline in Fru+HS rats and remained elevated from Day 17 through the 24th day. MAP progressively declined from Day 7 to Day 24 in the Fru+HS+T group such that there was no difference in MAP among Fru+NS, Fru+NS+T and Fru+HS+T groups by day 24; however, MAP of the Fru+HS group was significantly greater than any of the other three groups. SBP followed the same pattern as MAP. Glucose-fed rats in any of the groups did not display significant changes from baseline

or among the groups in MAP at any point of time (data not shown).

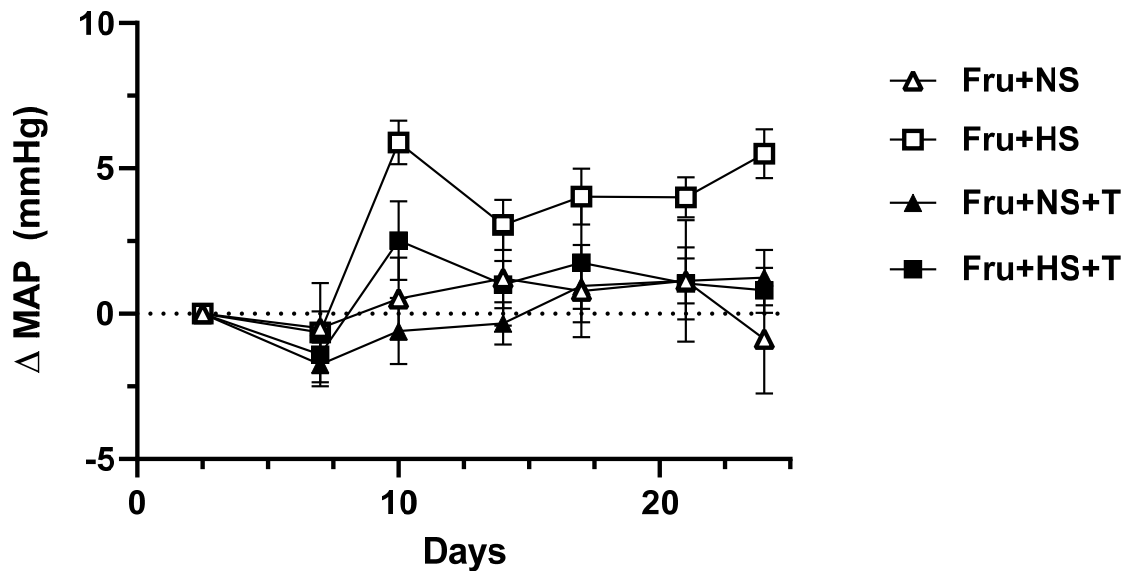


Figure 2.1: Change in mean arterial pressure (MAP) Timeline (over the 3-week period for the fructose-fed groups). Baseline MAP and delta MAP for glucose-fed groups did not change significantly over time (Table 2); not depicted graphically for simplicity. Fru+NS, 20% fructose+0.4% NaCl; Fru+HS, 20% fructose+4% NaCl; +T, indicates addition of 15 mg/400g BW Tempol; BW, body weight. * Values are mean \pm SE; n as in Table 2. * $P < 0.05$ vs baseline for Fru+HS; † $P < 0.05$ for Fru+HS vs all other fructose-fed groups by two-way ANOVA on Day 24.

Cardiovascular parameters measured by echocardiography

The increase in MAP in the Fru+HS group was accompanied by an increase in aortic pulse wave velocity (PWV) (803 ± 19 mm/s, $P < 0.005$) compared with Glu+NS (606 ± 48 mm/s), Glu+HS (645 ± 39 mm/s) or Fru+NS (700 ± 27 mm/s) groups (Figure 2.2A). Attenuation of free radical formation decreased aortic PWV in Fru+HS+T rats (686 ± 31 mm/s, $P < 0.005$) compared to their non-treated counterparts (Figure 2B), while it produced no change in PWV in other groups (Glu+NS: 681 ± 30 mm/s, Glu+HS+T: 630 ± 37 mm/s and Fru+NS+T: 684 ± 43 mm/s).

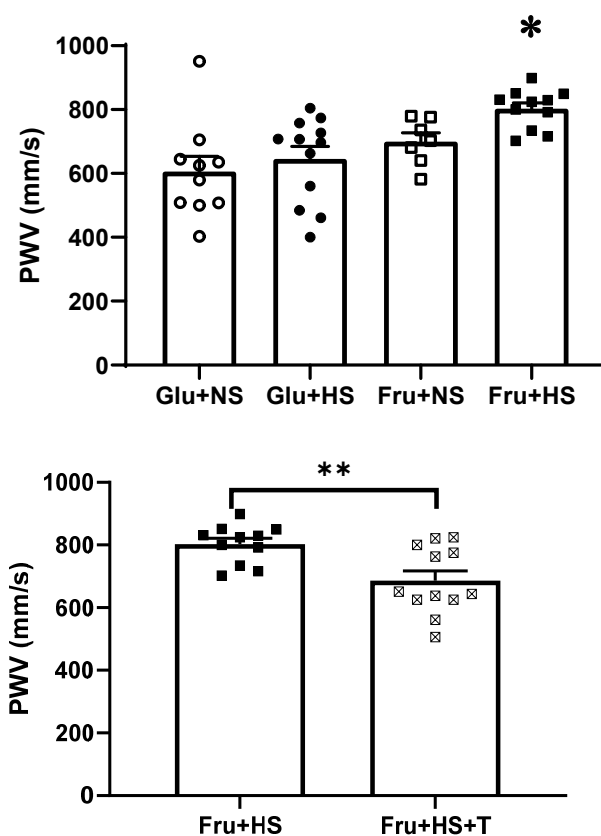


Figure 2.2: Aortic Pulse Wave Velocity (PWV) in (A) the four groups of rats: Glu+NS, 20% glucose+0.4% NaCl; Glu+HS, 20% glucose+4% NaCl; Fru+NS, 20% fructose+0.4% NaCl; Fru+HS, 20% fructose+4% NaCl. (B) Aortic pulse wave velocity in rats given either Fru+HS alone or with addition of 15 mg/400g BW Tempol (+T); BW, body weight, Fru+HS+T. Values are mean \pm SE; n as indicated per group; * $P < 0.005$ vs other three groups; ** $P < 0.005$ vs Fru+HS group.

Echocardiographic measures of systolic cardiac function revealed no overt phenotype in rats fed fructose and high salt diet. Ejection fraction, fractional shortening, left ventricle (LV) dimensions, and LV mass were similar across all groups (Table 2.3). Notably, only the Fru+HS rats displayed evidence of diastolic dysfunction (Figure 2.3). Specifically, the ratio of early (E) to late (A) transmitral filling velocities was decreased in Fru+HS rats (1.12 ± 0.03 , $P < 0.005$) compared with the rats on glucose (Glu+NS: 1.28 ± 0.04 and Glu+HS: 1.37 ± 0.05) or Fru+NS rats (1.37 ± 0.08). Supplementation with the antioxidant did not change E/A in Fru+HS rats (1.09 ± 0.07) nor in any of the other groups: Glu+NS+T (1.38 ± 0.07), Glu+HS+T

(1.25 ± 0.06) and Fru+NS+T (1.28 ± 0.04).

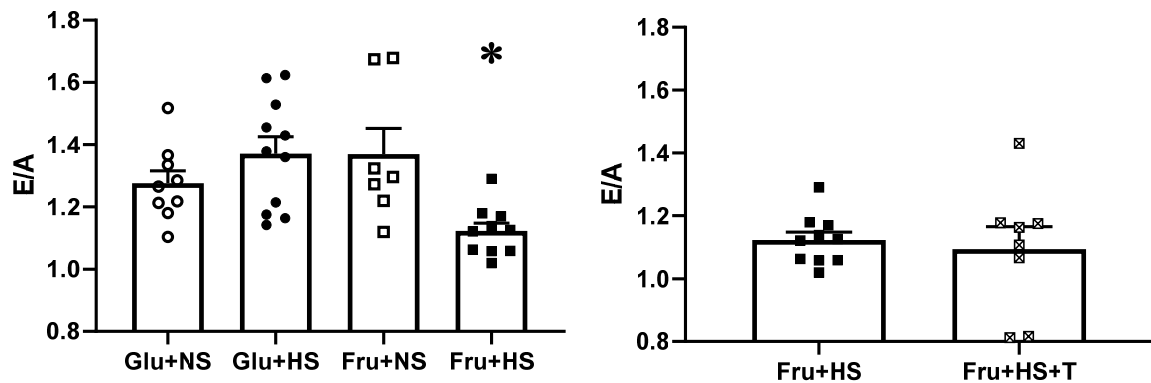


Figure 2.3: Ratio of Early to Late (E/A) Transmittal Filling Velocities. In (A) the four groups of rats and (B) rats fed fructose-high salt alone or with Tempol (+T). Group designations as in Figure 2. Values are mean \pm SE; n as indicated per group; * $P < 0.005$ vs other three groups.

The RRI, a measure of renal vascular stiffness or impedance, was significantly augmented in the Fru+HS group (0.60 ± 0.03 , $P < 0.05$), compared with Glu+NS (0.45 ± 0.03), Glu+HS (0.45 ± 0.04) or Fru+NS groups (0.47 ± 0.05) (Figure 5A). No differences were observed among the +T-treated groups (Glu+NS+T, 0.50 ± 0.04 ; Glu+HS+T, 0.53 ± 0.4 ; Fru+NS+T, 0.50 ± 0.02 ; and Fru+HS+T, 0.60 ± 0.05). Notably, the antioxidant failed to reverse the augmented RRI in rats fed fructose and high salt diet (Figure 2.5B).

Table 2.3: Echocardiographic Parameters in Control Groups.

	Glu+NS	Glu+HS	Fru+NS	Fru+HS
N	8	12	7	11
LVEF (%)	82 ± 3	78 ± 3	85 ± 2	75 ± 3
LVFS (%)	52 ± 3	48 ± 3	56 ± 3	47 ± 3
LVAWs (mm)	3.11 ± 0.15	2.92 ± 0.12	3.31 ± 0.10	2.82 ± 0.09
LVAWd (mm)	1.95 ± 0.06	1.98 ± 0.05	2.09 ± 0.09	1.85 ± 0.04
LVIDs (mm)	3.07 ± 0.32	3.22 ± 0.22	2.72 ± 0.32	2.58 ± 0.21
LVIDd (mm)	6.34 ± 0.19	6.34 ± 0.17	6.34 ± 0.27	6.58 ± 0.19
LVPWs (mm)	2.94 ± 0.18	3.17 ± 0.16	2.92 ± 0.15	2.81 ± 0.19
LVPWd (mm)	1.84 ± 0.09	1.96 ± 0.13	1.64 ± 0.14	1.84 ± 0.22
LV mass (mg)	645 ± 39	688 ± 38	663 ± 64	631 ± 33

Group definitions as in Table 1. LVEF, left ventricular ejection fraction; LVFS, left ventricular fractional shortening; HR, heart rate; LVAWs, left ventricular end-systolic wall thickness; LVAWd, left ventricular end-diastolic anterior all thickness; LVIDs, left ventricular end-systolic inner diameter; LVIDd, left ventricular end-diastolic inner diameter; LVPWs, end-systolic left ventricular posterior wall thickness; LVPWd, end-diastolic left ventricular posterior wall thickness. Values are mean \pm SE.

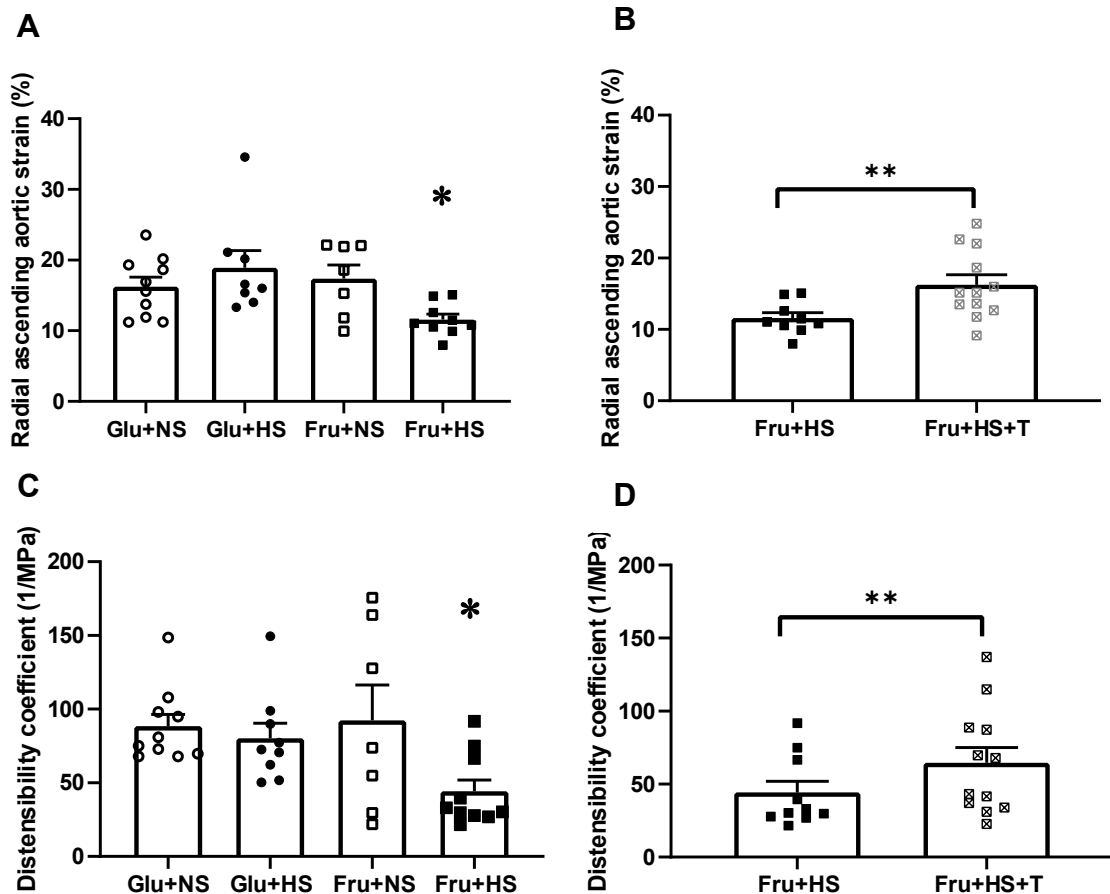


Figure 2.4: Elastic Properties of the Ascending Aorta. Radial ascending aortic strain and distensibility coefficient, respectively, in the four groups of rats (A, C) and in rats fed fructose-high salt alone or with Tempol (B, D). Group designations as in Figure 2. Values are mean \pm SE; n as indicated per group; * $P < 0.05$ vs other control groups; ** $P < 0.05$ vs Fru+HS group.

The RRI, a measure of renal vascular stiffness or impedance, was significantly augmented in the Fru+HS group (0.60 ± 0.03 , $P < 0.05$), compared with Glu+NS (0.45 ± 0.03), Glu+HS (0.45 ± 0.04) or Fru+NS groups (0.47 ± 0.05) (Figure 2.5A). No differences were observed among the +T-treated groups (Glu+NS+T, 0.50 ± 0.04 ; Glu+HS+T, 0.53 ± 0.04 ; Fru+NS+T, 0.50 ± 0.02 ; and Fru+HS+T, 0.60 ± 0.05). Notably, the antioxidant failed to reverse the augmented RRI in rats fed fructose and high salt diet (Figure 2.5B).

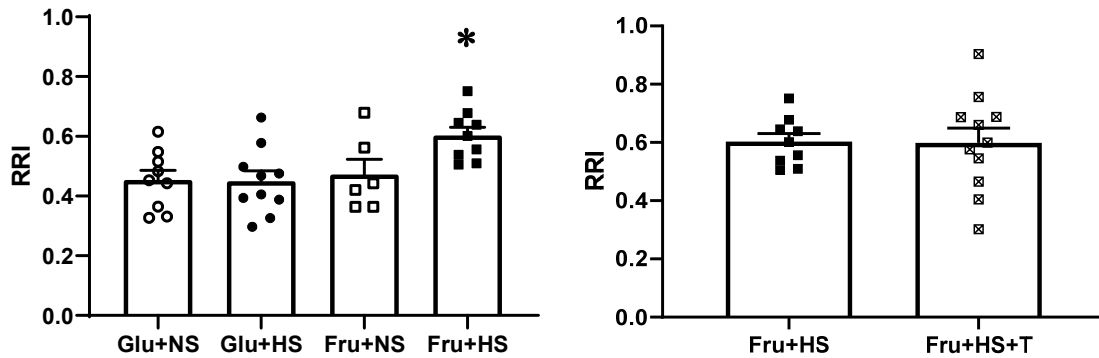


Figure 2.5: Renal Resistive Index (RRI). in (A) the four groups of rats and (B) rats fed fructose-high salt alone or with Tempol (+T). Group designations as in Figure 2. Values are mean \pm SE; n as indicated per group; * $P < 0.05$ vs other control groups; ** $P < 0.05$ vs Fru+HS group.

PRA, angiotensin II and insulin levels

High salt diet did not suppress PRA in either glucose-fed or fructose-fed rats (Table 2.4). In contrast, plasma Ang II was significantly lower in both Glu+HS and Fru+HS rats compared with rats fed the same sugar on normal salt diet. Plasma Ang II was attenuated in both Glu+NS+T and Fru+NS+T groups such that there were no differences among any of the +T-treated groups. Although kidney cortical tissue Ang II tended to be higher in the +T-treated normal salt groups vs the +T-treated high salt groups ingesting the same sugar, renal cortical tissue Ang II levels did not significantly differ among any of the groups. Non-fasting blood glucose values were similar among the groups (Table 2.4). Figure 2.6 shows that the glucose:insulin ratio was significantly diminished in the Fru+HS group ($P < 0.05$), indicative of insulin resistance compared with the other groups. The glucose:insulin ratio was restored in the Fru+HS+T group to a value significantly greater than the Fru+HS group ($P < 0.05$).

Table 2.4: Values for Plasma Glucose, PRA and Ang II and Renal Cortical Tissue Ang II after 3-Week Diet Regimen.

Diet	N	Glucose (mg/dL)	PRA (ng AngI per ml/hr)	Plasma Ang II (fmol/ml)	Kidney Tissue Ang II (fmol/g)
Glu+NS	8	132 ± 2	4.7 ± 1.5	34.2 ± 4.6	1,609 ± 222
Glu+HS	12	134 ± 7	5.6 ± 2.8	16.5 ± 4.2*	1,829 ± 269
Fru+NS	8	130 ± 5	5.6 ± 2.1	38.5 ± 5.8	1,667 ± 280
Fru+HS	10	137 ± 8	6.7 ± 2.8	22.2 ± 4.6‡	1,403 ± 223
Glu+NS+T	10	138 ± 6	4.9 ± 1.8	16.0 ± 2.3*	2,306 ± 396
Glu+HS+T	12	130 ± 4	5.1 ± 3.5	18.7 ± 4.3	1,376 ± 168
Fru+NS+T	9	142 ± 7	6.1 ± 3.0	25.4 ± 5.1	2,067 ± 241
Fru+HS+T	9	132 ± 3	5.3 ± 3.3	19.4 ± 3.5	1,509 ± 290

Group definitions as in Table 1. PRA, plasma renin activity; Ang II, angiotensin II. Values are mean ± SE. * $P < 0.05$ vs Glu-NS; ‡ $P < 0.05$ vs Fru-NS.

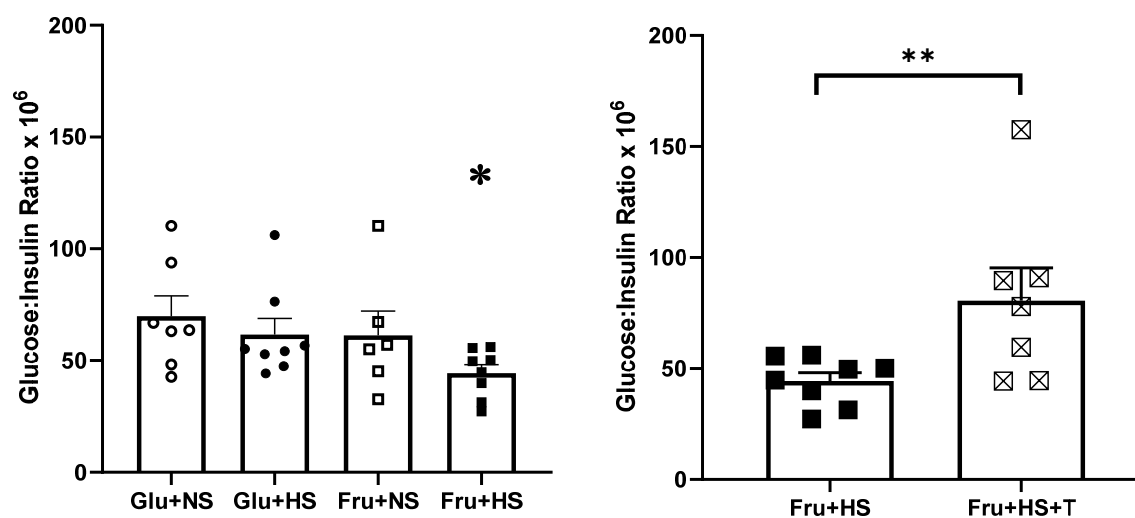


Figure 2.6: Glucose:insulin Ratio (nM/nM x 10⁶) in (A) the four groups of rats and (B) rats fed fructose-high salt alone or with Tempol (+T). Group designations as in Figure 2. Values are mean ± SE; n as indicated per group; * $P < 0.05$ vs other control groups; ** $P < 0.05$ vs Fru+HS group.

DISCUSSION

The major findings of the present investigation support the hypothesis that fructose and high salt feeding for as short a period as three weeks in rats results in salt sensitive

systolic hypertension, stiffening of the ascending aorta, and diastolic left ventricular dysfunction. This occurs at a time when the rats have insulin resistance but are not frankly diabetic. Free radical scavenging at least partially reverses the aortic stiffening but not the diastolic dysfunction. The vascular perturbations associated with combined fructose and high salt intake include increased ascending aortic PWV, decreased radial ascending aortic strain, and an impaired distensibility coefficient. The decreased E/A ratio denotes early diastolic left ventricular dysfunction. In addition, the increase in RRI in fructose-fed, high salt rats indicate impaired vascular compliance of the main renal artery that is not ameliorated by 4-hydroxy-2,2,6,6-tetramethylpiperidine-1-oxyl, suggesting a mechanistic basis other than oxidative stress. Interestingly, although PRA is not suppressed, the vasoactive hormone plasma Ang II is reduced after three weeks of high salt diet in both glucose- and fructose-fed animals. Intrarenal Ang II does not appear to be affected by either diet or antioxidant treatment.

Fructose, salt and blood pressure

The present studies confirm previous findings from our own [42] and other laboratories [41, 62, 66] showing that consumption of fructose at levels comparable to that ingested by the upper 20th percentile of the human population combined with high salt intake results in elevated arterial pressure. Although the increase in arterial pressure is modest when assessed in conscious unstressed rats by telemetry (vs tail cuff where there is the additional stress component of mild restraint), it is nonetheless reproducible, significant, and sustained. Moreover, the present data indicate that the elevation in arterial pressure is primarily due to a disproportionate rise in systolic pressure which may be more closely related to large artery stiffness (see below). The combination of high fructose and

high salt intake has the potential to alter arterial wall cell function and structure independent of blood pressure [107, 108]. Hypertension, in turn, can influence vascular stiffness via cellular and structural responses to mechanical pressure-induced wall stress [109]. Regardless of whether systolic hypertension is a cause or effect of arterial stiffness [109], the result is a complex interplay of factors that are influenced by consumption of fructose and high salt diet.

The observation that 4% NaCl diet does not suppress PRA in either glucose-fed or fructose-fed animals is distinctly different than the classic suppression of PRA by high salt diets in rats provided with normal carbohydrate diets [41, 110, 111]. Notably, earlier reports used higher salt diets (e.g., $\geq 8\%$ NaCl) that do not reflect typical human intake to inhibit PRA and did not report plasma Ang II levels [112, 113]. Although high salt diet when ingested with fructose suppresses plasma Ang II but not renal tissue Ang II. The persistence of high intrarenal Ang II, which has been shown to increase proximal tubular sodium reabsorption [62, 114]. may very well be responsible for cumulative positive sodium balance and hypertension observed in this model [41]. Furthermore, dietary fructose augments Ang II-stimulated superoxide formation by the kidney further enhancing proximal tubular sodium reabsorption and leading to volume-mediated hypertension [62, 111, 114]. Since antioxidant with +T treatment does not influence either plasma or intrarenal Ang II levels, it is more likely that its ability to decrease hypertension relates, at least in part, to its ability to decrease oxidative stress directly on the vasculature. More definitive data measuring vascular ROS and its products, which were beyond the scope of the present study, will be required to address this issue directly.

Left ventricular diastolic dysfunction

The axial heterogeneity of the aorta is well documented [115, 116]. For example, the ratio of elastic fibers to collagen changes from 3.1:1 in the ascending aorta to 2.8:1 in the thoracic aorta to 0.8:1 in the abdominal aorta [117]. Attenuation of the elastic properties of the proximal ascending aorta can have profound influence on end-systolic cardiac wall stress due to increased afterload, one of the most important factors in developing cardiac hypertrophy,[118] hence our choice to study the ascending aorta. In addition to the geometric properties of the left ventricle itself, aortic stiffness influences end-systolic cardiac wall stress [119]. Although there is no evidence of left ventricular hypertrophy, our echocardiographic studies were performed after only three weeks on the respective diets. Nevertheless, the reduced E/A ratio in the fructose-fed high salt rats reveals diastolic dysfunction which is the earliest indicator of hypertensive cardiac disease and precedes frank hypertrophy or systolic dysfunction [120]. Importantly, the diastolic impairment is significant despite the arterial pressure lowering effect of isoflurane anesthesia during the scan. Furthermore, inhibition of oxidative stress does not ameliorate this diastolic dysfunction despite lower arterial pressure suggesting involvement of alternative mechanisms.

Ingestion of fructose plus high salt even, in the short-term, in the present study results in mildly elevated non-fasting blood glucose and a depressed glucose:insulin ratio consistent with insulin resistance similar to human pre-diabetes. Long-term studies have unequivocally demonstrated the development of left ventricular hypertrophy in metabolic syndrome;[121] however, even prolonged pre-diabetes provides a constellation of physiological derangements that favor left ventricular remodeling in rats [122, 123] and humans [124]. In

fact, fructose alone, albeit at a higher concentration (60%), causes cardiac hypertrophy in mice after 10 weeks [125]. Moreover, direct fructation of structural proteins [107] or alterations in sympathetic cardiac innervation [126] have been associated with diastolic dysfunction. Thus, despite the lack of frank left ventricular hypertrophy, the presence of a pre-diabetic state and insulin resistance is likely also contributing to the diastolic dysfunction in the fructose plus high salt group [127].

Impairment of aortic and renal artery compliance

Diabetes[128, 129] and hypertension[130, 131] are each independently associated with increased PWV. The increased PWV along with diminished radial ascending aortic strain and distensibility coefficient in fructose salt-sensitive rats indicates that aortic compliance declines early with insulin resistance prior to overt diabetes. Greater aortic stiffness occurs with only modest (5-6 mmHg) elevations in systolic (and mean) arterial pressure in the fructose-fed high salt rats. Increases in PWV are typically associated greater pulse pressures. Although the change in pulse pressure was similar after three weeks of high salt, it is noteworthy that baseline pulse pressure in the fructose-fed high salt rats tended to be higher, albeit not statistically significant. Sympathetic innervation of the aorta is now recognized as a factor in aortic stiffening [132], and fructose-fed high salt rats display heightened renal sympathetic nerve activity. Renal denervation prevents the hypertension in this and other rodent models [42, 133] and ameliorates PWV in animal [133] and human systolic hypertension [134]. The contribution of cellular metabolic changes or ion-induced contractility cannot be totally excluded since triglycerides and cumulative salt balance are elevated in this model [41]. Thus, aortic stiffness is only partially dependent of blood pressure and may also be influenced by biophysical changes in the structure and/or function

of the arterial wall evoked by fructose plus high salt diet.

Increased oxidative stress has been implicated in decreased aortic compliance in disease [135] as well as normal aging [136, 137]. The agent, 4-hydroxy-2,2,6,6-tetramethylpiperidine-1-oxyl, is a nonselective superoxide dismutase mimetic that reduces free radical formation and peroxynitrite formation, thereby limiting inflammation. Similar to findings with free radical scavenging in aging mice [138], our results indicate that attenuation of oxidative stress in fructose salt-sensitive rats rescues some aspects of elastic properties of the aorta, restoring normal PWV and radial ascending aortic strain.

Like the aorta, renal artery compliance is reduced which is reflected by the elevated RRI in fructose-fed high salt rats. In contrast to the ascending aorta, renal artery stiffness does not improve after treatment with this antioxidant. Although 4-hydroxy-2,2,6,6-tetramethylpiperidine-1-oxyl has been shown to decrease renal superoxide anion and improve renal vascular resistance via a nitric oxide dependent mechanism,[111, 139] RRI tracks more closely with systemic vascular parameters, intrinsic renal artery compliance and pulsatility than with intrarenal vascular resistance [98]. This is not to say that this heightened pulsatility is not transmitted distally thereby ultimately resulting in hypertensive nephropathy and chronic kidney disease.

While the present hemodynamic measurements have been performed in conscious, freely moving rats, ultrasonography necessitates isoflurane anesthesia. Importantly, isoflurane anesthesia does not alter measures of arterial stiffness [140].

CONCLUSION

The rodent model used in these studies was chosen to mimic the amount of fructose and salt ingested by the upper fifth of the western population. Notably, impaired vascular

compliance of the proximal ascending aorta and renal artery occur after only short-term exposure to the fructose-high salt diet when insulin resistance but not frank hyperglycemia and only mild, but significantly elevated blood pressure occur. The loss of vascular compliance results in transmission of the elevated pressure wave downstream and may, thereby, predispose to hypertensive organ damage including nephrosclerosis. The presence of left ventricular diastolic dysfunction with preserved systolic function strongly suggests that that a diet of fructose combined with high salt exerts an independent effect on left ventricular relaxation. Importantly, antioxidant treatment normalizes fructose-induced salt sensitive hypertension and mitigates increase in aortic pulse wave velocity. These data, therefore, cannot distinguish whether aortic compliance is directly altered by reactive oxygen species induced by the high fructose plus high salt diet or indirectly via the elevation in arterial pressure or both. In contrast, left ventricular diastolic dysfunction and renal artery compliance are not altered by the free radical scavenger despite the decrease in blood pressure indicating that alternative mechanisms are responsible. Taken together, these findings indicate that a diet high in fructose and salt may lead to subtle, possibly progressive, pathophysiologic changes in the central cardiovascular system well before frank clinical disease is apparent. Changes in nutritional behavior and early assessment are imperative to foster cardiovascular health as we go forward.

CHAPTER 3: FRUCTOSE INDUCES CHRONIC SALT-SENSITIVITY AND RENAL DYSFUNCTION

INTRODUCTION

Environmental and lifestyle factors such as diet have become important contributors to the increasing prevalence of hypertension. The increase in hypertension has occurred concurrently with the rise in consumption of fructose-sweetened products [12, 141, 142]. Likewise, sodium consumption has remained high and is directly correlated to numerous cardiovascular and renal diseases [143, 144]. Recent research has shown that a diet high in fructose induces a state of increased sodium retention that leads to hypertension. Onset of this disease state occurs well before the development of metabolic syndrome or frank diabetes mellitus [41, 42]. Adolescents and young adults, particularly those from lower income levels, are the group consuming of the highest amounts of fructose, which is sourced predominately through sugar-sweetened beverages [12]. Despite this disparity, there are few studies investigating the chronic effects of these dietary regimens in youth and the potential impact later in life.

Particularly with polygenic disorders such as hypertension, full phenotypic manifestation does not generally occur before adulthood. The insults that shape disease progression and extent can often be traced back to early periods of development, or ontogeny [145]. The development of organs and physiologic systems can be attributed to specific time points; chiefly the earliest developmental stages of these systems are marked by the most rapid growth. During these windows of development, application of external stimuli can exert influence that can alter physical and mechanistic organ properties. These windows or time frames are referred to as critical developmental periods. While time frames vary and are approximate, readjustment of central hemodynamics in response to post-natal

growth occurs during prepuberty and sexual maturation, which occur between 4 and 6 weeks after birth [146-148]. Readjustment occurs predominately via morphogenesis, however additional maturation of pressor governing systems such as the baroreflex and renin-angiotensin-aldosterone-system (RAS) are simultaneously occurring [149-152].

In several preclinical models, a high salt diet in early life stages induces salt-sensitive hypertension that may not necessarily occur when the same challenge is applied in adulthood [153-156]. Likewise, various transient anti-hypertensive therapies applied in adolescence attenuate the development and degree of hypertension in genetically predisposed strains [157-159]. Notably, this effect coincides with the same critical time (4-9 weeks of age) periods used in salt-sensitivity programming via excess sodium loading, further indicating the importance of these time periods in hypertension induction.

The impact of fructose programming in neonates and adolescents is less well understood. GLUT5 is a glucose transporter that specifically transports fructose and is considered critical to the development of fructose induced salt-sensitive hypertension [160]. It is under-expressed in neonatal intestinal tissue. After weaning there is an abrupt increase in protein and mRNA expression, however, and these patterns can be enhanced if fructose is provided during weaning [161, 162]. Whereas cessation of fructose feeding is marked by restoration of fructose transport systems to control levels, the induction or maintenance of these transport mechanisms could conceivably lead to the development of salt-sensitivity and hypertension at a young age and beyond. Based on the observed effects of sodium programming in youth, it is possible that exposure to fructose early in life will exert long term effects. Thus, we hypothesize that a diet high in both fructose and salt, but not high in fructose alone, in rats aged 5 – 7 weeks will lead to salt-sensitive hypertension in adult life.

MATERIALS AND METHODS

Animals

Since previous reports were almost exclusively performed in male rats, our studies were performed in male rats to permit assessment of the impact of fructose in the context of existing studies. Male Sprague Dawley rats (Envigo Sprague Dawley, Shelby, MI) were housed under controlled conditions (21–23°C; 12-hr light/ dark cycles, lighting period 6 AM to 6 PM). Complete care provided to rats was in accordance with the principles of the National Institutes of Health *Guide for the Care and Use of Laboratory Animals*. All procedures and protocols were approved by the Wayne State University Institutional Animal Care and Use Committee (Protocol #19-03-1001).

Dietary regimen

Upon arrival, rats were acclimated in standard polyurethane caging and were permitted *ad libitum* access to water and standard rat chow for a minimum of 48 hours prior to enrollment in the experimental protocols. At the age of 4-5 weeks (body weight ~125 g), rats underwent placement of a hemodynamic telemetry transmitters and recovered in single housing for 3-5 days. Following recovery, rats were placed into metabolic housing units (Tecniplast USA, West Chester, PA) and randomly fed chow containing either 20% fructose or 20% glucose with 0.4% sodium. These diets were provided *ad libitum* for 5-7 days to permit baseline hemodynamic recordings. Then, the rats were formally entered into the phases of the protocol (Figure 3.1).

Phase I (Days 0 – 22±2): Rats were assigned to chow containing 20% glucose and 0.4% sodium group (glucose low sodium - GLS; ModTest Diet® 5755 – 5WZZ; n = 10); 20% fructose and 0.4% sodium (fructose low sodium - FLS; ModTest Diet® 5755 - 5W3Y, n = 9),

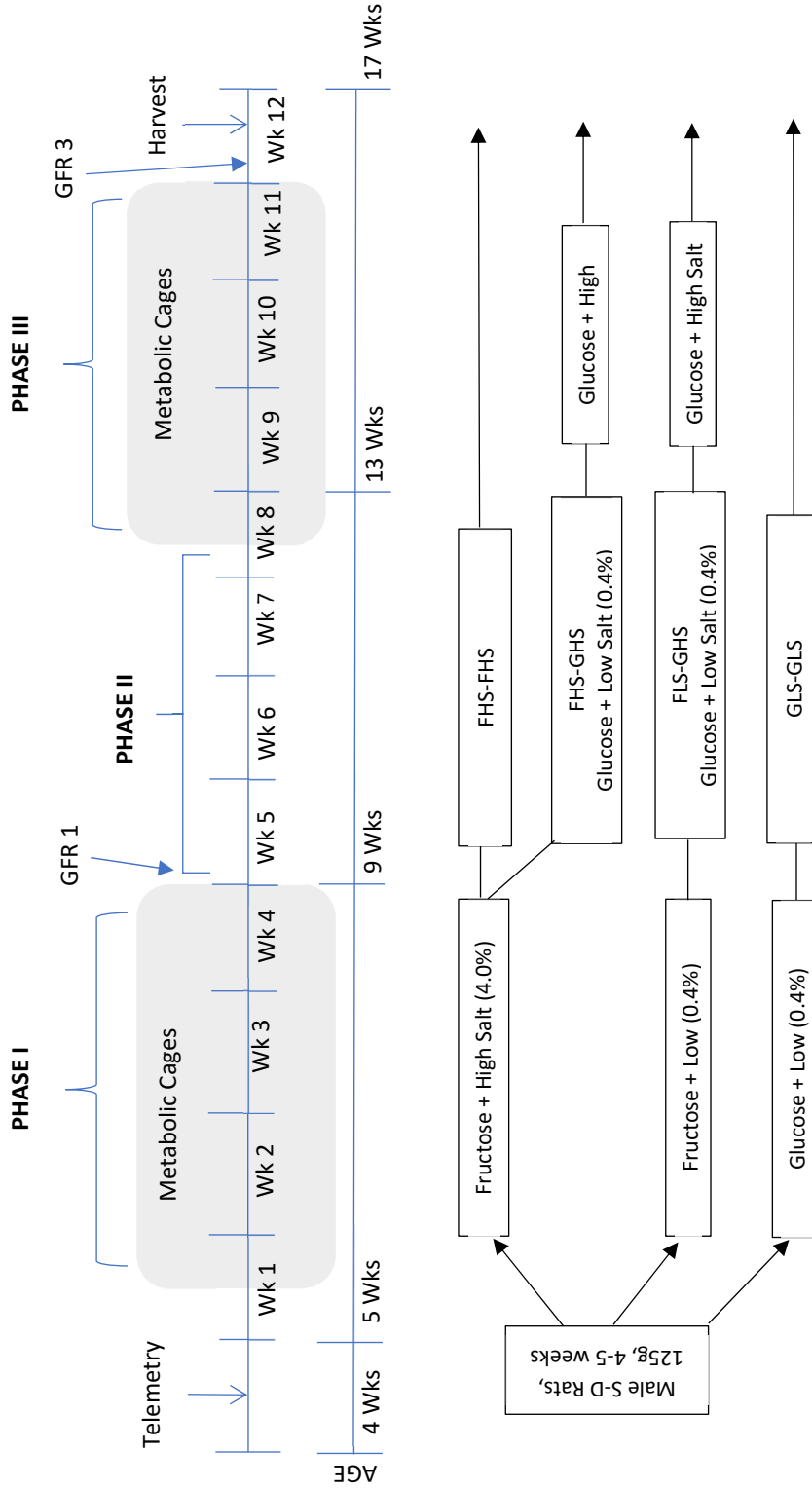


Figure 3.1: Timeline of Experimental Protocols, Division of Phases, and Allotment of Dietary Regimens and Groups.

or 20% fructose and 4.0% sodium (fructose high sodium - FHS; ModTest Diet® 5755 – 5WZ8; n = 18) for 3 weeks. Rats were pair-fed indexed to overall caloric intake due to account for differences in energy profiles (kcal/g) among the dietary formulations. Water provision in all groups remained *ad libitum* throughout the study.

Phase II (Days 23 – 44±2): The rats were returned to singly housed, polyurethane cages in which food and water were provided *ad libitum*. All rats on the GLS and FLS diets and 50% of the rats on the FHS diet were placed on the GLS diet. The remainder of the FHS rats remained on the FHS diet.

Phase III (Days 45 – 66±2): Rats were returned to metabolic housing units after three weeks and were permitted a three-day acclimation period. Rats fed fructose in Phase I were subjected to a high salt challenge with 20% glucose and 4.0% sodium (glucose high sodium - GHS; ModTest Diet® 5755 – 5WOW). As a control, the GLS group from Phase I remained on GLS diet. This resulted in four overall groups: 1) GLS-GLS, 2) FLS-GHS, 3) FHS-GHS, and 4) FHS-FHS. This regimen was continued for an additional three weeks at which time terminal studies were conducted.

Surgical procedures

Hemodynamic Telemetry Transmitter Placement. All surgical procedures were conducted under intraperitoneal ketamine (80 mg/kg; Mylan Institutional, LLC Rockford, IL) and AnaSed/xylazine (10 mg/kg; Akorn Animal Health, Inc., Lake Forest, IL) anesthesia and subcutaneous administration of buprenorphine SR (0.3 mg/kg) for analgesia. For hemodynamic telemetry unit placement, an inguinal incision was made, and the right femoral artery was exposed. Permanent ligation of the distal artery was placed using 3-0 silk suture while a proximal segment of the vessel was temporarily occluded using a vascular

clamp. A small arterial incision was made and the gel-filled catheter of the hemodynamic transmitter (HDS-10, Data Sciences International, MN) was inserted into the vessel using a 21-gauge needle as a guide. The vascular clamp was then removed and the catheter advanced into the abdominal aorta. The transmitter body was subcutaneously tunneled dorsally to the right flank and the incision was closed using surgical staples.

Vascular Catheter Placement. At the end of Phase III, catheters were placed into the left carotid artery and external jugular vein using anesthetic and analgesic regimen above as previously performed in our laboratory [42, 163]. Catheters were anchored using 3-0 silk suture, tunneled subcutaneously, and exteriorized between the scapulae. All incisions were closed using 4-0 Prolene suture (Ethicon, Johnson & Johnson, New Brunswick, NJ). The catheters were filled with heparinized saline (1000 units/mL) and secured. The rats were then permitted to recover in individual standard cages.

Analytical measurements and calculations

Telemetry. Acquisition of hemodynamic data was conducted using Ponemah software (Data Sciences International, MN). Measurement of systolic blood pressure (SBP), diastolic blood pressure (DBP), mean arterial pressure (MAP), and heart rate (HR) were sampled for 10 seconds every 4 minutes at a sampling rate of 500 samples/second. Pulse pressure (PP) was calculated separately using these values. Baseline measurements were averaged over three days following a three-day cage acclimation. Sampling was performed at this rate continuously throughout each study phase within metabolic cages.

Metabolic Assessment. Water intake, chow consumption, and urine volume were measured gravimetrically. Urinary sodium and potassium were measured via flame photometry using an internal lithium standard (Cole Parmer Instruments, Verner Hill, IL).

Transcutaneous Assessment of Renal Function. Glomerular filtration rate (GFR) was assessed at the end of each phase (Figure 3.1) using venous bolus injections of fluorescein-isothiocyanate-(FITC)-sinistrin as described by Schock-Kusch *et al* [164]. Rats were briefly anesthetized with isoflurane and a small adhesive patch with an LED-emitting optical transducer (Mannheim Pharma and Diagnostics GmbH, Mannheim, Germany) was placed on a shaved region on the dorsal aspect of the thorax. Baseline measurements were recorded for 3-5 minutes, thereafter a single bolus injection of FITC-sinistrin, 6 mg/100 g BW (Fresenius-Kabi, Linz, Austria) was administered via tail vein (Phases I and II) or venous catheter (Phase III). Rats were recovered in singly housed polyurethane cages and measurements were recorded for 2 hr. FITC-sinistrin disappearance kinetics were analyzed via a 3-compartment approach using MB Studio software (Mannheim Pharma and Diagnostics GmbH, Mannheim, Germany). GFR was calculated using the following formula:

$$^{[22]} \quad \text{GFR}[\text{ml}/\text{min}/100\text{g BW}] = \frac{31.26[\text{ml}/100\text{gBW}]}{t_{1/2}(\text{FITC-sinistrin})[\text{min}]}$$

Terminal Procedures and Hormonal Assessment. Following the GFR assessment after Phase III, the rats were permitted a 6-8 hour recovery period with no access to food before terminal harvest. Blood was collected from conscious rats via the carotid arterial catheter into pre-chilled tubes for hormonal analysis. Fasting glucose levels were determined using a One-Touch Ultra glucose monitor (LifeScan, Inc., Malpitas, CA). For plasma renin activity (PRA) assay, 1 mL of blood was collected into a tube containing 50 μL sodium ethylenediaminetetraacetic acid (EDTA). Blood (2 ml) was collected into a separate tube containing 120 μL of 500 mM sodium EDTA, 125 mM phenanthroline, 1 mM phenylmethanesulfonyl fluoride, 20 mM pepstatin, 1 mM enalapril and 10X phosphatase inhibitor cocktail for insulin assessment. Once collected, blood was immediately centrifuged

at 3000 rpm for 4 minutes at 4°C. Plasma was stored at -70°C until assayed.

Rats were then euthanized with sodium pentobarbital (120 mg/kg, iv). Kidneys were harvested, kept at 0°C in saline, and weighed. A segment of renal cortex was excised and stored at -70°C. A slice of kidney tissue was placed into formalin for 48 hr and paraffin embedded for histological analysis for future studies.

Statistical analysis. Between-group differences in the pattern of change over the study design were tested in a repeated-measure ANOVA framework, interpreting multivariate statistics as a profile analysis of longitudinal change. Consistent with the experimental design, hypothesis tests were conducted for Phase 1 and Phase 3 separately, without need for multiple comparison correction between phases in variable timeline assessments. Based on initial visual evaluation, the trajectories of daily change appeared non-linear, and an analytic approach was taken in which hypotheses were tested separately for Weeks 1 – 3 of each Phase. Type I error rate was controlled across the multiple tests by week with a Bonferroni correction for three comparisons ($\alpha' = 0.02$). Missing data points in daily measurements were adjusted for by substituting overall phase group means. Group sizes may among variables due to anatomic and or technical issues that precluded assessments of some measurements.

RESULTS

Acute and chronic hemodynamic effects of diet in adolescence. The addition of high salt to fructose fed rats led to a progressive increase in mean arterial pressure that was significantly elevated after four days (Figure 3.2). This increase was maintained for an additional two weeks before becoming statistically comparable to other groups at the end of Phase I. Whereas groups did not differ in Phase I final MAP levels, the overall change between

final and baseline values of Phase I in FHS groups was statistically greater than that of other groups ($p<0.01$). Throughout Phases II and III, FHS feeding led to a continuously increasing MAP, though this was not significant throughout the remainder of the study (Table 3.1).

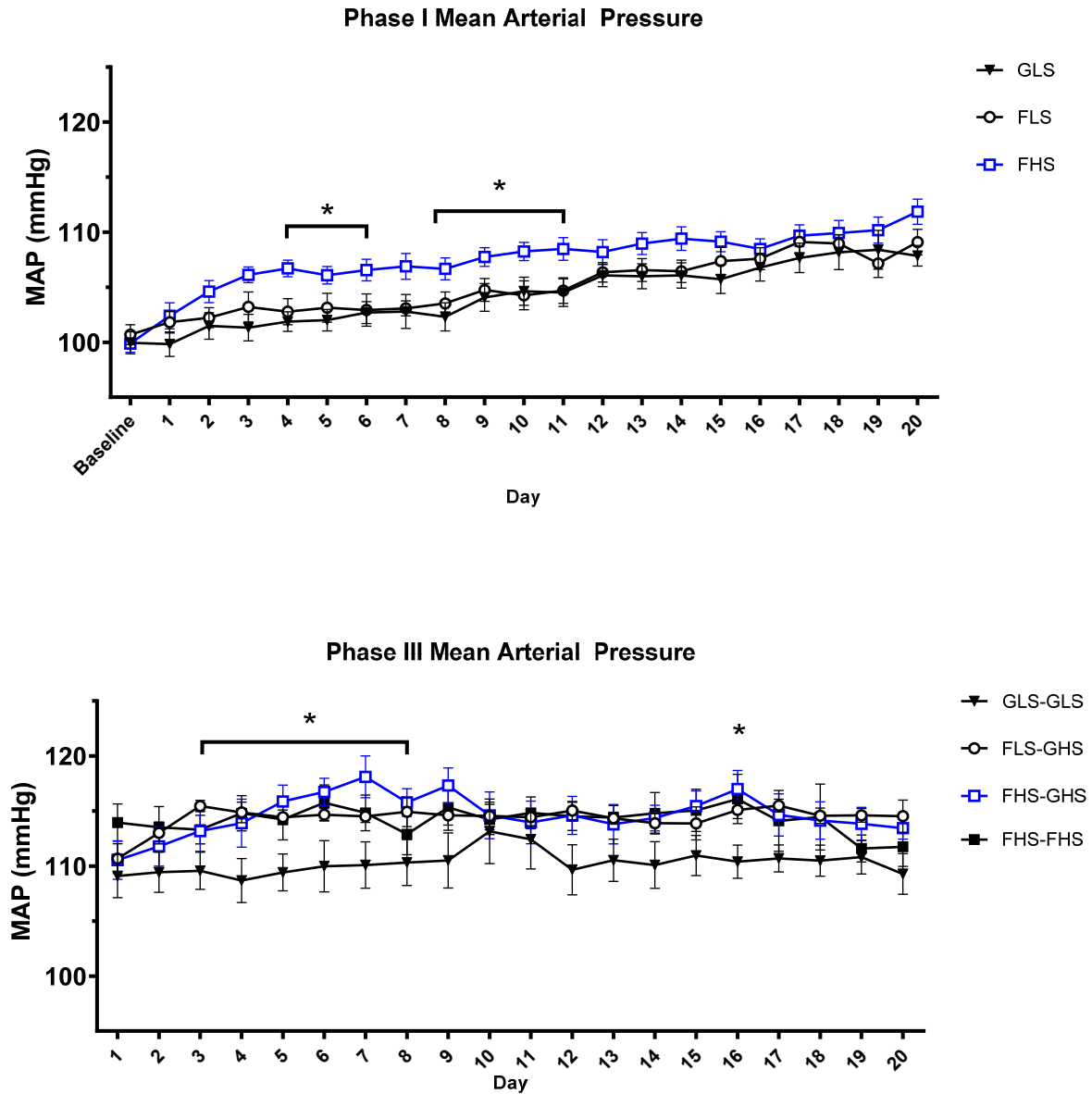


Figure 3.2: Timeline of Daily Mean Arterial Pressure. Measurements calculated as the average of 24 hour daily intervals. Measurements acquired from a catheter implanted into the abdominal aorta. Values are indicated as mean \pm SE, N as indicated per group; $*p<0.05$ FLS-GHS vs. GLS-GLS.

In phase III, mean arterial pressure significantly increased over the first week ($p < 0.001$) and the pattern of change differed among groups ($P = 0.001$): FHS-FHS and FLS-GHS demonstrated moderate increase, as compared to a relatively smaller increase in GLS-GHS, and stability of GLS-GLS. With one-way ANOVA to examine the specific group differences at Day 1 and Day 7, groups were overall equivalent at the start of Phase 3 ($P = 0.11$) but within a week group differences emerged ($P = 0.001$) following apparent elevation in FLS-GHS and FHS-FHS. Subsequent change over week 2 was also different among groups ($P = 0.015$) and by Day 14, FLS-GHS stabilized to average levels consistent with FHS-FHS ($P = 0.79$) and FHS-GHS ($P = 0.60$).

Table 3.1: Study-wide Changes in Hemodynamics.

DIETARY REGIMEN	N	STUDY Δ MAP (MMHG)	STUDY Δ SBP (MMHG)	STUDY Δ DBP (MMHG)	STUDY Δ HR (BPM)	STUDY Δ PP (MMHG)
GLS-GLS	7	10.0 \pm 1.0	11 \pm 2.2	11 \pm 1.2	-92 \pm 11	2.4 \pm 1.5
FLS-GHS	8	15 \pm 0.9*	18 \pm 0.9*	14 \pm 1.3	-103 \pm 18	4.2 \pm 1.6
FHS-GHS	8	15 \pm 1.4*	18 \pm 1.7*	13 \pm 1.7	-105 \pm 6	4.2 \pm 2.0
FHS-FHS	8	16 \pm 2.0**	19 \pm 2.3**	14 \pm 1.9	-89 \pm 14	4.6 \pm 1.4

Calculated as the difference between measurements taken at the end of Phase III and the baseline measurements taken at the beginning of Phase I. Values are indicated as mean \pm SE, N as indicated per group; * $P < 0.05$ vs. GLS-GLS controls. ** $P < 0.01$ vs. GLS-GLS controls.

Study-wide analysis (Table 3.1) evaluating the overall change in hemodynamic parameters throughout the entirety of the study indicated comparable increases between FLS-GHS and FHS-GHS groups that were significantly elevated above GLS-GLS controls ($P < 0.05$). The increases in FHS-FHS controls were elevated above this when compared to controls ($P < 0.01$). Overall study changes in SBP followed similar trends as MAP, but DBP and heart rate did not. While the change in DBP was not significant it increased sufficiently to prevent any statistically observable differences in pulse pressure.

Acute and chronic metabolic profiles of fructose and high salt programming during adolescence. Except during the initial baseline recordings, all rats in metabolic cages in Phases I and III were placed on a pair feeding paradigm. Chow consumption was assessed daily, and the amount provided was determined by caloric consumption, rather than direct gravimetric assessment. This protocol design was implemented as a more accurate correction to limit differences in total nutritional consumption due to the varying energy profiles (caloric content) of each type of chow. Statistical differences between caloric intake were observable initially following dietary changes to high salt feeds in both glucose and fructose groups in both Phases I and III, but these gradually normalized among groups. High Na⁺ intake was accompanied by increased fluid intake and urine excretion, both of which reached a maximum by the end of week 2 in Phases I and III (Table 3.2).

As defined in Methods, high and low salt feeds were comprised of 4.0% Na⁺ and 0.4% Na⁺, respectively. Consistent with a pair feeding strategy, low salt fed rats consumed approximately 10% of the amount of sodium consumed by high salt fed rats (Table 3.3). This increase in dietary sodium intake was accompanied by increases in both urine production and Na⁺ excretion. Albeit, sodium excretion was significantly increased compared to low salt diets, it was insufficient in maintaining a neutral bodily sodium balance. Net (Figure 3.3A&B) and cumulative (Figure 3.3C&D) Na⁺ balances are depicted in Figure 3.3. Phase I net Na⁺ balances changed over week 1 ($P < 0.001$) and groups differed in the pattern of change ($P < 0.001$): FHS-FHS and FLS-GHS both show faster increase over the initial 7 days of Phase I as compared to stable low levels of GLS-GLS and stable high levels of FHS-GHS. Over this period, groups differed on average ($P < 0.001$): GLS-GLS had a lower net Na⁺ balance as compared with all other groups (all $P < 0.001$), and FHS-GHS greater than FHS-FHS ($P = 0.04$). Between

group differences were only evident in week 1, and net Na⁺ did not change over week 2 ($P = 0.36$) or week 3 ($P = 0.09$). GLS-GLS remained significantly lower than all other groups over week 2 ($p < 0.001$) and week 3 ($p < 0.001$), however all other group comparisons were not statistically significant.

Table 3.2: Daily Metabolic Measurements.

		WEEK 1			WEEK 2			WEEK 3		
DIETARY REGIMEN	N	Caloric Intake (kcal/day)	Fluid Intake (mL/day)	Urine Output (mL/day)	Caloric Intake (kcal/day)	Fluid Intake (mL/day)	Urine Output (mL/day)	Caloric Intake (kcal/day)	Fluid Intake (mL/day)	Urine Output (mL/day)
GLS	9	61.5±5	30.4±8	13.7±3	68.4±4	33.6±4	16.4±3	66.0±6	33.0±5	15.3±3
FLS	9	60.7±8	32.5±4	17.9±3	67.2±4	34.4±5	19.0±4	65.7±5	34.3±4	19.2±3
FHS	9	51.9±7*	73.8±17*	56.2±16*	63.9±4	89.7±16*	70.0±17*	64.0±5	90.9±14*	68.8±13*
		WEEK 1			WEEK 2			WEEK 3		
DIETARY REGIMEN	N	Caloric Intake (kcal/day)	Fluid Intake (mL/day)	Urine Output (mL/day)	Caloric Intake (kcal/day)	Fluid Intake (mL/day)	Urine Output (mL/day)	Caloric Intake (kcal/day)	Fluid Intake (mL/day)	Urine Output (mL/day)
GLS-GLS	9	62.6±6	32.0±5	18.7±4	63.5±6	31.8±5	18.3±4	64.3±5	32.2±4	19.0±4
FLS-GHS	9	45.9±5*	65.5±14*†	49.9±15*†	54.4±4*	72.7±15*	56.3±15*	57.1±4†	79.7±18*	65.9±18*
FHS-GHS	8	50.1±7*	58.2±10*†	41.8±7*†	56.1±6*	69.6±11*	52.7±10*	59.9±6	76.6±12*	60.6±11*
FHS-FHS	9	60.5±5	86.6±20*	68.3±19*	63.9±6	86.2±16*	68.6±18*	66.4±8	91.6±18*	71.4±13*

Recorded at 5 PM each day. Caloric intake calculated using caloric profiles of 3.98 kcal/g and 3.61 kcal/g for low salt and high salt feed, respectively. Values are indicated as mean ± SE, N as indicated per group; * $p < 0.05$ vs. GLS-GLS; † $p < 0.05$ vs. FHS-FHS.

Table 3.3: Ionic Consumption and Excretion.

DIETARY REGIMEN	N	PHASE I						PHASE III					
		WEEK 1		WEEK 2		WEEK 3		WEEK 1		WEEK 2		WEEK 3	
		Consumption (mmols/day)		Excretion U_{xV} (mmols/day)		Consumption (mmols/day)		Excretion U_{xV} (mmols/day)		Consumption (mmols/day)		Excretion U_{xV} (mmols/day)	
	Na*	K*	Na*	K*	Na*	K*	Na*	K*	Na*	K*	Na*	K*	
GLS	9	3.0±0.3	4.9±0.5	2.4±0.1	3.9±0.1	3.0±0.1	4.8±0.1	2.7±0.2	4.1±0.3	2.9±0.1	4.67±0.1	2.6±0.2	4.1±0.2
FLS	9	2.7±0.1	4.3±0.2	3.0±0.2	4.1±0.2	3.0±0.1	4.8±0.1	3.4±0.1	4.6±0.2	3.2±0.3	5.17±0.6	2.8±0.2	4.3±0.1
FHS	9	24.9±1.0*	4.0±0.2	16.2±1.4*	3.6±0.2	30.9±1.8	5.0±0.1	22.2±1.5*	4.7±0.2	31.0±2.3*	5.0±0.1	20.8±1.6*	3.6±0.6
GLS-GLS	9	2.8±0.1	4.5±0.1	3.1±0.4	4.3±0.7	2.9±0.1	4.6±0.1	2.7±0.1	4.3±0.2	2.8±0.1	4.6±0.1	2.6±0.1	4.2±0.2
FLS-GHS	9	22.1±0.8**	3.6±0.1*†	15.8±1.3**	3.3±0.6	26.2±0.7*	4.2±0.1†	18.6±1.2*	4.1±0.9	27.5±0.6*	4.5±0.1	20.4±1.4*	4.9±1.3
FHS-GHS	8	23.3±1.2*	3.8±0.2*†	13.2±0.6**	3.7±0.6	26.0±0.8*	4.2±0.1†	16.7±1.0*†	4.0±0.2	27.7±0.6*	4.5±0.1	18.2±1.3*	4.6±0.6
FHS-FHS	9	27.5±0.8*	4.4±0.1	20.5±1.6*	4.4±0.3	29.0±0.3*	4.7±0.1	20.4±1.6*	4.3±0.3	29.9±1.0*	4.9±0.2	20.7±1.7*	4.5±0.2

Measurements obtained via flame photometry analysis of urine samples collected daily. Values are indicated as mean ± SE, N as indicated per group; * $p < 0.05$ vs. GLS-GLS controls; † $p < 0.05$ vs. FHS-FHS controls.

High and low salt feeds were comprised of 4.0% Na⁺ and 0.4% Na⁺, respectively. Consistent with a pair feeding strategy, low salt fed rats consumed approximately 10% of the amount of Na⁺ consumed by high salt fed rats (Table 3.3). This increase in dietary sodium intake was accompanied by increases in both urine production and sodium excretion. Although sodium excretion was significantly increased compared to low salt diets, it was insufficient in maintaining a neutral bodily Na⁺ balance. Balances are expressed in terms of net and cumulative Na⁺ balances in Figure 3.3.

Observed net Na⁺ balance in FHS rats in Phase I significantly increased from baseline to day 8 ($p < 0.001$), continued to change across week 2 ($P = 0.003$), but normalized by week 3 ($P = 0.25$). This trend was reflected by a continuously and significantly increasing cumulative balance throughout weeks 1-3 following baseline ($P < 0.01$). Phase III net Na⁺ balances changed over week 1 ($p < 0.001$) and groups differed in the pattern of change ($p < 0.001$): FHS-GHS and FLS-GHS both show faster increase over 7 days as compared to stable low levels of GLS-GLS and stable high levels of FHS-FHS. Over this period, groups differed on average ($p < 0.001$): GLS-GLS had a lower net Na⁺ balance as compared to all other groups (all $p < 0.001$), and FHS-GHS greater than FHS-FHS ($p = 0.04$). Between group differences were only evident in week 1, and net Na⁺ did not change over week 2 ($p = 0.36$) or week 3 ($p = 0.09$). GLS-GLS remained significantly lower than all other groups over week 2 ($p < 0.001$) and week 3 ($p < 0.001$), however all other group comparisons were not statistically significant.

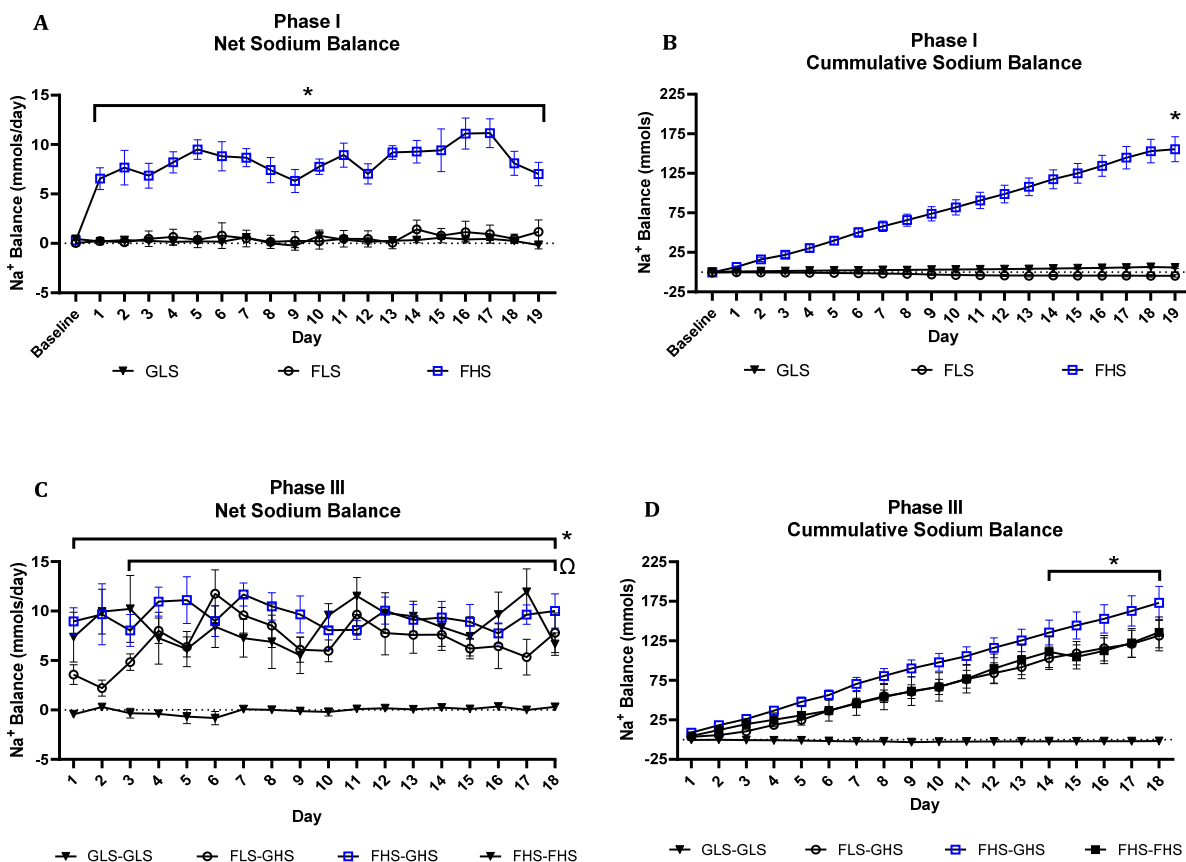


Figure 3.3: Bodily Sodium Balance. Measurements obtained via flame photometry analysis of urine samples collected daily. Values are indicated as mean \pm SE, N as indicated per group. A.) Phase I net sodium balances - $*p < 0.05$ vs. GLS-GLS controls. B.) Phase I Cumulative Sodium Balance - $*p < 0.05$ for rate and absolute values vs GLS. C.) Phase III Net Sodium Balances - $*p < 0.05$ FHS-GHS and FHS-FHS vs. GLS-GLS controls, $^{\Omega}p < 0.05$ FLS-GHS vs. GLS-GLS. Phase I Cumulative Sodium Balance - $*p < 0.05$ for rate and absolute values vs GLS. D.) Phase III Cumulative Sodium Balance - $*p < 0.05$ for absolute values of FHS-GHS vs. FHS-FHS.

Cumulative sodium balance increased all but GLS-GLS groups during Phase III: ($P < 0.001$), week 1-3 respectively. Groups differed in the magnitude of change across all weeks ($P < 0.001$). The group and day interaction was driven by GLS-GLS remaining stable while all other groups increased. A pattern of between-group differences emerged over the three weeks ($P < 0.001$), with all groups equivalent at week 1 and week 2 (except GLS-GLS, $P < 0.01$) and FHS-GHS observed with higher cumulative sodium balance than FHS-FHS ($P < 0.03$) by week 3. This effect by the last week appears to be due to a slight elevation at Day 1 and not necessarily a meaningfully different rate of increase; although the group difference

to start was small and not statistically significant, the meaningful effect in FHS-GHS emerged over time as a compounding effect in cumulative Na⁺ balance.

Table 3.4: Metabolic, Renal, and Endocrine Measurements.

DIETARY REGIMEN	N	INITIAL WEIGHT (G)	FINAL BODY WEIGHT (G)	LEFT KIDNEY WEIGHT (G/KG)	RIGHT KIDNEY WEIGHT (G/KG)	FASTING GLUCOSE	G:I RATIO (X10 ⁶)	PRA (NG ANG I/ML/HR)
GLS-GLS	9	125±4	380±27	3.3±0.3	3.2±0.2	128±13	64.7±6.4	1.82±0.20
FLS-GHS	9	132±4	346.7±30	3.7±0.4*	3.5±0.4*	129±24	74.6±12.6*	0.66±0.12**
FHS-GHS	8	128±3	362.2±33	3.5±0.3	3.4±0.2	126±14	31.6±1.9	1.35±0.28
FHS-FHS	9	127±5	365.8±36	3.7±0.3*	3.7±0.2*	118±11	43.0±8.3	1.09±0.29*

Assay values conducted using blood samples collected through an intra-arterial line extracted under conscious conditions. Rats were fasted for a minimum of 6 hours prior to collection. Values are indicated as mean ± SE, N as indicated per group; * $p < 0.05$ vs. GLS-GLS controls, ** $p < 0.01$ vs. GLS-GLS controls. Due to technical complications, G:I (Glucose:Insulin) ratio N values differ and are as follows: GLS-GLS - 5, FLS-GHS - 6, FHS-GHS - 7, FHS-FHS - 7.

Chronic effects on metabolism, endocrine systems, and renal function. Table 3.5 represents primary findings from terminal procedures. One-way ANOVA of final body weights did not find significant variance amongst groups, although the FLS-GHS group differed significantly from GLS-GLS controls. Likewise, there were no significant differences between right and left kidney weights. However, normalization to body weight found increased weight of both kidneys in FLS-GHS and FHS-FHS.

No significant differences in fasting plasma glucose levels were found among groups, and these levels did not vary from vendor specifications for Envigo® bred Sprague-Dawley rats. Plasma insulin levels indicated a reduced level of fasting insulin compared to other groups, but this was insufficient in producing any statistical trend when analyzed by ANOVA (data not shown). A glucose:insulin ratio was chosen as a measure of insulin sensitivity given our inability to perform overnight fasting for HOMA measurements of insulin resistance (due to IACUC restrictions) and the relevance of the glucose:insulin ratio to prior studies

conducted by our laboratory [42, 163]. The reduced insulin levels in FLS-GHS rats drove the significance in this group upon ANOVA analysis of G:I ratio. All other groups remained statistically similar. This decline was associated with a reduction in weight and caloric consumption in this group at the time of conversion to a high salt diet in Phase III.

Assessment of glomerular filtration rate (Figure 3.4) found no difference among groups at the end of Phase I and Phase II, with little change within each group between phases. GLS-GLS fed rats showed no significant differences over time. Conversely, FHS-FHS groups experienced a significant decline in GFR. Phase III was particularly characterized by this reduction in the FHS-FHS group. Reductions in GFR in this group were significant when compared to GLS-GLS in Phase I and Phase III, as well as in pairwise analysis of FHS-FHS changes over time. Whereas FHS-GHS did not significantly decline in Phase III compared to GLS-GLS rats, groupwise changes over time were significant. FLS-GHS fed rats followed a similar trend over time, but this did not achieve statistical significance. The reduction in GFR in the FLS-GHS group, chiefly between Phases II and III, is considered a product of tubuloglomerular feedback in response to the recent high salt challenge and increasing arterial pressure. In contrast, functional reductions in FHS-GHS and FHS-FHS groups are likely caused by vascular or morphologic changes and warrant further investigation.

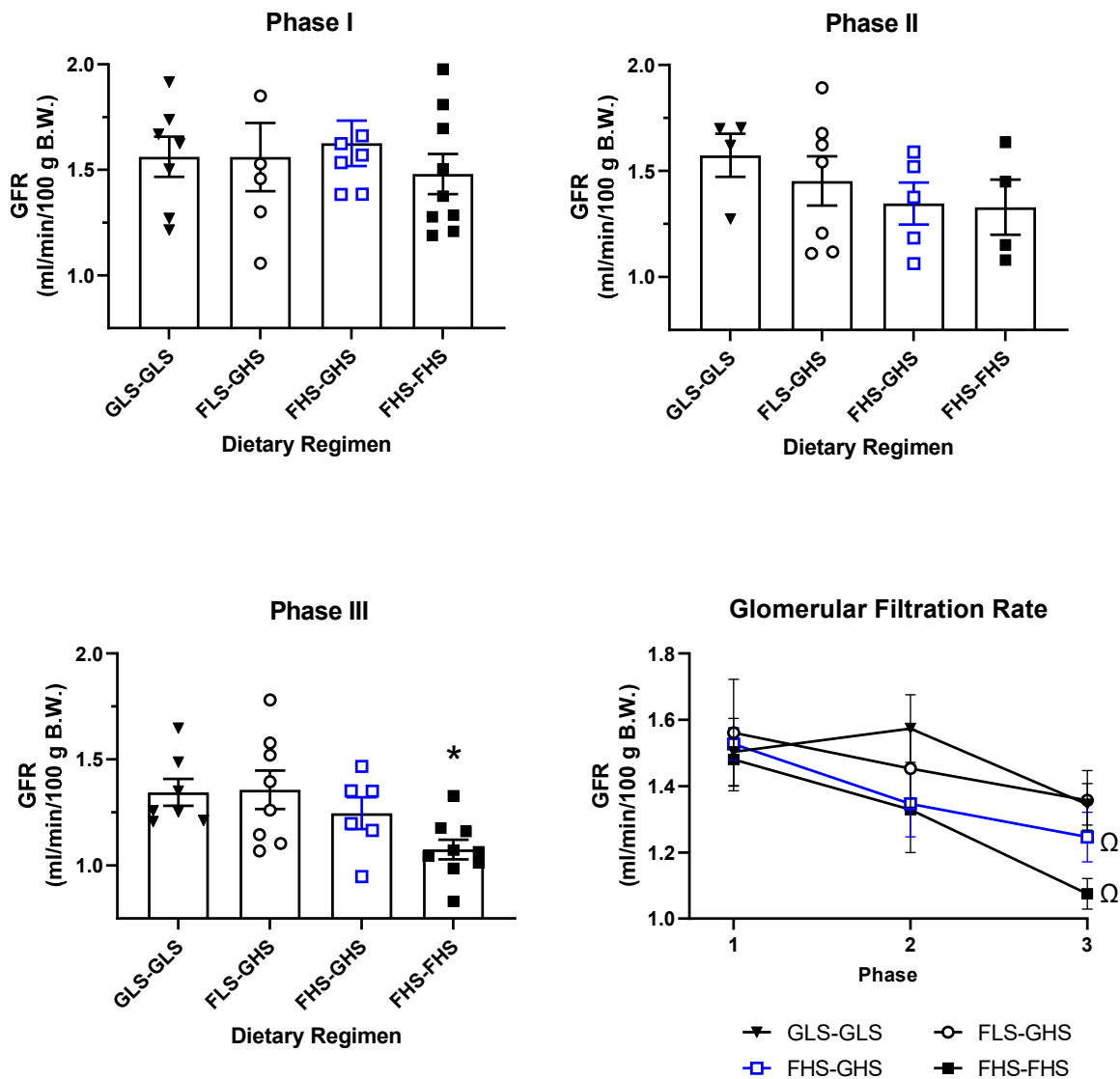


Figure 3.4: Assessment of Glomerular Filtration Rate. Measurements obtained at the end of each phase. Phase I measurements were obtained after randomization into final group assignments, permitting assessment of all 4 groups. N values per phase are demonstrated graphically. Values are indicated as mean \pm SE; * p <0.05 vs. GLS-GLS controls, $^{\Omega}p$ <0.05 vs initial Phase I measurements for the same group assessed via two-way ANOVA.

DISCUSSION

The present study provides support that high dietary fructose and sodium consumption patterns can induce hypertension in adolescence with chronic effects manifesting in later life when challenged only with high salt intake. The physiologic changes

that occur during these developmental periods have lasting effects that can render the body susceptible to hypertensive stimuli later in life. Hypertension induction in adult rat models via high salt loading alone would require prolonged periods of feeding, making the model unappealing due to economic and logistical constraints. These time periods would extend beyond the relatively brief periods critical to ontogenetic programming of hypertension. Indeed, the induction of hypertension in early life using high salt in rat models cannot, to our knowledge, be accomplished without additional manipulations that render the body more susceptible to the influence of sodium. Such manipulations include surgical deformation, either breeding or direct induction of genetic predispositions, chemical treatment (i.e. deoxycorticosterone-acetate), or severe metabolic disturbances [165-170]. Diets rich in fructose and sodium are immersed into western culture throughout all periods of life. The propensity for higher daily ingestion of fructose and salt in adolescents and young adults provides a strong basis for rigorous evaluation of the impact on subsequent cardiovascular and renal function and the relevance of this study.

The increases in arterial pressure in this model of fructose-induced salt-sensitive hypertension have been observed in several other studies [41, 42, 66]. These studies however used methods of blood pressure measurements that made discernment of individual contributions of each hemodynamic component difficult. In this study, chronic telemetry-based recording enabled a well-defined examination of BP changes over time. Analysis of change throughout the entire study unveiled significant increases in MAP in FLS-GHS, FHS-GHS, and FHS-FHS groups. Significant increases in systolic blood pressure were observed with no significant change in DBP occurred, indicating the increase in MAP was driven by systolic mechanisms.

The greatest increases in BP throughout the study were observed in the chronically fed FHS group, but values were only significantly elevated in Phase I and then proceeded to gradually increase throughout the remainder of the study. Significant increases in MAP that occur in any group throughout the study consistently coincide with the dietary addition of high salt. FHS-GHS groups experienced a significant increase in Phase I with a secondary increase when challenged with the addition of high salt in Phase III. BP patterns in the FLS-GHS group followed those of the GLS-GLS controls until Phase III, which was characterized by the most significant increase among all groups when given high salt. With regards to hemodynamic changes, the dietary addition of fructose during weeks 5 to 7 is as important in the development of susceptibility to salt sensitive hypertension later in life as sodium is itself.

Prior *in vivo* and *ex vivo* studies in adult rats have shown that both short term and chronic feeding, or acute perfusion of fructose increases activity and expression of fructose, sodium, and chloride transport systems within across the intestinal and renal epithelium. The osmotic gradient that develops in the intestine is important for absorption and initial increases of extracellular volume while the reabsorption mechanisms within the kidney serve to maintain and even potentiate this effect [40, 60, 160, 171-173]. Rats fed a FHS (both FHS-FHS and FHS-GHS groups) diet in Phase I had a significant increase in net sodium balance during Phase III, calculated as the difference between sodium consumption and urinary excretion. This was accompanied by an increase in net fluid balance, indicating increased fluid retention.

These trends follow those of similar studies using DOCA to induce salt-sensitive hypertension. Treatments initiated during early critical developmental periods elicited

robust increases in extracellular volume and arterial pressure that were not observable when treatments were initiated in adulthood [174]. Chronic increases in extracellular volume cannot perpetually drive increasing arterial pressure, however, as this would ultimately prove fatal. Pressure natriuresis in each high salt fed group was sufficient to prevent further increases in arterial pressure but unable to restore them to normotensive levels, potentially indicating baroreceptor resetting at central and renal levels.

The maintenance in post-pubertal arterial pressure indicates additional mechanisms in place, many of which have been investigated in other studies. Changes in autonomic activity that can modulate physiologic function both locally and regionally have been implicated with high salt, with and without the addition of dietary fructose [175]. This may serve to increase total peripheral resistance, cardiac function, or directly influence the RAS [176]. Indeed, renal sympathetic activity is increased in adult rats fed a fructose and high salt diet and stimulates renin secretion [42]. Thus, suppression of PRA by increased blood pressure and extracellular volume may be counteracted by enhanced sympathetic input to the kidney. Consistent with such a mechanism, the FLS-GHS group had the greatest extent of renin suppression (indicated by reduced PRA). In contrast, early exposure to FHS in the FHS-GHS and the FHS-FHS groups prevented suppression of PRA later in life. . Contrastingly, no reduction in PRA in FHS-GHS groups compared to GLS-GLS controls was observed which likely played a consequential role in the increased sodium reabsorption in Phase III and the elevated arterial pressure. Altered renal sympathetic activity and resetting renal autoregulatory mechanisms may be implicated in this but were not the focus the study [177-179]. Additionally, our laboratory has shown that reactive oxygen species has are also implicated in fructose and high salt diets. Oxidative stress can further induce vaso-

dysfunction, tubule sodium reabsorption, and renin secretion [180-183].

Perspectives

These mechanisms provide insight into the observed effects of the FHS-FHS and FHS-GHS groups in Phase III, all of which were likely exaggerated by ontogenetic programming [184]. Previous studies have demonstrated that high salt or even glucose combined with high salt does not increase net sodium balance in and of itself, nor does it have any significant impact on arterial pressure [41, 42, 163]. The present study found that a priming period of solely fructose feeding was necessary to promote a state of salt-sensitivity capable of eliciting increases in blood pressure following high salt challenge in the absence of fructose later in life. While alternative mechanisms acting to increase blood pressure such as increased sympathetic activity – regional or peripheral – or vascular dysfunction cannot be disregarded, the central role of the kidney in this model cannot be understated. Renal reabsorption of sodium plays an essential role in the development of hypertension in adolescence and the prolonged salt-sensitivity well into adulthood, despite the restoration of non-pressor inducing diets.

In light of research into protein and mRNA expression patterns of the relative sodium and fructose transport systems during fructose feeding, this period likely reflects a developmental, transport aggregational state. Singh *et al.* showed that within two weeks of fructose feeding, mRNA and protein abundance of intestinal transporters such as PAT1, GLUT5, NHE3 substantially increased and remained elevated with prolonged fructose feeding [160]. Similar patterns are observable within the kidney through post-translational and post-transcriptional mechanisms [172]. As discussed above, GLUT5 expression can be manipulated if fructose is provided to weanling rats, and this programming would likely

serve to amplify the already dramatic expression increases occurring in the presence of fructose. To our knowledge, expression of these transport systems has not been investigated following the cessation of fructose feeding. The extent and time length these transporters remain expressed would provide pathologic insights into the robust salt-sensitivity response to high salt challenge later in life, as observed in the FLS-GHS group.

CHAPTER 4: ACUTE AND CHRONIC CARDIO-RENAL CONSEQUENCES TO FRUCTOSE-INDUCED SALT-SENSITIVE HYPERTENSION INDUCED IN ADOLESCENCE

INTRODUCTION

The prevalence of hypertension has been increasing in the United States both independently and concurrently with the rise of diabetes throughout the past several decades. Elevated fructose consumption has been implicated in metabolic disorders and subsequent cardiovascular morbidity [12, 13, 32]. In most pre-clinical models, high levels - often exceeding 60% of daily caloric intake - of fructose consumption elicit hypertension and cardiovascular dysfunction, and implicate insulin signaling as the pathogenic mechanism [31, 32]. Ingestion of 20% fructose in drinking water together with a high salt diet, levels comparable to the diet ingested by the upper quintile in humans, results in sodium and fluid retention in rats, leading to a hypertensive state prior to development of frank metabolic syndrome or diabetes [41, 42].

Adolescence is marked by the continuous development and growth of physiologic systems. Particularly in earlier stages of life, various systems undergo substantial developmental changes and are susceptible to modulation by external stimuli. While there are several studies on the effect of fructose consumption on cardiorenal systems in adults, little is understood regarding the impact of diets rich in fructose alone on development during adolescence [77]. Notably, western diets use high fructose corn syrup extensively as a sweetener and are also high in sodium content [13]. In this regard the largest consumers of fructose are adolescents and young adults – particularly those of low-income families. Sugar sweetened beverages represent the main source of fructose intake and in young adults this accounts for as high as 20% of daily energy consumption [17, 185].

Since preclinical studies indicate that a diet high in both fructose and salt results in

hypertension, aortic stiffness, and early diastolic dysfunction, the question arises whether ingestion of high fructose and salt during a critical early life period predisposes to salt-sensitive hypertension and cardiovascular dysfunction in later life [41, 42, 66, 163, 186]. Particularly with cardiovascular development, rat models have shown that interventions during critical time periods of ontogeny known as developmental windows, may alter susceptibility to hypertension later in life and induce substantial physiologic and anatomical changes that render the animal prone to subsequent cardiovascular co-morbidities [187]. Currently, the predominant insights regarding how post-gestational insults affect arterial pressure development can be garnered from studies using genetically hypertensive strains rat (dahl salt-sensitive and spontaneously hypertensive, namely) to investigate the effects of environmental and genetic factors and their impact on disease progression [187]. In cases of salt-sensitivity, severe salt-deprivation during critical developmental periods (4-9 weeks) blunts hypertensive development while increased sodium intake accentuates it [188-190].

Salt-sensitivity can be assessed clinically using a variety of protocols; however, it can be defined generally as a 5-10% change in arterial pressure following a change in dietary sodium intake [191, 192]. We recently tested the hypothesis that a 20% fructose and 4% sodium diet provided early in life rats renders the animal prone to salt-sensitive hypertension later in life (Chapter 3). The purpose of the present study was to investigate the longitudinal functional alterations to function to provide mechanistic insights into disease progression. We hypothesized that rats consuming a diet with 20% fructose and with or without 4% sodium during weeks five to eight (inclusive) will develop elevated blood pressure, reduced arterial compliance, and diastolic left ventricular dysfunction in adulthood when challenged with high dietary sodium alone.

MATERIALS AND METHODS

All animal procedures and protocols were approved by the Wayne State University Institutional Animal Care and Use Committee (Protocol #19-03-1001). Animal care and experimentation was conducted in accordance with the guidelines and principles of National Institutes of Health Guide for the Care and Use of Laboratory Animals. Male Sprague Dawley rats (Envigo Sprague Dawley, Shelby, MI) were housed under controlled conditions (21–23°C; 12 hr light and 12 hr dark cycles, lighting period beginning at 6 AM).

Dietary regimen

Upon arrival rats were permitted to acclimate for at least 48 hours and provided standard lab chow and water, *ad libitum*. As depicted in Figure 1, when rats reached ~4.5 weeks of age and ~125 grams, a hemodynamic transmitter was implanted and the animal was permitted to recover in individual standard polyurethane caging. One week later, rats were placed into metabolic housing units (Tecniplast USA, West Chester, PA) and provided milled feed containing either 20% glucose and 0.4% Na⁺ (glucose low salt – GLS, ModTest Diet® 5755 – 5WZZ) or 20% fructose and 0.4% Na⁺ (fructose low salt - FLS, ModTest Diet® 5755 - 5W3Y). Rats were permitted a 3-day acclimation period followed by a 3-day baseline period where food and water were provided *ad libitum*. GLS rats (n = 9) were continued on the same diet. Rats receiving FLS chow were then randomly assigned into continue on FLS (n= 9) or 20% fructose and 4.0% Na⁺ (fructose high salt – FHS, ModTest Diet® 5755 – 5WZ8; n = 18). At this time, a pair feeding paradigm was initiated among groups to achieve equal caloric intake among the groups on a day-to-day basis. Water continued to be provided *ad libitum*. The diets were maintained for three weeks (Fig 4.1, weeks 2 to 4) during which fluid and urine outputs were assessed daily. The rats were then returned to standard individual

housing units (Figure 4.1, weeks 5 to 7). Rats on GLS feed were maintained on this diet for the remainder of the study. All rats on FLS feed were then placed on GLS chow. The rats on FHS chow were then further randomly assigned to receive GLS feeding (n = 9) or to continue the FHS diet (n = 10). The rats on FHS during Phase 2 remained on FHS through to the end of the study.

After 3 weeks, rats were returned to a metabolic cages and permitted to acclimate to the change in caging for three days. FLS and FHS fed rats that had been shifted to a GLS feed were then subjected to a high salt challenge without fructose for the remainder of the protocol using a 20% glucose and 4.0% Na⁺ chow (glucose high salt – GHS, ModTest Diet® 5755 – 5WOW). This produced four groups characterized by their dietary regimens in the early and late phases – Phase 1 and Phase 3, respectively (Figure 4.1) - of the protocol: a) GLS-GLS, b) FLS-GHS, c) FHS-GHS, and d) FHS-FHS. Rats were maintained on these diets for an additional 3 weeks; thereafter terminal studies were performed.

Surgical procedures

All surgical procedures were conducted under intraperitoneal ketamine (80 mg/kg; Mylan Institutional, LLC Rockford, IL) and xylazine (10 mg/kg; Akorn Animal Health, Inc., Lake Forest, IL) anesthesia and subcutaneous administration of buprenorphine SR (0.3 mg/kg) for analgesia.

Hemodynamic Transmitter Placement. Following right femoral artery isolation, a small arterial incision was made, and the gel-filled catheter of the hemodynamic transmitter (HDS-10, Data Sciences International, MN) was inserted into the vessel and advanced into the abdominal aorta. The catheter was then anchored in place within the femoral artery using 3-0 silk suture (Ethicon, Johnson & Johnson, New Brunswick, NJ) and the transmitter

body was subcutaneously tunneled to the right flank. Subcutaneous adipose tissue was reapproximated around the surgical sight and the incision was closed using surgical staples.

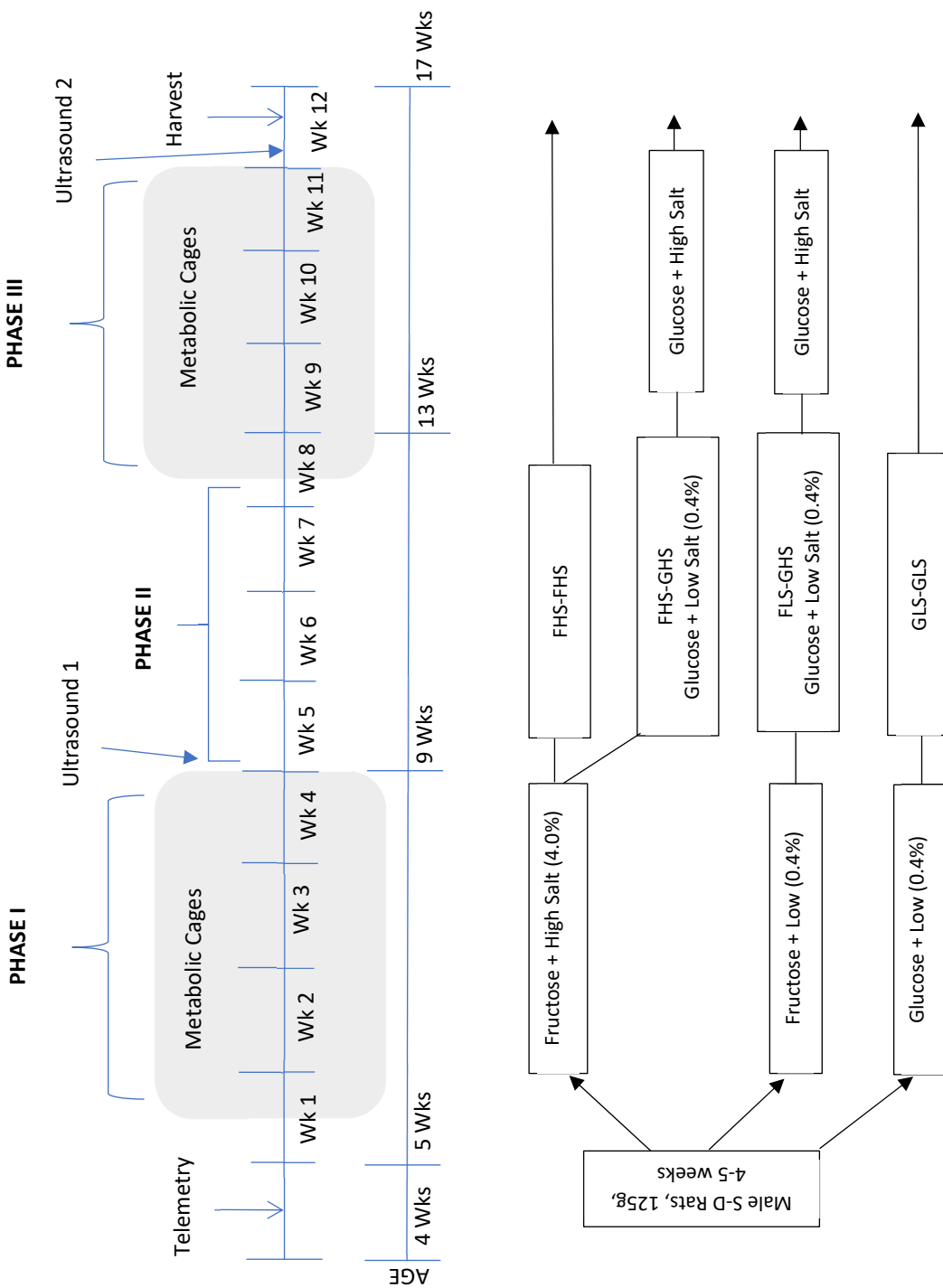


Figure 4.1: Timeline of Experimental Protocols, Division of Phases, and Allotment of Dietary Regimens and Groups. *Note: Figure adapted from Figure 3.1.

Vascular Catheter Placement. At the end of Phase III, catheters were placed into the left carotid artery and external jugular vein using the anesthetic and analgesic regimen above and as previously performed in our laboratory [42, 163]. Catheters were anchored using 3-0 silk suture and tunneled subcutaneously behind the scapulae for exteriorization. All incisions were closed using 4-0 Prolene suture (Ethicon, Johnson & Johnson, New Brunswick, NJ). The catheters were then filled with heparinized saline (1000 units/mL) and secured. The rats were then permitted to recover in individually housed polyurethane cages.

Ultrasonography

At the end of Phases I and III, rats were anesthetized in an induction chamber using 3% isoflurane and transferred to a pre-heated electronic ECG platform where 1-1.5% isoflurane was delivered via nosecone to maintain a sufficient plane of anesthesia. Fur from the chest and abdominal area was removed using an electric shaver followed by application of depilatory cream (Pharmaceutical Innovations, Newark, NJ). Electrode gel was placed on each of the ECG strips and the rat's limbs were situated in place using tape. Body temperature was measured via a rectal probe and contact gel preheated to 37°C was applied before performing echocardiography according to standard methods [103, 104].

Image acquisition was performed using the Vevo3100 Imaging system and MX250S transducer (Fujifilm Visualsonics, Inc., Toronto, ON). Assessment of left ventricular (LV) dimensions and systolic function was assessed using a short axis view in M-mode at the level of the papillary muscle. Left ventricular (LV) diastolic filling and function was assessed using pulsed wave doppler of transmitral blood flow velocities. These were located using color imaging superimposed over an apical four-chamber view. Myocardial function assessment was conducted using tissue doppler imaging (TDI) near the mitral annulus measured along

the apical axis. Pulse wave velocity (PWV) determination within the aortic arch was made via the determination of pulse transit time from the LV to a location measured proximally along the ascending aortic arch and one measured distally along the thoracic descending aorta. Distance between these points was measured using a B-mode image of this anatomical segment. Aortic PWV was calculated as the difference in pulse transit time (calculated using an ECG tracing as a reference) measured at these two points divided by the distance between them.

Renal resistive index (RRI) was determined using pulsed doppler measurements along the left main renal artery. RRI was calculated by taking the difference between systolic and diastolic velocity divided by the diastolic velocity at that time point [98]. Data analysis was performed offline using VevoLab and VevoVasc software (Fujifilm Visualsonics, Inc., Toronto, ON) in blinded fashion.

Analytical measurements and calculations

Hemodynamic Telemetry. Acquisition of hemodynamic data was conducted using Ponemah software (Data Sciences International, MN). Systolic blood pressure (SBP), diastolic blood pressure (DBP), mean arterial pressure (MAP), and heart rate (HR) were sampled for 10 seconds every 4 minutes at a sampling rate of 500 samples/second. Pulse pressure (PP) was calculated separately using these values. Baseline measurements were averaged over three days after cage acclimation. Sampling was performed at this rate continuously throughout Phases I and III within the metabolic cages.

Metabolic and Hormonal Assessment. Chow consumption was measured gravimetrically daily and caloric and sodium (Na⁺) values were determined based on dietary profiles for each feed.

At the end of Phase III and prior to terminal harvest, food was removed from caging at the beginning of the morning light cycles and terminal procedures were conducted at a minimum of 6 hours later to promote a semi-fasting state (as permitted by our Animal Use Committee). Glucose levels were determined using a One-Touch Ultra glucose monitor (LifeScan, Inc., Malpitas, CA) on 50 μ l blood from the arterial catheter. Arterial blood was collected into pre-chilled tubes containing ethylenediaminetetraacetic acid (EDTA) for plasma renin activity and into separate pre-chilled tubes containing 120 μ L of 500 mM sodium EDTA, 125 mM phenanthroline, 1 mM phenylmethanesulfonyl fluoride, 20 mM pepstatin, 1 mM enalapril and 10X phosphatase inhibitor cocktail for insulin. Once collected, blood was immediately centrifuged at 3000 rpm for 4 minutes at 4°C. Plasma was stored at -70°C until assay. PRA and insulin levels were measured using a standard Elisa kits (IBL International, Hamburg, Germany and Bertin Pharma SAS, Montigny-le-Bretonneux, France, respectively) Insulin sensitivity was calculated using the ratio of plasma glucose to insulin levels which was collected following a 6-hour minimum fasting period.

Rats were euthanized using sodium pentobarbital (120 mg/kg, IV) and hearts were excised and preserved in formalin solution for 24-48 hours before embedding for histological assessment.

Statistics. All values are presented as mean \pm standard error (SE). One-way analysis of variance (ANOVA) was used to determine differences among groups with a Sidak's multiple comparisons test for *post-hoc* analysis. To limit unnecessary reductions in adjusted statistical power resulting from excessive comparisons, once trends were discerned individual Holm-Sidak's tests were conducted on pre-selected groups. Two-way ANOVA's with repeated measures were performed to compare differences over time using a Sidak's

multiple comparisons test for *post-hoc* analysis. A *P*-value less than 0.05 was considered statistically significant. Due to the technical nature of many of these experimental techniques that required data acquisition of pre-determined anatomic sites for rigorous and reproducible analysis, *N*-values may differ across groups.

RESULTS

Caloric and sodium intakes. During baseline recordings, all rats in metabolic cages were placed on a pair feeding paradigm. Due to small but measurable differences in caloric profiles among diets, pair feeding was conducted using caloric consumption as an index rather than direct chow weight. Despite careful attempts to match caloric intakes, statistical differences among caloric intakes were observed following dietary changes from low salt to high salt feeds in Phase I, week 1 (FHS group) and in Phase III weeks 1 and 2 (FLS-GHS, FHS-GHS). Caloric intakes were no different among the groups by week 2 of Phase I and III except of the FLS-GHS group in Phase III that continued to ingest fewer calories (Table 4.1). Low salt fed rats consumed approximately 10% of the amount of sodium consumed by high salt fed rats consistent with their respective dietary sodium (Table 4.1).

Table 4.1: Daily Consumption Measurements.

		PHASE I					
		WEEK 1		WEEK 2		WEEK 3	
DIETARY REGIMEN	N	Caloric Intake (kcal/day)	Sodium Intake (mmols/day)	Caloric Intake (kcal/day)	Sodium Intake (mmols/day)	Caloric Intake (kcal/day)	Sodium Intake (mmols/day)
GLS	9	61.5±5	3.0± 0.3	68.4±4	3.0± 0.1	66.0±6	2.9± 0.1
FLS	9	60.7±8	2.7± 0.1	67.2±4	3.0± 0.1	65.7±5	3.2±0.3
FHS	19	51.9±7*	24.9±1.0*	63.9±4	30.9±1.8	64.0±5	31.0±2.3*
		PHASE III					
		WEEK 1		WEEK 2		WEEK 3	
DIETARY REGIMEN	N	Caloric Intake (kcal/day)	Sodium Intake (mmols/day)	Caloric Intake (kcal/day)	Sodium Intake (mmols/day)	Caloric Intake (kcal/day)	Sodium Intake (mmols/day)
GLS-GLS	9	62.6±6	2.8± 0.1	63.5±6	2.9± 0.1	64.3±5	2.8± 0.1
FLS-GHS	9	45.9±5*	22.1±0.8†	54.4±4*	26.2±0.7*	57.1±4†	27.5±0.6*
FHS-GHS	8	50.1±7*	23.3±1.2*	56.1±6*	26.0±0.8*	59.9±6	27.7±0.6*
FHS-FHS	9	60.5±5	27.5±0.8*	63.9±6	29.0±0.3*	66.4±8	29.9±1.0*

Table and data reconstituted from Chapter 3. Daily collection measurements recorded at 5 PM each day. Caloric intake calculated using caloric profiles of 3.98 kcal/g and 3.61 kcal/g for low salt and high salt feed, respectively. Values are indicated as mean ± SE, N as indicated per group; *p<0.05 vs. GLS-GLS controls; †-p<0.05 vs. FHS-FHS controls.

Hemodynamic effects. In Phase I, the addition of high salt in the diet of fructose fed rats led to a progressive increase in mean arterial pressure that was significantly elevated after four days (Data shown in Chapter 3, Figure 3.2). This increase was sustained for the subsequent two weeks. By the end of Phase I, the MAP had risen in all groups consistent with expected changes in blood pressure with maturation. Whereas the MAP did not differ among the groups at the end of Phase I, the change between baseline and final MAP values in the FHS group was statistically greater than that of other groups ($P<0.01$; Table 4.1A). The addition of high dietary salt to the FLS-GHS and FHS-GHS groups in Phase III led to significant increases in MAP within 1 week; levels which were maintained to the end of Phase III.

Table 4.2: Hemodynamic Measurements.

A	PHASE I			PHASE 3			
	GLS	FLS	FHS	GLS-FHS	FLS-GHS	FHS-GHS	FHS-FHS
MAP (MMHG)							
BASELINE	100.7±0.6	100.7±2.5	99.9±3.5	109.3±1.9	111.9±1.1	111.2±1.8	113.7±1.7
DELTA	6.8±0.7	7.6±1.1	10.5±0.7**	0.5±0.5	4.0±1.1*	3.8±1.1*	2.0±1.1

B		STUDY	STUDY	STUDY	STUDY	STUDY
DIETARY		Δ MAP	Δ SBP	Δ DBP	Δ HR	Δ PP
REGIMEN	N	(MMHG)	(MMHG)	(MMHG)	(BPM)	(MMHG)
GLS-GLS	7	10.0±1.0	11±2.2	11±1.2	-92±11	2.4±1.5
FLS-GHS	8	15±0.9*	18±0.9*	14±1.3	-103±18	4.2±1.6
FHS-GHS	8	15±1.4*	18±1.7*	13±1.7	-105±6	4.2±2.0
FHS-FHS	8	16±2.0**	19±2.3**	14±1.9	-89±14	4.6±1.4

A.) Hemodynamic calculations for MAP throughout phases. N-values are as follows: GLS – 9, FLS – 7, FHS – 18. B.) Study-wide changes in hemodynamics calculated as the difference between measurements taken at the end of Phase III and the baseline measurements taken at the beginning of Phase I. Values are indicated as mean ± SE, N as indicated per group; * $p < 0.05$ vs. GLS-GLS controls, ** $p < 0.01$ vs. GLS-GLS controls.

After the rats that had received fructose in Phase I with either low salt or high salt, were fed glucose-containing chow with high salt (FSL-GHS and FHS-GHS) or had been maintained on fructose and high salt throughout the protocol (FHS-FHS), systolic blood pressures at the end of Phase III had increased significantly compared with the GLS-GLS group that had ingested glucose and low salt chow throughout the study ($p < 0.05$). Diastolic blood pressures did not differ across any of the groups; MAP was significantly greater only in the FHS-FHS rats ($p < 0.01$). Therefore, the increases in MAP were driven predominately by systolic mechanisms. This did not, however, lead to a significant increase in pulse pressure. Additionally, no differences existed among groups when heart rate was assessed.

Early and late impairment of vascular compliance. Echocardiography and ultrasonography studies were performed immediately upon completion of Phases I and III. Regional measurements of vascular compliance were taken throughout the aortic arch and

the left main renal artery to assess PWV and RRI, respectively. In Phase I, FHS diet significantly increased PWV of the thoracic aorta, thereby indicating decreased aortic compliance compared to the GLS group (Figure 4.2). Maintenance of this diet throughout the protocol led to a significant increase in PWV in Phase III in both the FHS-GHS and FHS-FHS groups. No differences were observed in RRI of any of the groups at the end of Phase I (Figure 4.3). Similar to PWV values, FHS-GHS and FHS-FHS groups in Phase III displayed a statistically higher RRI than GLS-GLS rats. These trends were only elevated in Phase III and demonstrated no intra-group variability when compared to Phase I by two-way ANOVA.

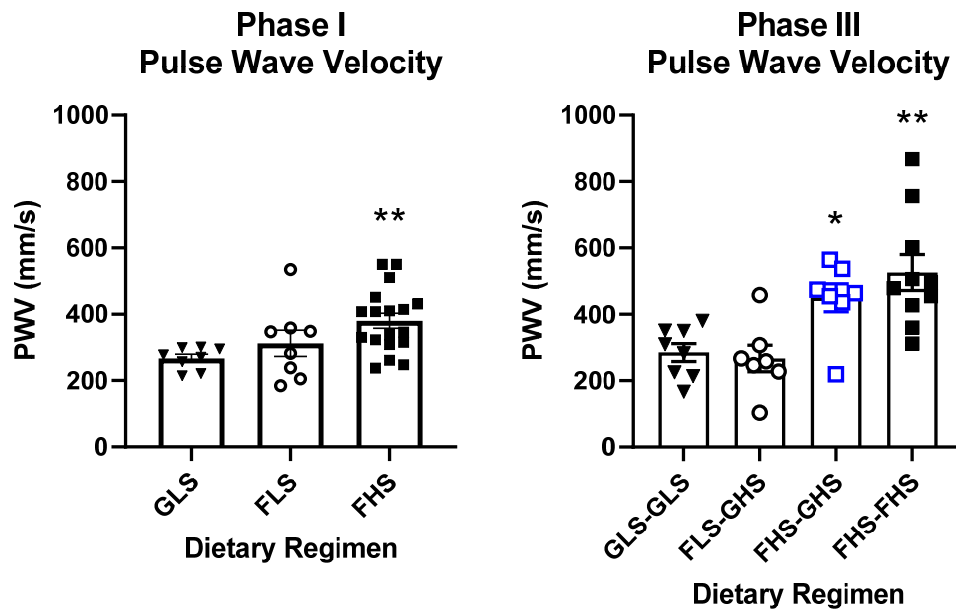


Figure 4.2: Assessment of Aortic Compliance. Measurements used for the assessment of thoracic aortic compliance in Phases 1 and 3. Values are indicated as mean \pm SE, N values are as follows: GLS-8, FLS-8, FHS-18, GLS-GLS - 8, FLS-GHS - 7, FHS-GHS - 8, FHS-FHS 10; * P <0.05 vs. GLS-GLS controls.

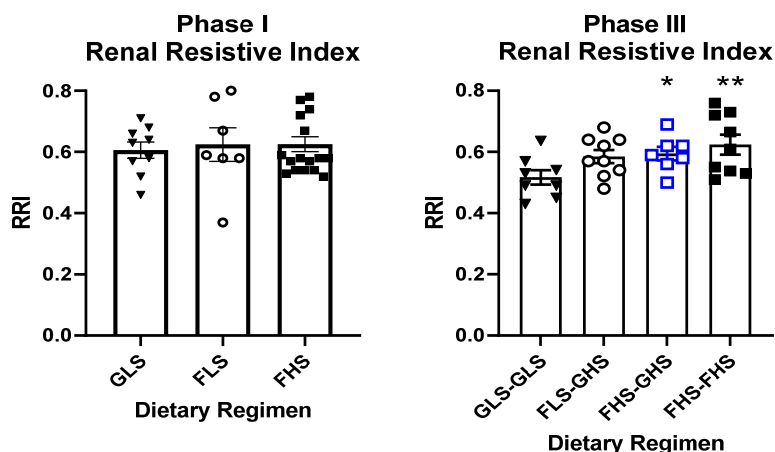


Figure 4.3: Assessment of Renal Resistive Index (RRI). Conducted in Phases 1 and 3. Doppler imaging measurements were made along the left main renal artery. Values are indicated as mean \pm SE, N values are as follows: GLS-9, FLS-6, FHS-16, GLS-GLS - 8, FLS-GHS - 9, FHS-GHS - 7, FHS-FHS - 9; * P <0.05 vs. GLS-GLS controls.

Table 4.3: Echocardiographic Parameters Assessed at the End of Phase III.

Group	GLS-GLS	FLS-GHS	FHS-GHS	FHS-FHS
<i>N</i>	9	8	8	10
<i>LVEF (%)</i>	74.9 \pm 3.4	77.3 \pm 4.4	80.3 \pm 3.7	78.2 \pm 2.3
<i>LVFS (%)</i>	46.0 \pm 3.4	49.1 \pm 4.4	51.9 \pm 4.4	48.8 \pm 2.4
<i>LVSID (mm)</i>	3.7 \pm 0.3	3.4 \pm 0.4	3.0 \pm 0.4	3.5 \pm 0.3
<i>LVDID (mm)</i>	6.7 \pm 0.3	6.5 \pm 0.3	6.1 \pm 0.4	6.9 \pm 0.4
<i>LVAW; Systole (mm)</i>	3.2 \pm 0.1	3.3 \pm 0.2	3.5 \pm 0.2	3.6 \pm 0.1
<i>LVAW; Diastole (mm)</i>	1.94 \pm 0.03	2.0 \pm 0.09	2.5 \pm 0.08**	2.2 \pm 0.14*
<i>LVPW; Systole (mm)</i>	3.5 \pm 0.1	3.5 \pm 0.2	4.0 \pm 0.3	4.0 \pm 0.2
<i>LVPW; Diastole (mm)</i>	2.3 \pm 0.1	2.4 \pm 0.1	3.0 \pm 0.3*	2.7 \pm 0.2
<i>LVTW; Systole (mm)</i>	6.8 \pm 0.2	6.8 \pm 0.4	7.4 \pm 0.3	7.6 \pm 0.4
<i>LVTW; Diastole (mm)</i>	4.3 \pm 0.1	4.4 \pm 0.2	5.6 \pm 0.4**	4.9 \pm 0.3
<i>LV Mass (mg)</i>	1190 \pm 73	1060 \pm 59	1401 \pm 56*	1373.0 \pm 75*

Abbreviations: LVEF, left ventricular ejection fraction; LVFS, left ventricular fractional shortening; LVSID, left ventricular systolic internal diameter; LVDID, left ventricular diastolic internal diameter; LVAW, left ventricular anterior wall width; LVPW, left ventricular posterior wall width; LVTW, left ventricular total wall width; LV Mass, Left ventricular mass. Values are mean \pm SE, n as indicated per group; * P <0.05 vs. GLS-GLS controls.

Echocardiographic assessment of dietary impacts. Physical assessment of the LV was performed using a short axis view and M-mode imaging. Table 4.3 depicts the results of LV echocardiography performed at the end of Phase III. No effect on standard systolic functional measures such as ejection fraction and fractional shortening were observed. LV mass

significantly increased in FHS-FHS and FHS-GHS test groups. Further assessment of structural morphology found changes in anterior and posterior wall thickness in FHS-GHS groups; these changes were more only significant during diastole. In the FHS-FHS group LV thickness only reached significance in the anterior wall. When assessed as a ratio of total wall thickness (sum of anterior and posterior walls) to diastolic diameter (radius cavity), there was a significant reduction in the ratio in FHS-GHS rats when compared with that of the GLS-GLS group (Figure 4.4). Taken together these measurements are indicative of ventricular hypertrophy and concentric remodeling.

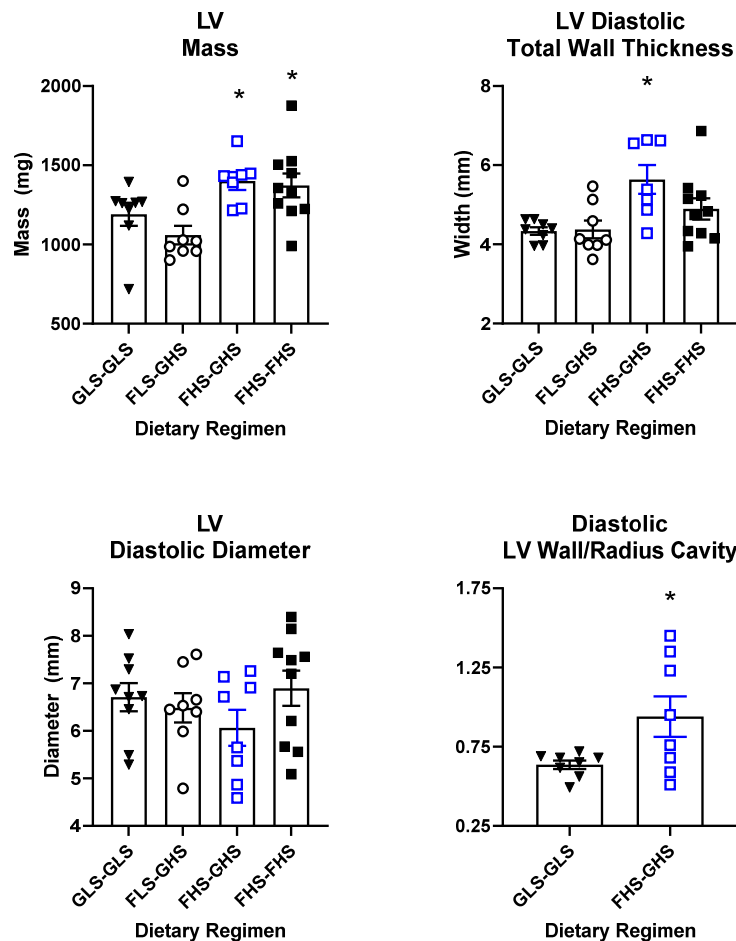


Figure 4.5. Assessment of Left Ventricular Morphology in Phase III. Conducted under a short axis view of the left ventricle using M-Mode. Total wall thickness is assessed as the sum of anterior and posterior LV wall widths and LV Wall/Radius cavity is assessed as the ratio of total wall thickness and end-diastolic diameter. Values are indicated as mean \pm SE, N as indicated per group; * $P < 0.05$ vs. GLS-GLS controls.

tissue doppler imaging of the mitral valve area. The ratio of early to late phase filling (E/A) demonstrated significant reductions in the FHS-FHS group. Values for E/A in Phase I and III, respectively, are shown in Figure 4.5. Reductions in the E/A ratio in the FLS-GHS and FHS-GHS test groups were also observed, although these values did not achieve significance. Likewise, decreases in mitral valve deceleration time were also observed across all groups when compared to the GLS-GLS group, however these were only significant in the FHS-FHS group. In contrast to these abnormal flow patterns, TDI did not observe any remarkable differences among groups.

Table 4.4: Parameters Associated with Diastolic Function Assessed at the End of Phase III.

Group	GLS-GLS	FLS-GHS	FHS-GHS	FHS-FHS
<i>N</i>	9	8	8	10
<i>Peak E (mm/s)</i>	706±22	630±45	652±41	641±39
<i>Peak A (mm/s)</i>	555±27	550±44	576±34	621±32
<i>E/A</i>	1.31±0.06	1.16±0.06	1.14±0.06*	1.03±0.04**
<i>DT (ms)</i>	39.5±4.0	28.0±2.2*	31.8±3.0	25.4±2.3**
<i>IVRT (ms)</i>	25.5±1.0	27.7±1.5	27.6±1.1	29.0±0.9 [†]
<i>E'(mm/s)</i>	34.1±2.6	32.3±4.6	34.2±4.0	27.4±1.8
<i>A'(mm/s)</i>	45.3±3.7	45.8±4.7	48±4.9	47.1±4.7
<i>E/E'</i>	22.5±1.9	25.2±6.2	21.1±3.3	24.3±2.3
<i>E'/A'</i>	0.81±0.01	0.71±0.09	0.81±0.15	0.64±0.01

Abbreviations: E, early phase ventricular filling; A, late phase ventricular filling; DT, mitral valve deceleration time; MV Area, mitral valve area; IVRT, isovolumetric relaxation time; E', mitral annulus early phase filling; A' Values are mean ± SE, n as indicated per group; * $p < 0.05$ vs. GLS-GLS controls, ** $p < 0.01$ vs. GLS-GLS controls. [†] $p < 0.05$ vs. GLS-GLS controls via unpaired student's t-test.



Figure 4.5: Assessment of Diastolic Function. Assessment of blood flow across the mitral valve as an indicator of diastolic function using the ratio of early phase left ventricular filling (E-Wave) and late phase left ventricular filling induced by atrial contraction (A-Wave) Values are indicated as mean \pm SE, GLS-9, FLS-7, FHS-18, GLS-GLS - 10, FLS-GHS - 9, FHS-GHS - 9, FHS-FHS - 10; * $p < 0.05$ vs. GLS-GLS controls, ** $p < 0.01$ vs. GLS-GLS controls.

Metabolic profiles are shown in Table 4.5. Initial weights and final weights demonstrated no differences among rats on different dietary regimens. FLS-GHS fed rats had a small, but insignificantly lower final body weight which was attributed to reduced caloric consumption at the beginning of Phase III following the change in chow from glucose with low salt to glucose with high salt content. Plasma glucose and insulin levels did not vary among the groups and were comparable to either vendor specifications for standard Sprague-Dawley rats on standard diets and rats fed control diets with no added sugar in similar studies [193-195]. Glucose: insulin ratio was significantly lower in the FHS-GHS group compared with GLS-GLS and FLS-GHS groups. FHS-FHS rats had an attenuated glucose:insulin ratio, but this was not significant. PRA was significantly reduced in FLS-GHS groups following high salt challenge at the end of Phase III. FHS-FHS rats had a similar, albeit

slightly blunted, inhibition of renin secretion that has been witnessed in prior studies [42]. Following high salt challenge, PRA was lower in FHS-GHS rats compared with GLS-GLS rats but did not achieve significance.

Table 4.5: Metabolic and Endocrine Assessment.

<i>Dietary Regimen</i>	<i>N</i>	<i>Initial weight (g)</i>	<i>Final Weight (g)</i>	<i>Heart Weight (g/kg)</i>	<i>Fasting Glucose (mg/dL)</i>	<i>Fasting Insulin (ng/mL)</i>	<i>G:I Ratio (x10⁶)</i>	<i>PRA (ng Ang I /mL/Hr)</i>
<i>GLS-GLS</i>	9	125±4	381±9	3.3±0.1	128±13	1.14±0.23	64.7±6.4	1.82±0.20
<i>FLS-GHS</i>	9	132±4	347±10	3.4±0.1	129±24	0.74±0.12	74.6±12.6	0.66±0.12**
<i>FHS-GHS</i>	8	128±3	362±12	3.2±0.1	126±14	1.33±0.12	31.6±1.9*	1.35±0.28
<i>FHS-FHS</i>	9	127±5	366±12	3.4±0.1	118±11	1.03±0.17	43.0±8.3	1.09±0.29*

Assay values conducted using blood samples collected through an intra-arterial line extracted under conscious conditions. Rats were fasted for a minimum of 6 hours prior to collection. Values are indicated as mean ± SE, N as indicated per group; * $P < 0.05$ vs. GLS-GLS controls, ** $P < 0.01$ vs. GLS-GLS controls. Due to technical complications, G:I (Glucose:Insulin) ratio N values differ and are as follows: GLS-GLS - 5, FLS-GHS - 6, FHS-GHS - 7, FHS-FHS - 7. *NOTE: Table adapted from Chapter 3, Table 4.

DISCUSSION

The major findings of this study support the hypothesis that fructose plus high salt programming early in life can have profound cardiovascular impacts in adulthood following the addition of high dietary sodium. Chronic feeding of FHS diet in our FHS-FHS group elicited more pronounced consequences than noted in prior studies conducted by our lab such as reduced aortic compliance and diastolic dysfunction [163]. Of note is the similar findings in cardiovascular parameters in FHS-GHS and FHS-FHS groups.

The addition of high salt to rats primed with a fructose diet elicits an increase in MAP driven by significant increases in systolic blood pressure. Slight increases in diastolic blood pressure occurred which prevented any statistically significant increases in pulse pressure. Study-wide increases in MAP were similar throughout all 3 groups fed with fructose. However, the statistically elevated MAP in the FLS-GHS groups were the result of the large increases observed in Phase III following high salt challenge. This alludes to the likelihood

that fructose alone (without the addition of high salt) is sufficient to chronically predispose the kidney to states of heightened salt-sensitivity that can lead to hypertension. Although the FLS-GHS group reach similar extents of hypertension, the problematic maladaptation of vascular stiffening and LV dysfunction were not as apparent as in other groups.

Pathologies underlying fructose-induced hypertension are increased sympathetic activity, endothelial dysfunction, and increased sodium retention leading to increased extracellular volume [52, 77]. Increased extracellular volume in the FHS group of Phase I is likely to play a large role in producing the increases in MAP. Increased extracellular volume is unlikely to be the only governing factor in prolonged FHS feeding, however. Indeed, increased arterial pressure over time alone can induce cellular and molecular alterations that deform the vascular wall [109]. Further, prolonged fructose feeding is associated with hyperinsulinemia which can cause increased circulating levels of endothelin-1 (ET-1), Ang II, and uric acid [32, 80, 196, 197]. It is of note that no significant differences in insulin levels or calculated insulin resistance via our modified G:I ratio approach were observed among groups. No evidence of hyperglycemia was present either. While it cannot be definitively concluded in this study that altered insulin signaling had no effect, the impact was likely nominal. Alternative pathologies such as reactive oxygen species (ROS) are more likely implicated in the observed endothelial dysfunction [66, 163].

Evidence of vascular dysfunction becomes evident in FHS groups by the end of Phase I as demonstrated by increased PWV, but in Phase III this effect becomes exacerbated in FHS-FHS groups both when compared to Phase III GLS-GLS controls as well as when compared to initial Phase I measurements using 2-way ANOVA with repeated measures. FHS-GHS fed rats exhibit a significant increase in PWV in Phase III that was not significantly elevated from

Phase I. Whether this is residual arterial dysfunction from Phase I or the result of additional factors is unclear. However, PRA was not significantly reduced from GLS-GLS controls at the time of terminal harvest despite the positive sodium balance observed in the FHS-GHS group. These levels differed from the significantly reduced PRA levels in FLS-GHS and FHS-FHS groups, indicating a contribution of the RAAS in maintaining the elevated MAP by the end of Phase III.

Numerous studies have been conducted to determine the capacity for clinical applicability of the renal resistive index (RRI) in determining renal function in association with the progression of hypertension, chronic nephropathy, and diabetes mellitus [198-201]. Further, many additional studies have found functional correlation between elevated RRI and intrarenal perfusion and renovascular resistance, but also correlation to various pathological conditions that occur in many of the above-mentioned diseases, such as tubulointerstitial damage and renal atherosclerosis [202-204].

While there is still controversy over the reliability of RRI as a measurement across all diseases [205], there is a general consensus regarding its relation to adverse cardiac and renal outcomes in hypertension [206, 207]. We observed significant increases in RRI in FHS-FHS and FHS-GHS groups only in Phase III. In some circumstances, the increase in renal artery resistance is a product of prolonged activation and/or resetting of renal autoregulatory mechanisms such as the myogenic response or tubuloglomerular feedback [208]. However, given the unremarkable response in RRI in the FLS-GHS group but statistical increase in FHS-GHS group to high salt challenge, it is unlikely that autoregulatory mechanisms play a significant role. Alternatively, renal resistance is also susceptible to changes in upstream and downstream vascular compliance and has been correlated to

increased pulsatility [98]. Concurrent with this theory is the decreased thoracic aortic compliance (calculated by PWV) observed in this present study.

Total peripheral resistance is a function of MAP and heart rate - an increase in either factor without a corresponding decrease in the other elevates total peripheral resistance [209]. In this study, this physiologic dysfunction is observed as both an increase in general systemic resistance and in lack of local aortic compliance. The net effect of these factors is an increase in ventricular afterload which can lead to left ventricular remodeling and subsequent hypertrophy [210]. Prior to the development of heart failure are the occurrence of early signs and symptoms of ventricular remodeling and mechanical dysfunction [211]. The significantly reduced E/A ratio in both FHS-GHS and FHS-FHS groups was evidence of diastolic dysfunction. In each of these groups ventricular wall sizes were increased, although this only statistically significant in FHS-GHS groups when compared to GLS-GLS controls. This implies hypertrophic growth that when assessed as a ratio of ventricular wall thickness to end-diastolic cavity size, a significant increase is observed. These changes did not result, however, in an overall increase in cardiac mass. These findings are consistent with concentric remodeling of the heart which is generally induced by chronic conditions of pressure-overload, such as in hypertension [212].

Whereas ventricular remodeling was not as pronounced in rats chronically fed FHS chow compared to the FHS-GHS group, mechanical dysfunction was more distinct. The decrease in the ratio of early to late diastolic filling was accompanied by an increase in isovolumetric relaxation time and decrease in mitral valve deceleration time. Mitral valve area is contrived from deceleration time and was therefore significantly increased. Shortening of the mitral valve deceleration time implies restrictive filling and has been

positively correlated to severe adverse cardiac events [213]. Each of these measurements are indicative of diastolic dysfunction and are phenotypes associated with either the development or presence of cardiomyopathy [214-216].

Limitations

Due to the overall protocol time length and material requirements, it was necessary to implement experimental group limitations to maintain consistent and equal allotment of animals into specified groups throughout each batch. Previous studies from differing labs have found no significant changes in arterial pressure or bodily sodium balance in rats fed a glucose and high salt diet in both acute and chronic settings. Concurrent with this are observations of no change in ultrasound and echocardiography studies. While the timeline of the study at present exceeds that of prior studies, we feel that our current choice of negative (GLS-GLS) and positive (FHS-FHS) control groups was sufficient to satisfactorily demonstrate changes associated with short term administration of high salt diet later in life.

Sex hormones play an important role in the development of hypertension following a high fructose diet. Female rats have been shown to be particularly resistant to the development of insulin resistance and therefore hyperinsulinemia specifically due to the presence of differing sex hormones. The purpose of this model is to demonstrate that hypertension can be induced using dietary regimens relevant to moderate consumption levels observed in modern society, and therefor with limited effects of insulin. While these effects are limited, they cannot be entirely negated; effective comparisons among groups with previous findings therefore necessitated the use of only one sex. Studies in female rats will be needed in the future.

Perspectives

Several studies demonstrating the effects of chronic carbohydrate consumption and the development of cardiomyopathy and heart failure exist, but these specifically rely on the development of diabetes and the associated pathologies [214, 217]. Hyperglycemia, hyperinsulinemia, and insulin resistance are associated even with pre-diabetic states and play an important role in developing the observed cardiovascular abnormalities [186]. In the present study we did not find remarkable evidence of any of these pathologies. The administration of free radical scavengers in this model prevents the development of hypertension and ameliorates aortic stiffening in matured rats [66, 163]. The vascular insults observed via ultrasound following Phase I grew progressively worse in the FHS-FHS controls and likely played a considerable pathologic role in the developed diastolic dysfunction. As the FLS-GHS groups did not display any aortic stiffening following the high salt challenge in Phase III, it can be speculated that what was observed in the FHS-GHS group was in part residual reductions in compliance from Phase I that may have been exacerbated by the addition of high dietary sodium. Alternatively, the exposure to both fructose *and* high salt early in life in Phase I is an important factor for later development of the vasculopathy and cardiomyopathy.

On the other hand, fructose feeding alone, without the addition of high dietary sodium during the critical developmental period is sufficient to induce a state of salt-sensitivity later in life which renders the body susceptible to hypertension. Chronically this can lead to various cardiac and renal co-morbidities such as heart failure and chronic kidney disease [218, 219]. Even FLS-GHS groups that became hypertensive only later in life had a reduction in diastolic function, indicated by the E/A ratio, but this was not significant. Contrastingly,

the addition of high salt to a moderate fructose diet during pubescent, developmental years had lasting effects on cardiac and renal function evidenced by diastolic dysfunction, ventricular hypertrophy, and failed renin suppression. This detriment occurred in rats that were fed this fructose and high salt diet chronically and those that were allowed a period of reprise from poor dietary conditions (FHS-GHS) groups. Indeed, diets with fructose fed early in life - with or without the presence of elevated sodium - promote adaptations that render the body increasingly vulnerable to complications caused by even modest dietary insults; these insults are long lasting and with severe consequence.

CHAPTER 5: CONCLUSIONS AND FUTURE DIRECTIONS

The present studies indicate that consumption of even a moderate fructose diet induces states of salt-sensitivity that can result in hypervolemia and rapid induction of hypertension. The robust initial increase in arterial pressure does not necessarily continue to progress as numerous regulatory mechanisms such as diuresis become increasingly active. While these responses are sufficient to curb the rising arterial pressure, they are unable to entirely restore normotensive states, indicating abnormally functioning regulatory systems. The result is a modest overall increase in arterial pressure that can lead to cardiovascular and renal dysfunction in relatively short periods of time.

Whereas further studies are necessary to determine the permanence of fructose-induced complications, it is apparent from the studies at present that provision of fructose during developmental periods in youth leads to a programmed salt-sensitivity which extend into adulthood. In this model the salt-sensitivity is driven by renal mechanisms. A particularly novel observation made in these studies was that this state of salt-sensitivity is no longer dependent on the concomitant consumption of fructose. Further, the increases in arterial pressure that arise from the addition of high dietary sodium are accompanied by phenotypes of cardiovascular and renal dysfunction similar in nature and extent to those of rats chronically fed a fructose and high sodium diet since early adolescence.

The ratio of early to late phase ventricular filling (E/A ratio) assessed via trans-mitral flow imaging is effectively the most reliable indicator of diastolic function. Unfortunately, there is an inherent degree of bluntness behind its use as it serves as an overall index of function and provides very little mechanistic insight, thereby necessitating several other measurements to not only confirm the presence of dysfunction, but also to determine the

precise pathologic origins. Furthermore, it is subject to error particularly in animal models where heart rate is much higher than that of a human. Indeed, subjects with elevated resting heart rates make not only the discernment of E and A waves challenging, but it can also affect the magnitude itself of each wave form [220]. Such inaccuracies can ultimately sufficiently affect statistical analyses such that observable trends become dismissed.

The dismissal of such trends is not indicative of Type 1 error so much as it is a result of various pitfalls associated with standard echocardiography. Regional measurements of the rate of deformation by which cardiac fibers displace themselves throughout the cardiac cycle, also known as strain and strain rate assessment, provides a unique methodology by which to measure changes in cardiac function. This technique observes trends in myocardial detriment with greater sensitivity and is favorable in instances in which frank cardiac disturbances are only beginning to manifest, such as in early stages of diabetes. Particularly in FLS-GHS groups, where the E/A ratio declined but ultimately did not reach significance, strain and strain rate assessment may provide additional insight. Furthermore, this technique may reveal preliminary changes that occur in youth that were previously unobservable. The subtlety by which diastolic dysfunction occurs in this model warrants further investigation. Early detection of these malignant adaptations is critical for the employment of interventional strategies in the prevention of severe future complications.

APPENDIX A
IACUC Protocol Approval Letters



**INSTITUTIONAL ANIMAL
CARE AND USE COMMITTEE**
87 E. Canfield, Second Floor
Detroit, MI 48201-2011
Telephone: (313) 577-1629
Fax Number: (313) 577-1941

ANIMAL WELFARE ASSURANCE # A3310-01

PROTOCOL # A 05-01-16 (VAMC)

Protocol Effective Period: June 10, 2016 – May 31, 2019

Year 2 Annual Review Date: June 1, 2017

TO: Dr. Noreen Rossi
Department of Internal Medicine
Division of Nephrology
LL 313 Veterans Administration Medical Center

FROM: Lisa Anne Polin, Ph.D. *Lisa Anne Polin*
Chairperson
Institutional Animal Care and Use Committee

SUBJECT: Approval of Protocol # A 05-01-16 (VAMC)
"Exercise training and blood pressure in hypertension: integrated mechanisms (VAMC)"

DATE: May 1, 2017

The Annual Review of your animal research protocol and any applicable grant applications has been conducted and approved by the Wayne State University Institutional Animal Care and Use Committee (IACUC). The species and number of animals approved for the duration of this protocol are listed below.

<u>Species</u>	<u>Strain</u>	<u>Qty.</u>	<u>Cat.</u>
RATS.....	Sprague Dawley, male, 200-250 gm.....	608.....	D
RATS.....	Sprague Dawley, male, 200-250 gm.....	576.....	E
RATS.....	Sprague Dawley, female, 200-250 gm.....	96.....	D
RATS.....	Sprague Dawley, female, 200-250 gm.....	320.....	E

<u>Species Amendments</u>	<u>Strain</u>	<u>Qty.</u>	<u>Cat.</u>
RATS.....	Sprague Dawley, male 200-250 g.....	100.....	D

Be advised that any change in the procedures used, a change in species, or additional numbers of animals requires prior approval by the IACUC. Any animal work on this research protocol beyond the expiration date will require the submission of a new IACUC protocol form and full committee review.

The Guide for the Care and Use of Laboratory Animals is the primary reference used for standards of animal care at Wayne State University. The University has submitted an appropriate assurance statement to the Office of Laboratory Animal Welfare (OLAW) of the National Institutes of Health. The animal care program at Wayne State University is accredited by the Association for Assessment and Accreditation of Laboratory Animal Care International (AAALAC).



Institutional Animal Care and Use Committee

87 East Canfield, Second Floor
Detroit, MI 48201
Phone: (313) 577-1629
www.research.wayne.edu/iacuc/

ANIMAL WELFARE ASSURANCE # D16-00198 (A3310-01)

TO: Noreen Rossi
Internal Medicine

FROM: Institutional Animal Care and Use Committee

DATE: February 17, 2020

SUBJECT: Approval of Amendment to Protocol IACUC-19-03-1001

TITLE: Exercise training and blood pressure in hypertension: integrated mechanisms (VAMC)

Protocol Effective Period: February 17, 2020 - May 21, 2022

The recent amendment to your animal research protocol has been approved by the Wayne State University Institutional Animal Care and Use Committee (IACUC).

Be advised that this protocol must be reviewed by the IACUC on an annual basis to remain active. Any changes (e.g. procedures, lab personnel, strains, additional numbers of animals) must be submitted as amendments and require prior approval by the IACUC. Any animal work on this research protocol beyond the expiration date will require the submission of a new IACUC protocol application for committee review and approval.

The *Guide for the Care and Use of Laboratory Animals* (the Guide, NRC 2011) is the primary reference used for standards of animal care at Wayne State University. The University has submitted an appropriate assurance statement to the Office for Laboratory Animal Welfare (OLAW) of the National Institutes of Health. The animal care program at Wayne State University is accredited by the Association for Assessment and Accreditation of Laboratory Animal Care International (AAALAC).

APPENDIX B

CHAPTER 1 LICENCE AGREEMENT

*Komnenov D, ***Levanovich PE**, Perecki N, Chung CS, Rossi NF. Aortic Stiffness and Diastolic Dysfunction in Sprague Dawley Rats Consuming Short-Term Fructose Plus High Salt Diet. Integr Blood Press Control. 2020 Sep 28;13:111-124. doi: 10.2147/IBPC.S257205. eCollection 2020. PMID: 33061560 **Free PMC article**. *Indicates Co-first authorship.

This work is published and licensed by **Dove Medical Press Limited**. The full terms of this license are available at <https://www.dovepress.com/terms.php> and incorporate the Creative Commons Attribution – Non Commercial (unported, v3.0) License (<http://creativecommons.org/licenses/by-nc/3.0/>). By accessing the work you hereby accept the Terms. Non-commercial uses of the work are permitted without any further permission from Dove Medical Press Limited, provided the work is properly attributed. For permission for commercial use of this work, please see paragraphs 4.2 and 5 of our Terms (<https://www.dovepress.com/terms.php>).

creative commons | Share your work | Use & remix | What We do | Blo

Help us build a vibrant, collaborative global commons [Donate Now](#)

This page is available in the following languages: English

Attribution-NonCommercial 3.0 Unported (CC BY-NC 3.0)

This is a human-readable summary of (and not a substitute for) the license. [Disclaimer](#).

You are free to:

- Share** — copy and redistribute the material in any medium or format
- Adapt** — remix, transform, and build upon the material

The licensor cannot revoke these freedoms as long as you follow the license terms.

Under the following terms:

- Attribution** — You must give appropriate credit, provide a link to the license, and indicate if changes were made. You may do so in any reasonable manner, but not in any way that suggests the licensor endorses you or your use.
- NonCommercial** — You may not use the material for commercial purposes.

No additional restrictions — You may not apply legal terms or technological measures that legally restrict others from doing anything the license permits.

Notices:

You do not have to comply with the license for elements of the material in the public domain or where your use is permitted by an applicable [exception or limitation](#).

No warranties are given. The license may not give you all of the permissions necessary for your intended use. For example, other rights such as [publicity, privacy, or moral rights](#) may limit how you use the material.

APPENDIX C

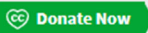
CHAPTER 2 LICENCE AGREEMENT

*Komnenov D, ***Levanovich PE**, Rossi NF. Hypertension Associated with Fructose and High Salt: Renal and Sympathetic Mechanisms. *Nutrients*. 2019 Mar 7;11(3):569. doi: 10.3390/nu11030569. PMID: 30866441 **Free PMC article**. *Indicates Co-first authorship.

Licensee MDPI, Basel, Switzerland. This article is an open access article distributed under the terms and conditions of the Creative Commons Attribution (CC BY) license (<http://creativecommons.org/licenses/by/4.0/>).

Search for CC images | Global Network | Newsletters | Store | Contact |   

 | [Share your work](#) | [Use & remix](#) | [What We do](#) | [Blog](#)

Help us build a vibrant, collaborative global commons 

This page is available in the following languages:  English

Attribution 4.0 International (CC BY 4.0)

This is a human-readable summary of (and not a substitute for) the license. [Disclaimer](#)

You are free to:

Share — copy and redistribute the material in any medium or format

Adapt — remix, transform, and build upon the material for any purpose, even commercially.

The licensor cannot revoke these freedoms as long as you follow the license terms.



Under the following terms:

 **Attribution** — You must give [appropriate credit](#), provide a link to the license, and [indicate if changes were made](#). You may do so in any reasonable manner, but not in any way that suggests the licensor endorses you or your use.

No additional restrictions — You may not apply legal terms or [technological measures](#) that legally restrict others from doing anything the license permits.

Notices:

You do not have to comply with the license for elements of the material in the public domain or where your use is permitted by an applicable [exception or limitation](#).

No warranties are given. The license may not give you all of the permissions necessary for your intended use. For example, other rights such as [publicity, privacy, or moral rights](#) may limit how you use the material.

REFERENCES

1. Carretero, O.A. and S. Oparil, *Essential hypertension. Part I: definition and etiology.* *Circulation*, 2000. **101**(3): p. 329-35.
2. Messerli, F.H., B. Williams, and E. Ritz, *Essential hypertension.* *Lancet*, 2007. **370**(9587): p. 591-603.
3. Egan, B.M., Y. Zhao, and R.N. Axon, *US trends in prevalence, awareness, treatment, and control of hypertension, 1988-2008.* *JAMA*, 2010. **303**(20): p. 2043-50.
4. Yano, Y., et al., *Association of Blood Pressure Classification in Young Adults Using the 2017 American College of Cardiology/American Heart Association Blood Pressure Guideline With Cardiovascular Events Later in Life.* *JAMA*, 2018. **320**(17): p. 1774-1782.
5. Dorans, K.S., et al., *Trends in Prevalence and Control of Hypertension According to the 2017 American College of Cardiology/American Heart Association (ACC/AHA) Guideline.* *J Am Heart Assoc*, 2018. **7**(11).
6. Mills, K.T., et al., *Global Disparities of Hypertension Prevalence and Control: A Systematic Analysis of Population-Based Studies From 90 Countries.* *Circulation*, 2016. **134**(6): p. 441-50.
7. Taylor, B.C., T.J. Wilt, and H.G. Welch, *Impact of diastolic and systolic blood pressure on mortality: implications for the definition of "normal".* *J Gen Intern Med*, 2011. **26**(7): p. 685-90.
8. Bowe, B., et al., *Changes in the US Burden of Chronic Kidney Disease From 2002 to 2016: An Analysis of the Global Burden of Disease Study.* *JAMA Netw Open*, 2018. **1**(7): p. e184412.

9. Lerman, L.O., et al., *Animal models of hypertension: an overview*. J Lab Clin Med, 2005. **146**(3): p. 160-73.
10. Warden, C.H. and J.S. Fisler, *Comparisons of diets used in animal models of high-fat feeding*. Cell Metab, 2008. **7**(4): p. 277.
11. Alberti, K.G., et al., *Harmonizing the metabolic syndrome: a joint interim statement of the International Diabetes Federation Task Force on Epidemiology and Prevention; National Heart, Lung, and Blood Institute; American Heart Association; World Heart Federation; International Atherosclerosis Society; and International Association for the Study of Obesity*. Circulation, 2009. **120**(16): p. 1640-5.
12. Bray, G.A., S.J. Nielsen, and B.M. Popkin, *Consumption of high-fructose corn syrup in beverages may play a role in the epidemic of obesity*. Am J Clin Nutr, 2004. **79**(4): p. 537-43.
13. Tappy, L. and K.A. Le, *Metabolic effects of fructose and the worldwide increase in obesity*. Physiol Rev, 2010. **90**(1): p. 23-46.
14. Zhang, D.M., R.Q. Jiao, and L.D. Kong, *High Dietary Fructose: Direct or Indirect Dangerous Factors Disturbing Tissue and Organ Functions*. Nutrients, 2017. **9**(4).
15. Marshall, R.O. and E.R. Kooi, *Enzymatic conversion of D-glucose to D-fructose*. Science, 1957. **125**(3249): p. 648-9.
16. Hanover, L.M. and J.S. White, *Manufacturing, composition, and applications of fructose*. Am J Clin Nutr, 1993. **58**(5 Suppl): p. 724S-732S.
17. Marriott, B.P., N. Cole, and E. Lee, *National estimates of dietary fructose intake increased from 1977 to 2004 in the United States*. J Nutr, 2009. **139**(6): p. 1228S-1235S.

18. Jayalath, V.H., et al., *Total fructose intake and risk of hypertension: a systematic review and meta-analysis of prospective cohorts*. J Am Coll Nutr, 2014. **33**(4): p. 328-39.
19. Jayalath, V.H., et al., *Sugar-sweetened beverage consumption and incident hypertension: a systematic review and meta-analysis of prospective cohorts*. Am J Clin Nutr, 2015. **102**(4): p. 914-21.
20. Benjamin, E.J., et al., *Heart Disease and Stroke Statistics-2018 Update: A Report From the American Heart Association*. Circulation, 2018. **137**(12): p. e67-e492.
21. Beunza, J.J., et al., *Sedentary behaviors and the risk of incident hypertension: the SUN Cohort*. Am J Hypertens, 2007. **20**(11): p. 1156-62.
22. Bowman, T.S., et al., *A prospective study of cigarette smoking and risk of incident hypertension in women*. J Am Coll Cardiol, 2007. **50**(21): p. 2085-92.
23. Forman, J.P., M.J. Stampfer, and G.C. Curhan, *Diet and lifestyle risk factors associated with incident hypertension in women*. JAMA, 2009. **302**(4): p. 401-11.
24. Wang, L., et al., *Meat intake and the risk of hypertension in middle-aged and older women*. J Hypertens, 2008. **26**(2): p. 215-22.
25. Ford, C.D., et al., *Psychosocial Factors Are Associated With Blood Pressure Progression Among African Americans in the Jackson Heart Study*. Am J Hypertens, 2016. **29**(8): p. 913-24.
26. Hall, J.E., *The kidney, hypertension, and obesity*. Hypertension, 2003. **41**(3 Pt 2): p. 625-33.
27. Jones, D.W., et al., *Body mass index and blood pressure in Korean men and women: the Korean National Blood Pressure Survey*. J Hypertens, 1994. **12**(12): p. 1433-7.
28. Le, M.T., et al., *Effects of high-fructose corn syrup and sucrose on the pharmacokinetics*

- of fructose and acute metabolic and hemodynamic responses in healthy subjects.* Metabolism, 2012. **61**(5): p. 641-51.
29. Johnson, R.J., et al., *Hypothesis: could excessive fructose intake and uric acid cause type 2 diabetes?* Endocr Rev, 2009. **30**(1): p. 96-116.
30. Hwang, I.S., et al., *Fructose-induced insulin resistance and hypertension in rats.* Hypertension, 1987. **10**(5): p. 512-6.
31. Martinez, F.J., R.A. Rizza, and J.C. Romero, *High-fructose feeding elicits insulin resistance, hyperinsulinism, and hypertension in normal mongrel dogs.* Hypertension, 1994. **23**(4): p. 456-63.
32. Tran, L.T., V.G. Yuen, and J.H. McNeill, *The fructose-fed rat: a review on the mechanisms of fructose-induced insulin resistance and hypertension.* Mol Cell Biochem, 2009. **332**(1-2): p. 145-59.
33. Brown, C.M., et al., *Fructose ingestion acutely elevates blood pressure in healthy young humans.* Am J Physiol Regul Integr Comp Physiol, 2008. **294**(3): p. R730-7.
34. Perez-Pozo, S.E., et al., *Excessive fructose intake induces the features of metabolic syndrome in healthy adult men: role of uric acid in the hypertensive response.* Int J Obes (Lond), 2010. **34**(3): p. 454-61.
35. Dai, S. and J.H. McNeill, *Fructose-Induced Hypertension in Rats Is Concentration-Dependent and Duration-Dependent.* Journal of Pharmacological and Toxicological Methods, 1995. **33**(2): p. 101-107.
36. Glushakova, O., et al., *Fructose induces the inflammatory molecule ICAM-1 in endothelial cells.* J Am Soc Nephrol, 2008. **19**(9): p. 1712-20.
37. Aroor, A.R., et al., *The role of tissue Renin-Angiotensin-aldosterone system in the*

- development of endothelial dysfunction and arterial stiffness*. Front Endocrinol (Lausanne), 2013. **4**: p. 161.
38. Katakam, P.V., et al., *Endothelial dysfunction precedes hypertension in diet-induced insulin resistance*. Am J Physiol, 1998. **275**(3 Pt 2): p. R788-92.
 39. Singh, A.K., et al., *Fructose-induced hypertension: essential role of chloride and fructose absorbing transporters PAT1 and Glut5*. Kidney International, 2008. **74**(4): p. 438-447.
 40. Cabral, P.D., et al., *Fructose stimulates Na/H exchange activity and sensitizes the proximal tubule to angiotensin II*. Hypertension, 2014. **63**(3): p. e68-73.
 41. Gordish, K.L., et al., *Moderate (20%) fructose-enriched diet stimulates salt-sensitive hypertension with increased salt retention and decreased renal nitric oxide*. Physiol Rep, 2017. **5**(7).
 42. Soncrant, T., et al., *Bilateral renal cryodenervation decreases arterial pressure and improves insulin sensitivity in fructose-fed Sprague-Dawley rats*. Am J Physiol Regul Integr Comp Physiol, 2018. **315**(3): p. R529-R538.
 43. de Wardener, H.E., F.J. He, and G.A. MacGregor, *Plasma sodium and hypertension*. Kidney Int, 2004. **66**(6): p. 2454-66.
 44. Haddy, F.J., *Role of dietary salt in hypertension*. Life Sci, 2006. **79**(17): p. 1585-92.
 45. Karppanen, H. and E. Mervaala, *Sodium intake and hypertension*. Prog Cardiovasc Dis, 2006. **49**(2): p. 59-75.
 46. Meneton, P., et al., *Links between dietary salt intake, renal salt handling, blood pressure, and cardiovascular diseases*. Physiol Rev, 2005. **85**(2): p. 679-715.
 47. Cheeseman, C.I. and B. Harley, *Adaptation of glucose transport across rat enterocyte*

- basolateral membrane in response to altered dietary carbohydrate intake.* J Physiol, 1991. **437**: p. 563-75.
48. Gould, G.W., et al., *Expression of human glucose transporters in Xenopus oocytes: kinetic characterization and substrate specificities of the erythrocyte, liver, and brain isoforms.* Biochemistry, 1991. **30**(21): p. 5139-45.
 49. Kane, S., M.J. Seatter, and G.W. Gould, *Functional studies of human GLUT5: Effect of pH on substrate selection and an analysis of substrate interactions.* Biochemical and Biophysical Research Communications, 1997. **238**(2): p. 503-505.
 50. Leturque, A., et al., *The role of GLUT2 in dietary sugar handling.* Journal of Physiology and Biochemistry, 2005. **61**(4): p. 529-537.
 51. Wang, Z., et al., *Identification of an apical Cl(-)/HCO3(-) exchanger in the small intestine.* Am J Physiol Gastrointest Liver Physiol, 2002. **282**(3): p. G573-9.
 52. Soleimani, M. and P. Alborzi, *The role of salt in the pathogenesis of fructose-induced hypertension.* Int J Nephrol, 2011. **2011**: p. 392708.
 53. Dudeja, P.K., et al., *Intestinal distribution of human Na⁺/H⁺ exchanger isoforms NHE-1, NHE-2, and NHE-3 mRNA.* Am J Physiol, 1996. **271**(3 Pt 1): p. G483-93.
 54. Seidler, U., et al., *Sodium and chloride absorptive defects in the small intestine in Slc26a6 null mice.* Pflugers Arch, 2008. **455**(4): p. 757-66.
 55. Dantzler, W.H., *Comparative physiology of the vertebrate kidney.* Zoophysiology. 1989, Berlin ; New York: Springer-Verlag. x, 198 p.
 56. Boron, W.F. and E.L. Boulpaep, *Medical physiology : a cellular and molecular approach.* Updated second edition. ed. 2012, Philadelphia, PA: Saunders/Elsevier. xiii, 1337 pages.

57. Aldred, K.L., P.J. Harris, and E. Eitle, *Increased proximal tubule NHE-3 and H⁺-ATPase activities in spontaneously hypertensive rats*. J Hypertens, 2000. **18**(5): p. 623-8.
58. Tank, J.E., O.W. Moe, and W.L. Henrich, *Abnormal regulation of proximal tubule renin mRNA in the Dahl/Rapp salt-sensitive rat*. Kidney Int, 1998. **54**(5): p. 1608-16.
59. Alpern, R.J., M.G. Cogan, and F.C. Rector, Jr., *Effect of luminal bicarbonate concentration on proximal acidification in the rat*. Am J Physiol, 1982. **243**(1): p. F53-9.
60. Queiroz-Leite, G.D., et al., *Fructose acutely stimulates NHE3 activity in kidney proximal tubule*. Kidney Blood Press Res, 2012. **36**(1): p. 320-34.
61. Gonzalez-Vicente, A., et al., *Dietary Fructose Enhances the Ability of Low Concentrations of Angiotensin II to Stimulate Proximal Tubule Na(+) Reabsorption*. Nutrients, 2017. **9**(8).
62. Gonzalez-Vicente, A., et al., *Dietary Fructose Increases the Sensitivity of Proximal Tubules to Angiotensin II in Rats Fed High-Salt Diets*. Nutrients, 2018. **10**(9).
63. Song, J., et al., *Effects of dietary fat, NaCl, and fructose on renal sodium and water transporter abundances and systemic blood pressure*. Am J Physiol Renal Physiol, 2004. **287**(6): p. F1204-12.
64. Ares, G.R., K.M. Kassem, and P.A. Ortiz, *Fructose acutely stimulates NKCC2 activity in rat thick ascending limbs (TALs) by increasing surface NKCC2 expression*. Am J Physiol Renal Physiol, 2018.
65. Xu, C., et al., *Activation of Renal (Pro)Renin Receptor Contributes to High Fructose-Induced Salt Sensitivity*. Hypertension, 2017. **69**(2): p. 339-348.
66. Zenner, Z.P., K.L. Gordish, and W.H. Beierwaltes, *Free radical scavenging reverses fructose-induced salt-sensitive hypertension*. Integr Blood Press Control, 2018. **11**: p.

- 1-9.
67. Giacchetti, G., et al., *The tissue renin-angiotensin system in rats with fructose-induced hypertension: overexpression of type 1 angiotensin II receptor in adipose tissue.* J Hypertens, 2000. **18**(6): p. 695-702.
 68. Dhar, I., et al., *Increased methylglyoxal formation with upregulation of renin angiotensin system in fructose fed Sprague Dawley rats.* PLoS One, 2013. **8**(9): p. e74212.
 69. Yokota, R., et al., *Intra-Renal Angiotensin Levels Are Increased in High-Fructose Fed Rats in the Extracorporeal Renal Perfusion Model.* Front Physiol, 2018. **9**: p. 1433.
 70. Esler, M.D., et al., *Catheter-based renal denervation for treatment of patients with treatment-resistant hypertension: 36 month results from the SYMPPLICITY HTN-2 randomized clinical trial.* Eur Heart J, 2014. **35**(26): p. 1752-9.
 71. Krum, H., et al., *Percutaneous renal denervation in patients with treatment-resistant hypertension: final 3-year report of the Symplicity HTN-1 study.* Lancet, 2014. **383**(9917): p. 622-9.
 72. Osborn, J.W. and J.D. Foss, *Renal Nerves and Long-Term Control of Arterial Pressure.* Compr Physiol, 2017. **7**(2): p. 263-320.
 73. DiBona, G.F., *Physiology in perspective: The Wisdom of the Body. Neural control of the kidney.* Am J Physiol Regul Integr Comp Physiol, 2005. **289**(3): p. R633-41.
 74. Teff, K.L., et al., *Dietary fructose reduces circulating insulin and leptin, attenuates postprandial suppression of ghrelin, and increases triglycerides in women.* J Clin Endocrinol Metab, 2004. **89**(6): p. 2963-72.
 75. Zeng, W., et al., *Sympathetic neuro-adipose connections mediate leptin-driven lipolysis.*

- Cell, 2015. **163**(1): p. 84-94.
76. Tappy, L. and K.A. Le, *Does fructose consumption contribute to non-alcoholic fatty liver disease?* Clin Res Hepatol Gastroenterol, 2012. **36**(6): p. 554-60.
77. Klein, A.V. and H. Kiat, *The mechanisms underlying fructose-induced hypertension: a review.* J Hypertens, 2015. **33**(5): p. 912-20.
78. Tran, L.T., K.M. MacLeod, and J.H. McNeill, *Selective alpha(1)-adrenoceptor blockade prevents fructose-induced hypertension.* Mol Cell Biochem, 2014. **392**(1-2): p. 205-11.
79. Li, R.Z., et al., *Beneficial Effect of Genistein on Diabetes-Induced Brain Damage in the ob/ob Mouse Model.* Drug Des Devel Ther, 2020. **14**: p. 3325-3336.
80. Verma, S., S. Bhanot, and J.H. McNeill, *Effect of chronic endothelin blockade in hyperinsulinemic hypertensive rats.* Am J Physiol, 1995. **269**(6 Pt 2): p. H2017-21.
81. Jiang, J., et al., *Endothelin-1 blockade prevents COX2 induction and TXA2 production in the fructose hypertensive rat.* Can J Physiol Pharmacol, 2007. **85**(3-4): p. 422-9.
82. Tran, L.T., K.M. MacLeod, and J.H. McNeill, *Endothelin-1 modulates angiotensin II in the development of hypertension in fructose-fed rats.* Mol Cell Biochem, 2009. **325**(1-2): p. 89-97.
83. Shinozaki, K., et al., *Evidence for a causal role of the renin-angiotensin system in vascular dysfunction associated with insulin resistance.* Hypertension, 2004. **43**(2): p. 255-62.
84. Coker, M.L., et al., *Matrix metalloproteinase expression and activity in isolated myocytes after neurohormonal stimulation.* Am J Physiol Heart Circ Physiol, 2001. **281**(2): p. H543-51.
85. Benjamin, E.J., et al., *Heart Disease and Stroke Statistics-2019 Update: A Report From*

- the American Heart Association. Circulation, 2019. 139(10): p. e56-e528.*
86. Lewington, S., et al., *Age-specific relevance of usual blood pressure to vascular mortality: a meta-analysis of individual data for one million adults in 61 prospective studies. Lancet, 2002. 360(9349): p. 1903-13.*
 87. Brown, I.J., et al., *Sugar-Sweetened Beverage, Sugar Intake of Individuals, and Their Blood Pressure International Study of Macro/Micronutrients and Blood Pressure. Hypertension, 2011. 57(4): p. 695-+.*
 88. Palanisamy, N. and A.C. Venkataraman, *Beneficial effect of genistein on lowering blood pressure and kidney toxicity in fructose-fed hypertensive rats. Br J Nutr, 2013. 109(10): p. 1806-12.*
 89. Kopp, U.C. and G.F. Dibona, *Interaction between Epinephrine and Renal Nerves in Control of Renin Secretion Rate. American Journal of Physiology, 1986. 250(6): p. F999-1007.*
 90. Cooper, L.L., et al., *Components of hemodynamic load and cardiovascular events: the Framingham Heart Study. Circulation, 2015. 131(4): p. 354-61; discussion 361.*
 91. Kaess, B.M., et al., *Aortic stiffness, blood pressure progression, and incident hypertension. JAMA, 2012. 308(9): p. 875-81.*
 92. Cavalcante, J.L., et al., *Aortic stiffness: current understanding and future directions. J Am Coll Cardiol, 2011. 57(14): p. 1511-22.*
 93. Teixeira, R., et al., *Ultrasonographic vascular mechanics to assess arterial stiffness: a review. Eur Heart J Cardiovasc Imaging, 2016. 17(3): p. 233-46.*
 94. Ben-Shlomo, Y., et al., *Aortic Pulse Wave Velocity Improves Cardiovascular Event Prediction An Individual Participant Meta-Analysis of Prospective Observational Data*

- From 17,635 Subjects*. Journal of the American College of Cardiology, 2014. **63**(7): p. 636-646.
95. Vlachopoulos, C., K. Aznaouridis, and C. Stefanadis, *Prediction of Cardiovascular Events and All-Cause Mortality With Arterial Stiffness A Systematic Review and Meta-Analysis*. Journal of the American College of Cardiology, 2010. **55**(13): p. 1318-1327.
96. Bjallmark, A., et al., *Ultrasonographic strain imaging is superior to conventional non-invasive measures of vascular stiffness in the detection of age-dependent differences in the mechanical properties of the common carotid artery*. Eur J Echocardiogr, 2010. **11**(7): p. 630-6.
97. Bu, Z., et al., *Ascending Aortic Strain Analysis Using 2-Dimensional Speckle Tracking Echocardiography Improves the Diagnostics for Coronary Artery Stenosis in Patients With Suspected Stable Angina Pectoris*. J Am Heart Assoc, 2018. **7**(14).
98. O'Neill, W.C., *Renal resistive index: a case of mistaken identity*. Hypertension, 2014. **64**(5): p. 915-7.
99. Kuznetsova, T., et al., *Doppler Indexes of Left Ventricular Systolic and Diastolic Flow and Central Pulse Pressure in Relation to Renal Resistive Index*. American Journal of Hypertension, 2015. **28**(4): p. 535-545.
100. O'Rourke, M.F. and M.E. Safar, *Relationship between aortic stiffening and microvascular disease in brain and kidney - Cause and logic of therapy*. Hypertension, 2005. **46**(1): p. 200-204.
101. Morimoto, A., et al., *Sodium sensitivity and cardiovascular events in patients with essential hypertension*. Lancet, 1997. **350**(9093): p. 1734-7.
102. Weinberger, M.H., et al., *Salt sensitivity, pulse pressure, and death in normal and*

- hypertensive humans*. Hypertension, 2001. **37**(2 Pt 2): p. 429-32.
103. Coatney, R.W., *Ultrasound imaging: principles and applications in rodent research*. ILAR J, 2001. **42**(3): p. 233-47.
 104. Lindsey, M.L., et al., *Guidelines for measuring cardiac physiology in mice*. Am J Physiol Heart Circ Physiol, 2018. **314**(4): p. H733-H752.
 105. Lee, L., et al., *Aortic and Cardiac Structure and Function Using High-Resolution Echocardiography and Optical Coherence Tomography in a Mouse Model of Marfan Syndrome*. PLoS One, 2016. **11**(11): p. e0164778.
 106. Rossi, N.F., et al., *Hemodynamic and neural responses to renal denervation of the nerve to the clipped kidney by cryoablation in two-kidney, one-clip hypertensive rats*. Am J Physiol Regul Integr Comp Physiol, 2016. **310**(2): p. R197-208.
 107. Amani, S. and S. Fatima, *Glycation with Fructose: The Bitter Side of Nature's Own Sweetner*. Curr Diabetes Rev, 2020.
 108. Park, K.H., et al., *Fructated apolipoprotein A-I showed severe structural modification and loss of beneficial functions in lipid-free and lipid-bound state with acceleration of atherosclerosis and senescence*. Biochem Biophys Res Commun, 2010. **392**(3): p. 295-300.
 109. Humphrey, J.D., et al., *Central Artery Stiffness in Hypertension and Aging: A Problem With Cause and Consequence*. Circ Res, 2016. **118**(3): p. 379-81.
 110. Huang, Y. and D.H. Wang, *Role of renin-angiotensin-aldosterone system in salt-sensitive hypertension induced by sensory denervation*. Am J Physiol Heart Circ Physiol, 2001. **281**(5): p. H2143-9.
 111. Yang, N., A. Gonzalez-Vicente, and J.L. Garvin, *Angiotensin II-induced superoxide and*

- decreased glutathione in proximal tubules: effect of dietary fructose.* Am J Physiol Renal Physiol, 2020. **318**(1): p. F183-F192.
112. Hayakawa, Y., et al., *High salt intake damages the heart through activation of cardiac (pro) renin receptors even at an early stage of hypertension.* PLoS One, 2015. **10**(3): p. e0120453.
113. Chandramohan, G., et al., *Effects of dietary salt on intrarenal angiotensin system, NAD(P)H oxidase, COX-2, MCP-1 and PAI-1 expressions and NF-kappaB activity in salt-sensitive and -resistant rat kidneys.* Am J Nephrol, 2008. **28**(1): p. 158-67.
114. Gonzalez-Vicente, A., et al., *Fructose reabsorption by rat proximal tubules: role of Na(+)-linked cotransporters and the effect of dietary fructose.* Am J Physiol Renal Physiol, 2019. **316**(3): p. F473-F480.
115. Wilson, J.S., W.R. Taylor, and J. Oshinski, *Assessment of the regional distribution of normalized circumferential strain in the thoracic and abdominal aorta using DENSE cardiovascular magnetic resonance.* J Cardiovasc Magn Reson, 2019. **21**(1): p. 59.
116. Cox, R.H., *Regional, species, and age related variations in the mechanical properties of arteries.* Biorheology, 1979. **16**(1-2): p. 85-94.
117. Apter, J.T., *Correlation of visco-elastic properties with microscopic structure of large arteries. IV. Thermal responses of collagen, elastin, smooth muscle, and intact arteries.* Circ Res, 1967. **21**(6): p. 901-18.
118. Vakili, B.A., P.M. Okin, and R.B. Devereux, *Prognostic implications of left ventricular hypertrophy.* Am Heart J, 2001. **141**(3): p. 334-41.
119. Grossman, W., D. Jones, and L.P. McLaurin, *Wall stress and patterns of hypertrophy in the human left ventricle.* J Clin Invest, 1975. **56**(1): p. 56-64.

120. Sorrentino, M.J., *The Evolution from Hypertension to Heart Failure*. Heart Fail Clin, 2019. **15**(4): p. 447-453.
121. Jorgensen, P.G., et al., *Burden of Uncontrolled Metabolic Risk Factors and Left Ventricular Structure and Function in Patients With Type 2 Diabetes Mellitus*. J Am Heart Assoc, 2018. **7**(19): p. e008856.
122. D'Souza, A., et al., *Left ventricle structural remodelling in the prediabetic Goto-Kakizaki rat*. Exp Physiol, 2011. **96**(9): p. 875-88.
123. Mizushige, K., et al., *Alteration in left ventricular diastolic filling and accumulation of myocardial collagen at insulin-resistant prediabetic stage of a type II diabetic rat model*. Circulation, 2000. **101**(8): p. 899-907.
124. Rospleszcz, S., et al., *Association of glycemic status and segmental left ventricular wall thickness in subjects without prior cardiovascular disease: a cross-sectional study*. BMC Cardiovasc Disord, 2018. **18**(1): p. 162.
125. Park, J.H., et al., *Amelioration of High Fructose-Induced Cardiac Hypertrophy by Naringin*. Sci Rep, 2018. **8**(1): p. 9464.
126. Liu, Y., et al., *Improvement of cardiac dysfunction by bilateral surgical renal denervation in animals with diabetes induced by high fructose and high fat diet*. Diabetes Res Clin Pract, 2016. **115**: p. 140-9.
127. Waddingham, M.T., et al., *Diastolic dysfunction is initiated by cardiomyocyte impairment ahead of endothelial dysfunction due to increased oxidative stress and inflammation in an experimental prediabetes model*. J Mol Cell Cardiol, 2019. **137**: p. 119-131.
128. Agnoletti, D., et al., *Clinical interaction between diabetes duration and aortic stiffness*

- in type 2 diabetes mellitus.* J Hum Hypertens, 2017. **31**(3): p. 189-194.
129. Rahman, S., et al., *Early manifestation of macrovasculopathy in newly diagnosed never treated type II diabetic patients with no traditional CVD risk factors.* Diabetes Res Clin Pract, 2008. **80**(2): p. 253-8.
130. Guers, J.J., et al., *Voluntary Wheel Running Attenuates Salt-Induced Vascular Stiffness Independent of Blood Pressure.* Am J Hypertens, 2019. **32**(12): p. 1162-1169.
131. Armstrong, M.K., et al., *Aortic-to-brachial artery stiffness gradient is not blood pressure independent.* J Hum Hypertens, 2019. **33**(5): p. 385-392.
132. Holwerda, S.W., et al., *Elevated Muscle Sympathetic Nerve Activity Contributes to Central Artery Stiffness in Young and Middle-Age/Older Adults.* Hypertension, 2019. **73**(5): p. 1025-1035.
133. Hohl, M., et al., *Modulation of the sympathetic nervous system by renal denervation prevents reduction of aortic distensibility in atherosclerosis prone ApoE-deficient rats.* J Transl Med, 2016. **14**(1): p. 167.
134. Fengler, K., et al., *Pulse Wave Velocity Predicts Response to Renal Denervation in Isolated Systolic Hypertension.* J Am Heart Assoc, 2017. **6**(5).
135. Kals, J., et al., *Inflammation and oxidative stress are associated differently with endothelial function and arterial stiffness in healthy subjects and in patients with atherosclerosis.* Scand J Clin Lab Invest, 2008. **68**(7): p. 594-601.
136. Zhou, R.H., et al., *Mitochondrial oxidative stress in aortic stiffening with age: the role of smooth muscle cell function.* Arterioscler Thromb Vasc Biol, 2012. **32**(3): p. 745-55.
137. Canugovi, C., et al., *Increased mitochondrial NADPH oxidase 4 (NOX4) expression in aging is a causative factor in aortic stiffening.* Redox Biol, 2019. **26**: p. 101288.

138. de Picciotto, N.E., et al., *Nicotinamide mononucleotide supplementation reverses vascular dysfunction and oxidative stress with aging in mice*. *Aging Cell*, 2016. **15**(3): p. 522-30.
139. Patterson, M.E., et al., *Interactive effects of superoxide anion and nitric oxide on blood pressure and renal hemodynamics in transgenic rats with inducible malignant hypertension*. *Am J Physiol Renal Physiol*, 2005. **289**(4): p. F754-9.
140. Morgan, E.E., et al., *In vivo assessment of arterial stiffness in the isoflurane anesthetized spontaneously hypertensive rat*. *Cardiovasc Ultrasound*, 2014. **12**: p. 37.
141. Welsh, J.A., et al., *Overweight among low-income preschool children associated with the consumption of sweet drinks: Missouri, 1999-2002*. *Pediatrics*, 2005. **115**(2): p. e223-9.
142. Poirier, P., et al., *Obesity and cardiovascular disease: pathophysiology, evaluation, and effect of weight loss: an update of the 1997 American Heart Association Scientific Statement on Obesity and Heart Disease from the Obesity Committee of the Council on Nutrition, Physical Activity, and Metabolism*. *Circulation*, 2006. **113**(6): p. 898-918.
143. Farquhar, W.B., et al., *Dietary sodium and health: more than just blood pressure*. *J Am Coll Cardiol*, 2015. **65**(10): p. 1042-50.
144. Kalogeropoulos, A.P., et al., *Dietary sodium content, mortality, and risk for cardiovascular events in older adults: the Health, Aging, and Body Composition (Health ABC) Study*. *JAMA Intern Med*, 2015. **175**(3): p. 410-9.
145. Barker, D.J., *The fetal and infant origins of disease*. *Eur J Clin Invest*, 1995. **25**(7): p. 457-63.
146. Albrecht, I., *Critical period for the development of spontaneous hypertension in rats*.

- Mech Ageing Dev, 1974. **3**(1): p. 75-9.
147. Albrecht, I., *The hemodynamics of early stages of spontaneous hypertension in rats. Part I: Male study.* Jpn Circ J, 1974. **38**(11): p. 985-90.
148. Folkow, B. and A. Svanborg, *Physiology of cardiovascular aging.* Physiol Rev, 1993. **73**(4): p. 725-64.
149. Andresen, M.C., S. Kuraoka, and A.M. Brown, *Baroreceptor function and changes in strain sensitivity in normotensive and spontaneously hypertensive rats.* Circ Res, 1980. **47**(6): p. 821-8.
150. Su, D.F., et al., *Arterial baroreflex control of heart period is not related to blood pressure variability in conscious hypertensive and normotensive rats.* Clin Exp Pharmacol Physiol, 1992. **19**(11): p. 767-76.
151. Jelinek, J., E. Hackenthal, and R. Hackenthal, *Role of the renin-angiotensin system in the adaptation to high salt intake in immature rats.* J Dev Physiol, 1990. **14**(2): p. 89-94.
152. Pohlova, I. and J. Jelinek, *Components of the renin-angiotensin system in the rat during development.* Pflugers Arch, 1974. **351**(3): p. 259-70.
153. Musilova, H., J. Jelinek, and I. Albrecht, *The age of factor in experimental hypertension of the DCA type in rats.* Physiol Bohemoslov, 1966. **15**(6): p. 525-31.
154. Brownie, A.C., et al., *The influence of age and sex on the development of adrenal regeneration hypertension.* Lab Invest, 1966. **15**(8): p. 1342-56.
155. Kunes, J. and J. Jelinek, *Influence of age on saline hypertension in subtotal nephrectomized rats.* Physiol Bohemoslov, 1984. **33**(2): p. 123-8.
156. Zicha, J. and J. Kunes, *Haemodynamic changes induced by short- and long-term sodium chloride or sodium bicarbonate intake in deoxycorticosterone-treated rats.* Acta Physiol

- Scand, 1994. **151**(2): p. 217-23.
157. Weiss, L. and Y. Lundgren, *Chronic antihypertensive drug treatment in young spontaneously hypertensive rats: Effects on arterial blood pressure, cardiovascular reactivity and vascular design*. Cardiovasc Res, 1978. **12**(12): p. 744-51.
 158. Benetos, A., et al., *Life survival and cardiovascular structures following selective beta-blockade in spontaneously hypertensive rats*. Am J Hypertens, 1994. **7**(2): p. 186-92.
 159. Adams, M.A., A. Bobik, and P.I. Korner, *Enalapril can prevent vascular amplifier development in spontaneously hypertensive rats*. Hypertension, 1990. **16**(3): p. 252-60.
 160. Singh, A.K., et al., *Fructose-induced hypertension: essential role of chloride and fructose absorbing transporters PAT1 and Glut5*. Kidney Int, 2008. **74**(4): p. 438-47.
 161. Toloza, E.M. and J. Diamond, *Ontogenetic development of nutrient transporters in rat intestine*. Am J Physiol, 1992. **263**(5 Pt 1): p. G593-604.
 162. Jiang, L. and R.P. Ferraris, *Developmental reprogramming of rat GLUT-5 requires de novo mRNA and protein synthesis*. Am J Physiol Gastrointest Liver Physiol, 2001. **280**(1): p. G113-20.
 163. Komnenov, D., et al., *Aortic Stiffness and Diastolic Dysfunction in Sprague Dawley Rats Consuming Short-Term Fructose Plus High Salt Diet*. Integr Blood Press Control, 2020. **13**: p. 111-124.
 164. Schock-Kusch, D., et al., *Transcutaneous measurement of glomerular filtration rate using FITC-sinistrin in rats*. Nephrol Dial Transplant, 2009. **24**(10): p. 2997-3001.
 165. Dietz, R., et al., *Contribution of the sympathetic nervous system to the hypertensive effect of a high sodium diet in stroke-prone spontaneously hypertensive rats*. Hypertension,

1982. **4**(6): p. 773-81.
166. Folkow, B. and D.L. Ely, *Dietary sodium effects on cardiovascular and sympathetic neuroeffector functions as studied in various rat models.* J Hypertens, 1987. **5**(4): p. 383-95.
167. Dlouha, H., J. Krecek, and J. Zicha, *Hypertension in rats with hereditary diabetes insipidus. The role of age.* Pflugers Arch, 1977. **369**(2): p. 177-82.
168. Jelinek, J., *Blood volume in rats with DOCA-hypertension elicited at different ages.* Physiol Bohemoslov, 1972. **21**(6): p. 581-8.
169. Winternitz, S.R. and S. Oparil, *Sodium-neural interactions in the development of spontaneous hypertension.* Clin Exp Hypertens A, 1982. **4**(4-5): p. 751-60.
170. Wyss, J.M., et al., *Salt-induced hypertension in normotensive spontaneously hypertensive rats.* Hypertension, 1994. **23**(6 Pt 1): p. 791-6.
171. Antoine, B., et al., *Role of the GLUT 2 glucose transporter in the response of the L-type pyruvate kinase gene to glucose in liver-derived cells.* J Biol Chem, 1997. **272**(29): p. 17937-43.
172. Ares, G.R., K.M. Kassem, and P.A. Ortiz, *Fructose acutely stimulates NKCC2 activity in rat thick ascending limbs by increasing surface NKCC2 expression.* Am J Physiol Renal Physiol, 2019. **316**(3): p. F550-F557.
173. Barone, S., et al., *Slc2a5 (Glut5) is essential for the absorption of fructose in the intestine and generation of fructose-induced hypertension.* J Biol Chem, 2009. **284**(8): p. 5056-66.
174. Dobesova, Z., J. Kunes, and J. Zicha, *Body fluid alterations and organ hypertrophy in age-dependent salt hypertension of Dahl rats.* Physiol Res, 1995. **44**(6): p. 377-87.

175. Campese, V.M., et al., *Abnormal relationship between sodium intake and sympathetic nervous system activity in salt-sensitive patients with essential hypertension*. *Kidney Int*, 1982. **21**(2): p. 371-8.
176. Farah, V., K.M. Elased, and M. Morris, *Genetic and dietary interactions: role of angiotensin AT1a receptors in response to a high-fructose diet*. *Am J Physiol Heart Circ Physiol*, 2007. **293**(2): p. H1083-9.
177. Thomson, S.C., R.C. Blantz, and V. Vallon, *Increased tubular flow induces resetting of tubuloglomerular feedback in euvolemic rats*. *Am J Physiol*, 1996. **270**(3 Pt 2):p. F461-8.
178. Blantz, R.C., et al., *The complex role of nitric oxide in the regulation of glomerular ultrafiltration*. *Kidney Int*, 2002. **61**(3): p. 782-5.
179. Thomson, S.C., V. Vallon, and R.C. Blantz, *Resetting protects efficiency of tubuloglomerular feedback*. *Kidney Int Suppl*, 1998. **67**: p. S65-70.
180. Gonzalez-Vicente, A. and J.L. Garvin, *Effects of Reactive Oxygen Species on Tubular Transport along the Nephron*. *Antioxidants (Basel)*, 2017. **6**(2).
181. Gonzalez-Vicente, A., N. Hong, and J.L. Garvin, *Effects of reactive oxygen species on renal tubular transport*. *Am J Physiol Renal Physiol*, 2019. **317**(2): p. F444-F455.
182. Grillo, A., et al., *Sodium Intake and Hypertension*. *Nutrients*, 2019. **11**(9).
183. Thorup, C. and A.E. Persson, *Inhibition of locally produced nitric oxide resets tubuloglomerular feedback mechanism*. *Am J Physiol*, 1994. **267**(4 Pt 2): p. F606-11.
184. Kunes, J., et al., *Critical developmental periods in the pathogenesis of hypertension*. *Physiol Res*, 2012. **61**(Suppl 1): p. S9-17.
185. Park, Y.K. and E.A. Yetley, *Intakes and food sources of fructose in the United States*. *Am*

- J Clin Nutr, 1993. **58**(5 Suppl): p. 737S-747S.
186. Nunes, S., et al., *Early cardiac changes in a rat model of prediabetes: brain natriuretic peptide overexpression seems to be the best marker*. Cardiovasc Diabetol, 2013. **12**: p. 44.
 187. Zicha, J. and J. Kunes, *Ontogenetic aspects of hypertension development: analysis in the rat*. Physiol Rev, 1999. **79**(4): p. 1227-82.
 188. Wilczynski, E.A. and F.H. Leenen, *Dietary sodium intake and age in spontaneously hypertensive rats: effects on blood pressure and sympathetic activity*. Life Sci, 1987. **41**(6): p. 707-15.
 189. Louis, W.J., R. Tabei, and S. Spector, *Effects of sodium intake on inherited hypertension in the rat*. Lancet, 1971. **2**(7737): p. 1283-6.
 190. Ely, D.L., et al., *Blood pressure and heart rate responses to mental stress in spontaneously hypertensive (SHB) and normotensive (WKY) rats on various sodium diets*. Acta Physiol Scand, 1985. **123**(2): p. 159-69.
 191. Sullivan, J.M., *Salt sensitivity. Definition, conception, methodology, and long-term issues*. Hypertension, 1991. **17**(1 Suppl): p. I61-8.
 192. Nichols, J., F. Eljovich, and C.L. Laffer, *Lack of validation of a same-day outpatient protocol for determination of salt sensitivity of blood pressure*. Hypertension, 2012. **59**(2): p. 390-4.
 193. D'Angelo, G., et al., *Fructose feeding increases insulin resistance but not blood pressure in Sprague-Dawley rats*. Hypertension, 2005. **46**(4): p. 806-11.
 194. Reaven, G.M., H. Ho, and B.B. Hoffman, *Attenuation of fructose-induced hypertension in rats by exercise training*. Hypertension, 1988. **12**(2): p. 129-32.

195. Johnson, M.D., H.Y. Zhang, and T.A. Kotchen, *Sucrose does not raise blood pressure in rats maintained on a low salt intake*. *Hypertension*, 1993. **21**(6 Pt 1): p. 779-85.
196. Katakam, P.V., et al., *Endothelial dysfunction precedes hypertension in diet-induced insulin resistance*. *Am J Physiol*, 1998. **275**(3): p. R788-92.
197. Nakagawa, T., et al., *A causal role for uric acid in fructose-induced metabolic syndrome*. *Am J Physiol Renal Physiol*, 2006. **290**(3): p. F625-31.
198. Gazhonova, V.E., et al., *[Prognostic value of renal resistance index in estimating the progression of chronic kidney disease]*. *Ter Arkh*, 2015. **87**(6): p. 29-33.
199. Radermacher, J., S. Ellis, and H. Haller, *Renal resistance index and progression of renal disease*. *Hypertension*, 2002. **39**(2 Pt 2): p. 699-703.
200. Parolini, C., et al., *Renal resistive index and long-term outcome in chronic nephropathies*. *Radiology*, 2009. **252**(3): p. 888-96.
201. Mendonca, S. and S. Gupta, *Resistive index predicts renal prognosis in chronic kidney disease*. *Nephrol Dial Transplant*, 2010. **25**(2): p. 644; author reply 644.
202. Ikee, R., et al., *Correlation between the resistive index by Doppler ultrasound and kidney function and histology*. *Am J Kidney Dis*, 2005. **46**(4): p. 603-9.
203. Boddi, M., et al., *Renal resistive index early detects chronic tubulointerstitial nephropathy in normo- and hypertensive patients*. *Am J Nephrol*, 2006. **26**(1):p. 16-21.
204. Sugiura, T., et al., *Evaluation of tubulointerstitial injury by Doppler ultrasonography in glomerular diseases*. *Clin Nephrol*, 2004. **61**(2): p. 119-26.
205. Tublin, M.E., R.O. Bude, and J.F. Platt, *Review. The resistive index in renal Doppler sonography: where do we stand?* *AJR Am J Roentgenol*, 2003. **180**(4): p. 885-92.
206. Heine, G.H., et al., *Renal resistive index and cardiovascular and renal outcomes in*

- essential hypertension*. Hypertension, 2013. **61**(2): p. e22.
207. Doi, Y., et al., *Renal resistive index and cardiovascular and renal outcomes in essential hypertension*. Hypertension, 2012. **60**(3): p. 770-7.
208. Just, A., *Mechanisms of renal blood flow autoregulation: dynamics and contributions*. Am J Physiol Regul Integr Comp Physiol, 2007. **292**(1): p. R1-17.
209. Boron, W.F. and E.L. Boulpaep, *Medical physiology*. Third edition. ed. 2017, Philadelphia, PA: Elsevier. xii, 1297 pages.
210. Tham, Y.K., et al., *Pathophysiology of cardiac hypertrophy and heart failure: signaling pathways and novel therapeutic targets*. Arch Toxicol, 2015. **89**(9): p. 1401-38.
211. Zile, M.R. and D.L. Brutsaert, *New concepts in diastolic dysfunction and diastolic heart failure: Part I: diagnosis, prognosis, and measurements of diastolic function*. Circulation, 2002. **105**(11): p. 1387-93.
212. Katz, D.H., et al., *Prevalence, clinical characteristics, and outcomes associated with eccentric versus concentric left ventricular hypertrophy in heart failure with preserved ejection fraction*. Am J Cardiol, 2013. **112**(8): p. 1158-64.
213. Popovic, A., et al., *Serial assessment of left ventricular chamber stiffness after acute myocardial infarction*. Am J Cardiol, 1996. **77**(5): p. 361-4.
214. Satpathy, C., et al., *Diagnosis and management of diastolic dysfunction and heart failure*. Am Fam Physician, 2006. **73**(5): p. 841-6.
215. Huynh, K., et al., *Diabetic cardiomyopathy: mechanisms and new treatment strategies targeting antioxidant signaling pathways*. Pharmacol Ther, 2014. **142**(3): p. 375-415.
216. Schannwell, C.M., et al., *Left ventricular diastolic dysfunction as an early manifestation of diabetic cardiomyopathy*. Cardiology, 2002. **98**(1-2): p. 33-9.

217. Battiprolu, P.K., et al., *Diabetic cardiomyopathy and metabolic remodeling of the heart*. Life Sci, 2013. **92**(11): p. 609-15.
218. Drazner, M.H., *The progression of hypertensive heart disease*. Circulation, 2011. **123**(3): p. 327-34.
219. Griffin, K.A., *Hypertensive Kidney Injury and the Progression of Chronic Kidney Disease*. Hypertension, 2017. **70**(4): p. 687-694.
220. Chung, C.S. and L. Afonso, *Heart Rate Is an Important Consideration for Cardiac Imaging of Diastolic Function*. JACC Cardiovasc Imaging, 2016. **9**(6): p. 756-8.

ABSTRACT**CARDIO-RENAL MECHANISMS OF FRUCTOSE-INDUCED SALT-SENSITIVE HYPERTENSION**

by

PETER E. LEVANOVICH**August 2021****Advisor:** Noreen F. Rossi, MD**Major:** Physiology**Degree:** Doctor of Philosophy

Dietary consumption of fructose facilitates increased intestinal fluid absorption and renal sodium reabsorption, thereby increasing fluid retention. The net result of this is a sustained increase in extracellular fluid volume that leads to states of hypervolemia and subsequent hypertension. Simultaneously, arterial pressure is being elevated by increased autonomic drive stemming from the sympathetic nervous system and various other endovascular proteins that induce vasoconstriction. Under these conditions, the addition of high dietary sodium promotes hypertension prior to the development of significant metabolic disturbances; the subtlety of which may go unnoticed by patients for prolonged periods. While much is understood regarding the multifactorial pathologies of this model of hypertension, few studies have investigated the chronic effects of this disease and the end-organ damage that may result. The highest consumers of fructose are adolescents and young adults, and despite this demographic factor a disparity in the amount of research investigating the chronic effects of such a diet on developing physiologic systems exists. Using techniques such as ultrasonography, telemetry, and metabolic caging systems, we sought to determine the acute and chronic effects of fructose and high salt feeding in both adult and

adolescent rats. The results of these studies confirmed conclusions from prior studies in that fructose induces a state of salt-sensitivity. Over time this prolonged period of hypertension eventually leads to diastolic dysfunction and left ventricular hypertrophy. The novel-most finding of this study, however, was the discovery that fructose feeding at a young age induces salt-sensitive states governed by renal mechanisms and that this sensitivity is retained into adulthood even following the restoration of a healthy diet. Taken together, these results indicate the inherent risks associated with moderate fructose consumption and highlight the importance healthy dietary habits in promoting cardiovascular and renal health throughout life.

AUTOBIOGRAPHICAL STATEMENT

Peter E. Levanovich

EDUCATION

<i>Ph.D. Candidate in Physiology,</i> <i>Wayne State University, Detroit, MI</i>	2015– Present
<i>B.S.B.A. Real Estate and Construction Management,</i> <i>University of Denver, Denver, CO</i>	2010

AWARDS AND HONORS

Detroit Cardiovascular Training (T32) Grant	2019-2021
Interdisciplinary Biomedical Sciences Fellowship	2016-2018
1 st Place Abstract	2015
<ul style="list-style-type: none"> • American Urology Association 2015, New Orleans, LA 	

PEER-REVIEWED PUBLICATIONS

ORIGINAL OBSERVATIONS

1. Komnenov, D., ***Levanovich, PE.**, Perecki, N., Chung, C., Rossi, NF. 2020. Aortic Stiffness and Diastolic Dysfunction in Sprague Dawley Rats consuming Short-Term Fructose Plus High Salt Diet. *Integrated Blood Pressure Control*. Volume 2020:13 Pages 111-124. *Indicates Co-first authorship
2. **Levanovich PE**, Diaczok A, Rossi NF. Clinical and Molecular Perspectives of Monogenic Hypertension. *Curr Hypertens Rev*. 2019 Apr 9. doi: 10.2174/1573402115666190409115330. PMID: 30963979.
3. Komnenov, D., ***Levanovich, P.**, Rossi, NF. 2019. Hypertension Associated with Fructose and High Salt: Renal and Sympathetic Mechanisms. *Nutrients*. 11(3), 569. *Indicates Co-first authorship.
4. Rajaganapathy, B.R., Janicki, J., **Levanovich, P.**, Tyagi, P., Hafron, J., Chancellor, M.B., Krueger, S., Marples, B. 2015. Intravesical Liposomal Tacrolimus Protects Against Radiation Cystitis Induced by 3-Beam Targeted Bladder Radiation. *Journal of Urology*. 194(2): 578–584.
5. **Levanovich, P.**, Diokno, A., Hasenau, D.L., Lajiness, M., Pruchnic, R., Chancellor. M.B. 2015. Intradetrusor injection of adult muscle-derived cells for the treatment of underactive bladder: pilot study. *International urology and nephrology*. 47:465-467.
6. Smith, P.P., P. Tyagi, G.A. Kuchel, S. Pore, C. Chermansky, M. Chancellor, N. Yoshimura, **Levanovich, P.** 2014. Advanced therapeutic directions to treat the underactive bladder. *International urology and nephrology*. 46 Suppl 1:S35-44.
7. Chancellor, M.B., **Levanovich, P.**, Rajaganapathy, B.R., Vereecke, A.J. 2014. Optimum Management of Overactive Bladder: Medication vs Botox® vs InterStim® vs Urgent® PC. *Urology Practice*. 1:7-12.